

1-1-2011

Characterization of the role of yadK in the pathogenesis of enterohaemorrhagic E. coli O157:H7

Yijing Yu
Ryerson University

Follow this and additional works at: <http://digitalcommons.ryerson.ca/dissertations>



Part of the [Biology Commons](#)

Recommended Citation

Yu, Yijing, "Characterization of the role of yadK in the pathogenesis of enterohaemorrhagic E. coli O157:H7" (2011). *Theses and dissertations*. Paper 677.

This Thesis is brought to you for free and open access by Digital Commons @ Ryerson. It has been accepted for inclusion in Theses and dissertations by an authorized administrator of Digital Commons @ Ryerson. For more information, please contact bcameron@ryerson.ca.

**CHACTERIZATION OF THE ROLE OF YADK IN THE
PATHOGENESIS OF ENTEROHAEMORRHAGIC
E. COLI O157:H7**

by

Yijing Yu

BSc. MSc. Anhui Medical University, Anhui, China 2008

A thesis

presented to Ryerson University

in partial fulfillment of the
requirements for the degree of

Master of Science

in the Program of

Molecular Science

Toronto, Ontario, Canada, 2011

© Yijing Yu 2011

Author's Declaration

I hereby declare that I am the sole author of this thesis.

I authorize Ryerson University to lend this thesis to other institutions or individuals for the purpose of scholarly research.

I further authorize Ryerson University to reproduce this thesis by photocopying or by other means, in total or in part, at the request of other institutions or individuals for the purpose of scholarly research.

Abstract

CHACTERIZATION OF THE ROLE OF YADK IN THE PATHOGENESIS OF ENTEROHAEMORRHAGIC *E. COLI* O157:H7

Yijing Yu, MSc. in Molecular Science, Ryerson University, 2011

Enterohaemorrhagic *Escherichia coli* (EHEC) O157:H7 can cause serious diarrhea and haemolytic uremic syndrome. Various virulence factors including adhesins contribute to pathogenesis of EHEC. Previous studies suggested that *yadK* gene, which encodes a putative fimbrial adhesin in EHEC, may be involved in response of EHEC to acid stress. To characterize role of YadK protein in the pathogenesis of EHEC, recombinant YadK protein was generated and used to immunize rabbit to obtain anti-YadK antiserum, which was able to specifically recognize over-expressed YadK protein in EHEC. Western blotting with anti-YadK revealed a higher level of YadK expression in EHEC under acid adapted-acid stress compared to EHEC under unstressed conditions, which confirmed earlier *yadK* mRNA studies and indicated that YadK is upregulated in EHEC under acid stress. Finally, we observed that anti-YadK antiserum was able to specifically reduce adhesion of acid stressed EHEC to human epithelial cells compared to adhesion level of unstressed EHEC.

Acknowledgements

It was a great experience to study for my Master of Science (MSc.) in the Molecular Science Program, Ryerson University. There are several people who helped me during the course of my project. Amongst them are my committee members: **Dr. Roberto Botelho** and **Dr. Celine Levesque**. I am also grateful to my committee members for their great support and suggestions at various intervals throughout the project. I am thankful to members of Dr. Botelho and Dr. John Marshall labs for sharing with me their equipments and research reagents at several occasions.

I am also grateful to all the members of Dr. Foster lab: Frances, Shahnaz, Julianne, Seavly and Ahferom. I owe Ryerson University for the Ryerson Graduate Student Stipends and Scholarships throughout my 2-year MSc. studies.

Most importantly, I am deeply grateful to my dearest supervisor **Dr. Debora Foster** for having recruited me as part of her great research team. Without her, this project would not have been possible in the first place. Her continuous great support and supervision to my research project has kept me moving forward on the way of making scientific discovery. It would be less if I just say “thank you” to my supervisor. It is much more than that, for which she will remain in my heart and in my memory for years.

Table of Contents

1. Introduction.....	1
1.1 Enterohemorrhagic <i>Escherichia coli</i> O157:H7.....	2
1.2 Bacterial responses to environmental stress.....	4
1.3 Response of EHEC O157:H7 to acid response.....	6
1.4 Virulence factors.....	8
1.5 Bacterial adhesins.....	11
1.6 YadK: a putative fimbrial protein.....	22
1.7 Rationale.....	28
1.8 Hypothesis.....	29
1.9 Thesis objectives.....	29
2. Materials and Methods.....	31
2.1 Bacteria strains and growth conditions.....	31
2.2 Cell culture.....	31
2.3 Plasmid purification.....	33
2.4 PCR analysis.....	35
2.5 Preparation of chemically competent cells.....	37
2.6 Restriction enzyme digestion.....	37
2.7 Gel extraction.....	38
2.8 Ligation.....	38
2.9 Transformation of chemically competent cells.....	38
2.10 YadK protein over-expression.....	38
2.11 SDS and western blotting.....	38
2.12 Protein extraction from BL21 (DE3).....	41
2.13 Isolation of proteins from inclusion bodies.....	41
2.14 Affinity column purification.....	42
2.15 Animal immunization.....	42
2.16 Fimbrial proteins sample preparation.....	43
2.17 Acid stress treatment.....	43
2.18 Preparation of electrocompetent cells.....	44
2.19 Adhesion assay.....	44
2.20 Construction of the <i>yadK</i> deletion mutant.....	46
2.21 Promoter activity assay.....	46
2.22 Statistical analysis.....	48
3. Results.....	49
3.1.1 Successful construction of pGEX-4T3- <i>yadK</i>	49
3.1.2 GST-YadK expressed as inclusion bodies in BL21 (DE3).....	51

3.2.1 Successful construction of pET23d- <i>yadK</i>	54
3.2.2 T7-YadK-His expressed as inclusion bodies in BL21 (DE3).....	56
3.2.3 T7-YadK-His purification from inclusion bodies.....	58
3.2.4 Specific anti-YadK polyclone antibodies were generated.....	60
3.3 Successful construction of EDL933 $\Delta yadK$	62
3.4 Increased YadK expression was observed under acid-adapted acid stress.....	65
3.5 Anti-YadK inhibits host adhesion of acid-stressed EHEC	67
3.6.1 Successful construction of predicted promoter constructs for <i>yadK</i>	69
3.6.2 Up-regulation of promoter activity of <i>PyadN</i> was observed under acid-adapted acid stress.....	74
 4. Discussion.....	75
 5. Future Directions.....	81
 6. References.....	83

List of Tables

Table 2.1	List of strains used in this study.....	32
Table 2.2	List of plasmids used in this study.....	33
Table 2.3	Primers used for PCR in this study.....	35

List of Figures

Figure 1.1 Model of glutamate-dependent acid resistance in <i>E. coli</i>	6
Figure 1.2 The Virulence factors in EHEC O157:H7.....	9
Figure 1.3 The proposed working model for Shiga-toxin.....	10
Figure 1.4 Genetic organization among fimbriae operons identified expressed in EHEC.....	13
Figure 1.5 Type I fimbriae in <i>E. coli</i> under electron microscope	15
Figure 1.6 Donor strand exchange mechanism in type I fimbria.....	22
Figure 1.7 A: <i>yadK</i> mRNA expression under no-acid (UU) and acid adapted acid (AA) stress.....	24
Figure 1.7 B: Adhesion of EHEC wild type and $\Delta yadK$ under stress condition.....	24
Figure 1.8 Genes in Locus 2 with up-regulated transcription level on microarray chip after acid adaptation and acid stress.....	26
Figure 1.9 A: The genetic organization of Locus 2 is similar to the genetic organization of type I fimbriae.....	27
Figure 1.9 B: Predicted Locus 2 fimbriae assembling process.....	27
Figure 2.1 Molecule cloning construct and protein purification procedure in this study.....	34
Figure 2.2 Predicted promoter regions in the locus 2.....	48
Figure 3.1.1 PCR product of <i>yadK</i> full length from DH5 α /pGEX-4T3- <i>yadK</i>	49
Figure 3.1.2 Representative gene sequencing result of <i>yadK</i> amplified from DH5 α /pGEX4T3- <i>yadK</i>	50
Figure 3.1.3 Coomassie blue staining of BL21(DE3) and BL21(DE3)/pGEX4T3- <i>yadK</i> lysate on SDS-PAGE gel.....	52
Figure 3.1.4 Western blotting of GST and BL21(DE3)/pGEX4T3- <i>yadK</i> with anti-GST70K antibodies.....	52
Figure 3.1.5 Coomassie blue staining of soluble and insoluble fraction of BL21(DE3)/pGEX4T3- <i>yadK</i> lysate.....	53
Figure 3.1.6 Western blotting of soluble and insoluble fraction of BL21(DE3) /pGEX4T3- <i>yadK</i> lysate.....	53
Figure 3.2.1 Western blotting of soluble and insoluble fraction of BL21(DE3) /pGEX4T3- <i>yadK</i> lysate.....	54
Figure 3.2.2 Gene sequencing result of <i>yadK</i> amplified from DH5 α /pET23d- <i>yadK</i>	55
Figure 3.2.3 Coomassie blue staining of BL21 (DE3)/pET23d- <i>yadK</i> lysate.....	56
Figure 3.2.4 Western blotting of BL21(DE3)/pET23d- <i>yadK</i> lysate.....	57
Figure 3.2.5 Coomassie blue staining of soluble and insoluble fraction of BL21(DE3)/pET23d- <i>yadK</i> lysate.....	57
Figure 3.2.6 Coomassie blue staining of soluble fraction of detergent-treated BL21(DE3)/pET23d- <i>yadK</i> lysate.....	58
Figure 3.2.7 Coomassie blue staining of purified T7-YadK-His protein from BL21(DE3)/pET23d- <i>yadK</i> lysate.....	59

Figure 3.2.8 Western blotting of purified T7-YadK-His protein from BL21 (DE3)/pET23d- <i>yadK</i> lysate.....	59
Figure 3.2.9 Western blotting of 85170Δ <i>yadK</i> and 85170Δ <i>yadK</i> /pGEX-4T3- <i>yadK</i> with anti-YadK antibodies.....	60
Figure 3.2.10 Western blotting of BL21(DE3) and BL21(DE3)/pET23d- <i>yadK</i> with anti-YadK antibodies.....	61
Figure 3.2.11 Western blotting of 85170Δ <i>yadK</i> and 85170Δ <i>yadK</i> /pBlueSK- <i>yadK</i> with anti-YadK antibodies.....	61
Figure 3.3.1 PCR product of <i>yadK</i> -Kan- <i>yadK</i> amplified from EDL933 Δ <i>yadK</i>	63
Figure 3.3.2 Sequencing result of PCR product amplified from EDL933Δ <i>yadK</i> using internal <i>yadK</i> primers.	64
Figure 3.4.1 Western blotting of EDL933 and EDL933Δ <i>yadK</i> lysates with anti-YadK antibodies.....	66
Figure 3.4.2 Quantitative analysis of the blotting band intensity of YadK versus DnaK revealed that the YadK protein level in EHEC AA group was significantly higher than that in EHEC UU group.....	66
Figure 3.5 Adhesion was assessed and compared among three different incubation groups.....	67
Figure 3.6.1 PCR products of putative <i>yadK</i> promoter regions from DH5α/pMC-PyadN, DH5α/pMC-PyadM and DH5α/pMC-PyadK colonies, respectively.....	69
Figure 3.6.2 Sequencing result of potential <i>yadK</i> promoter regions amplified from pMC1403-PyadN, pMC1403-PyadK and pMC1403-PyadM in DH5α, respectively.....	72
Figure 3.6.3 Promoter activity of EHEC 85170/pMC1403-PyadN under unstressed or acid-adapted acid stress.....	73
Figure 3.6.4 Promoter activity of EHEC 85170/pMC1403-PyadM under unstressed or acid-adapted acid stress.....	74
Figure 3.6.5 Promoter activity of EHEC 85170/pMC1403-PyadK under unstressed or acid-adapted acid stress.....	74
Figure 4.1 A: The effect of acid stress on EHEC adhesion to human epithelial cells.....	79
Figure 4.1 B: Enhanced EHEC adhesion to large intestine after EHEC encounter acid stress in the stomach	79

List of Abbreviations

AA	Acid adapted acid stress
AA30	Acid adapted acid stress 30 minutes
A/E	Attaching and effacing lesions
AI-2	Autoinducer-2
ATCC	American Type Culture Collection
AR	Acid resistance
AR1	Oxidative repressed acid resistance
AR2	Glutamate decarboxylase-dependent acid resistance
AR3	Argines decarboxylase-dependent acid resistance
ATR	Acid tolerance response
cAMP	3',5'-cyclic adenosine monophosphate
Caco-2	Colonic adenocarcinoma cells
CFU	Colony forming units
CRP	cAMP receptor protein
DMEM	Dulbecco's MEM
ECP	<i>E. coli</i> Common Pilus
EDTA	Ethylenediaminetetraacetic acid
EHEC	Enterohemorrhagic <i>Escherichia coli</i>
FBS	Fetal bovine serum
GABA	γ -amino butyric acid
Gb3	Glycolipid globotriaosylceramide-3 receptor
Gb4	Glycolipid globotriaosylceramide-4 receptor
GI	Gastrointestinal
HC	Hemorrhagic colitis
HEp-2	Laryngeal carcinoma cells
H-NS	Heat-stable nucleoid-structuring protein
HUS	Hemolytic-uremic syndrome
IPTG	Isopropyl β -D-1-thiogalactopyranoside
IHF	Integration host fact
LB	Luria-Bertani
LEE	Locus of enterocytes effacement
LPS	Lipopolysaccharide
LPF	Long polar fimbriae
LRP	Leucine-responsive regulatory protein
MEM	Minimal essential media
MLC	Myosin light chain
PBS	Phosphate buffered saline
PCR	Polymerase chan reaction
RpoS	Stress response regulon
RT-PCR	Quantitative Real-Time PCR
Stx	Shiga toxin
SF	Sorbitol-fermenting

TccP	Tir-cytoskeleton coupling protein
TNF	Tumor necrosis factor
Tir	Translocated intimin receptor
TTSS	Type III secretion system
UU	unshocked control for its counterpart acid stress
UU30	unadapted unstressed counterpart for acid stress 30 minutes
Vtx	Verocytotoxin
WT	Wild type

1. Introduction

Escherichia coli (*E. coli*) is commonly found in the environment. Most *E. coli* strains are harmless to humans; however, some strains, such as enterohaemorrhagic *E. coli* O157:H7 (EHEC O157:H7), present a major threat to human health primarily through food or water contamination. Unlike most commensal strains of *E. coli*, EHEC disrupts the physiological balance of resident flora in the gastrointestinal (GI) tract. EHEC infection can cause serious bloody or non-bloody diarrhea and haemolytic uremic syndrome (HUS) in human patients¹. The 1982 outbreaks of EHEC O157:H7 infection in the United States of America posed a serious problem to the public health. A recent EHEC O104:H4 outbreak in Europe has been reported to infect more than 2400 people².

Enteric pathogens, including EHEC, must be able to survive the harsh environment of GI tract in order to cause infection. EHEC, on route to the site of colonization in the large intestine, encounter harsh conditions, including acid stress in the stomach, bile salt stress in small intestine, and short fatty acid stress in large intestine³. While there has been considerable progress in understanding the pathogenesis of EHEC, we still know relatively little about changes in EHEC virulence in response to stress.

Adhesion to host cells, a critical virulence property, is an integral event for bacterial colonization to the host cell surfaces, and is often an essential step during bacterial infection. Adhesins are the bacterial surface components that are responsible for the

attachment of bacteria to specific host receptors. The types of host cells targeted by bacteria are determined by the bacterial adhesins⁴. Shiga-toxin (Stx) or Verocytotoxin (Vtx), is the most important virulence factor in EHEC. In addition, a number of non-toxin virulence factors have been reported⁵⁻⁷. Fimbrial adhesins, which are one group of non-toxin virulence factors, participate in the adherence of EHEC O157:H7 to eukaryotic cells and play an essential role in biofilm formation⁸. However, the regulatory mechanisms of fimbrial expression are not well understood.

1.1 Enterohemorrhagic *Escherichia coli* O157:H7

EHEC O157:H7 are Gram-negative rod shaped bacteria. EHEC O157:H7 are distinguished from other pathogenic strains of *E. coli* by the lack of β -glucuronidase production¹. But like other kinds of pathogenic *E. coli* bacteria, several virulence factors encoded in the locus of enterocyte effacement (LEE) and the phage encoded Shiga-toxin (Stx) genes were also found in EHEC O157:H7⁹⁻¹⁰. These virulence factors are essential for the survival and infection of these EHEC.

Individuals infected with EHEC O157:H7 typically develop watery diarrhea which progresses to bloody diarrhea or hemorrhagic colitis (HC) within a week. Most of them recover gradually. However, about 5-10% of HC cases will progress to systemic complications known as hemolytic uremic syndrome (HUS)¹¹. HUS is characterized

by hemolytic anemia, thrombocytopenia and acute renal failure¹². Children and the elderly have the highest incidence of developing this life-threatening syndrome¹².

The major transmission of EHEC from animals to humans occurs via food chain contamination. The consumption of contaminated bovine-derived products, such as ground beef and raw milk, has been linked to O157:H7 outbreaks. Manure contaminated runoff is another source of EHEC contamination in crop irrigation systems, as the EHEC-colonized cattle can continuously shed off EHEC bacteria, thus contaminating drinking water¹³⁻¹⁴; other waterborne outbreaks can be traced to contaminated fruits and vegetables. Person to person transmission is also possible, as the infectious dose could be achieved at a very low dose (i.e. 10^2 organisms)¹⁵.

So far, effective therapies to prevent and treat EHEC infection are limited. Many antibiotics including ciprofloxacin and trimethoprim/sulfamethoxazole could produce rapid bactericidal activity, but still allowing continuous toxin synthesis before cell death. In contrast, azithromycin was able to reduce the Stx production even when O157:H7 remained at high viability¹⁶. A recent report has revealed that an antibody therapy (the monoclonal C5 antibody eculizumab) successfully inhibited and reversed kidney damage and neurological symptoms in 3 years old EHEC infected children¹⁷. To develop better therapeutic treatments, an understanding of EHEC O157:H7 virulence responses and pathogenesis is required.

1.2 Bacterial responses to acid stress

Bacterial growth and survival can be affected by many environmental factors, and bacteria have to adapt and survive under various environmental challenges. Most of *E. coli* strains have an optimal growth condition range (i.e. pH, oxygen, nutrition compounds and temperature), which is suitable for growth in natural or laboratory conditions¹⁸.

Many studies have shown that adhesion of EHEC O157:H7 to host cells is influenced by exposure to selected stresses³. It has been demonstrated that acid shock (pH 3.0) preceded by adaptation to mild acid stress (pH 5.0) for 1h significantly increased EHEC adhesion to human epithelial cells³. Another study reported that adhesion of EHEC to Caco-2 cells was significantly increased after long-term adaptation to salt stress, compared to the standard condition (i.e. no salt)¹⁹. In yet another study, the lack of lactose resulted in the inhibition of LEE genes expression, leading to decreased EHEC adhesion to HEp-2 cells²⁰.

Studies have shown that low pH can cause damage to bacteria through affecting the cytoplasmic membrane, denaturing essential proteins, disrupting the intracellular enzyme function and damaging the chromosome DNA²¹. *E. coli* has evolved acid resistance (AR) mechanisms to survive in an acidic environment. The definition of AR in *E. coli* is the ability to withstand the acid challenge at pH 2.5 or even lower pH. Three types of acid response system have been investigated in acid resistance of *E.*

*coli*²². The oxidative repressed acid resistance (AR1) is a glucose-repressed system, which is associated with the alternative sigma factor σ^s (encoded by *rpoS* gene) and the cAMP receptor protein (CRP)²³. Mutations in the *rpoS* gene have been found in natural and laboratory strains, but these mutant strains still survive under acid stress, indicating that other *rpoS*-independent AR systems are involved in recovering the acid tolerance response²⁴.

The other two acid response systems belong to amino acid decarboxylase-dependent systems: one requires glutamate (AR2) while the other needs arginine (AR3). *E. coli* usually could not survive in highly acidic (i.e. below pH 2.5) LB in the absence of glucose, unless glutamate or arginine was present²². Generally speaking, AR1 system is thought to be sufficient for *E. coli* survival in the mildly acidic environment, while AR2 and AR3 are responsible for *E. coli* survival under relatively low pH acid stress (i.e. pH 2-3)²⁵. The AR2 system has been more extensively studied compared to other two AR systems²³. AR2 system are composed of proteins encoded by three genes (i.e. *gadA*, *gadB* and *gadC*), respectively. *gadA* and *gadB* encode highly homologous glutamate decarboxylase isozymes (GadA and GadB), while *gadC* encodes the γ -aminobutyric acid (GABA) antiporter (**Figure 1.1**)²⁴. For AR3, arginine decarboxylase AdiA (encoded by *adiA*) converts arginine to agmatine, while the antiporter AdiC transports arginine and agmatine across the membrane in opposite directions²⁶.

The mechanism of AR is to induce bacterial pH homeostasis, by keeping intracellular pH less acidic. As shown in **Figure 1.1**, the low pH extracellular environment allows the proton to move into the bacterial cells and the proton is then consumed by GadA and GadB through decarboxylation of glutamate into GABA. As a membrane bound transporter, GadC transports glutamate into cell while transporting GABA out of cell. In this way, an intracellular pH homeostasis can be maintained.

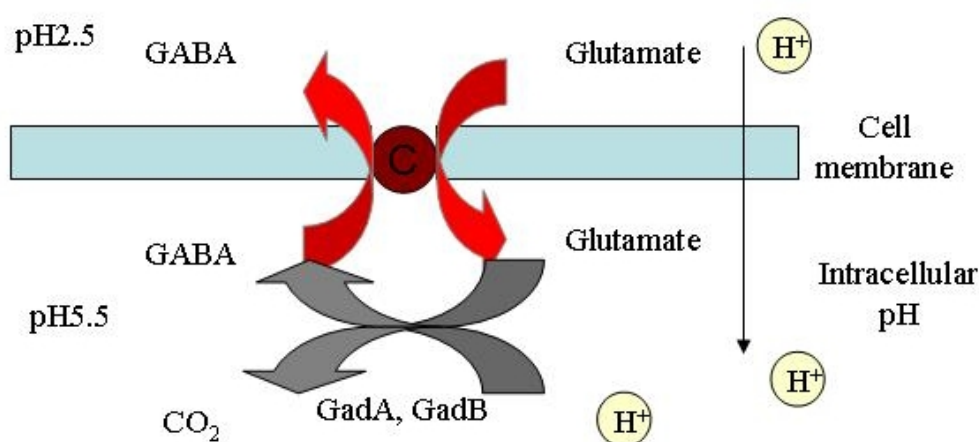


Figure 1.1 Model of glutamate-dependent acid resistance in *E. coli*²⁴. C indicates GadC, an antiporter; GABA represents γ -amino butyric acid. GadA and GadB are glutamate decarboxylase isoforms, which mediate decarboxylation of glutamate into GABA. When the extracellular pH reaches low, the proton can travel into bacterial cells. To maintain intracellular pH homeostasis, GadA and GadB consume a proton into CO₂ by decarboxylation of glutamate into GABA. The antiporter GadC transports glutamate in and GABA out of bacteria, to consume more protons.

1.3 Response of EHEC O157:H7 to acid stress

Low pH (i.e. pH 1.5-3) in the stomach is one of the first host defenses that foodborne pathogens encounter in the human GI tract. Exposure to stomach acid stress is a survival challenge for many foodborne pathogens before reaching to final

colonization sites, but EHEC O157:H7 is able to survive passage through the acidic environment of GI tract³. In vitro studies found that EHEC O157:H7 can also survive for periods of time in other acidic environments, such as apple cider (pH 3.6-4), mayonnaise (pH 3.6-3.9 and fermented sausage (pH 4.5)²⁷.

EHEC O157:H7 has also been reported to show enhanced survival in acute acid if pre-adapted by exposure to mild acid²⁷. EHEC O157:H7 shows enhanced growth in apple cider (pH 3.6), if it is pre-adapted in broth (pH 5)²⁸. Another study showed that pre-exposure of a clinical isolate of EHEC O157:H7 to pH 4.5 resulted in greater tolerance to acute acidic conditions as low as pH 3.0²⁹. Acid adaptation also influences the tolerance of EHEC to other environmental stresses. For example, the acid-adapted EHEC O157:H7 has increased tolerance to thermal stress and higher sodium chloride concentrations³⁰. It also has been demonstrated that acid-adaption of EHEC O157:H7 induces cross-protection against activated lactoperoxidase and lactic lactoperoxidase, which are used to control EHEC O157:H7 contamination in the milk industry³¹.

The adhesion of pathogenic *E. coli* to epithelial cells was also enhanced under acid stress^{3, 32}. Exposure either to acute acid stress or acid-adapted acid stress significantly enhances adhesion of EHEC to human epithelial cells³. Similar to EHEC, enhanced bacterial adhesion to human epithelial cells after acid stress was also observed for diarrhaegenic pathogen EPEC³².

Through transcriptomic and proteomic analysis of EHEC O157:H7 under various culture conditions, the potential genes involved in the response of EHEC to acid stress were explored^{3, 33-35}. It has been shown that exposure of EHEC to the mild acid stress of apple juice (pH 3.5) was associated with significant up-regulation of several genes encoding shock proteins and putative membrane proteins³³. Recently, mRNA extractions from *E. coli* K12 and EHEC O157:H7 exposed to acetic, lactic and hydrochloric acid (pH 5.5) are compared³⁴. The universal acid response genes that are up-regulated in acid shocked EHEC O157:H7, but not in *E. coli* K12, were involved in heat shock response, osmoregulation, inorganic ion and nucleotide transport and metabolism, translation and energy production³⁴. A DNA microarray study revealed that exposure of EHEC to a variety of acid adaptation and acid shock conditions resulted in a significant increase in the expression of a variety of virulence factors, including molecules involved in adhesion, motility and type III secretion³. Mass spectrometry studies of EHEC O157:H7 have demonstrated that numerous proteins involved in metabolism were increased in an acidic environment, including GadA and GadB (acid resistance) and ompA (outer membrane protein)³⁵.

1.4 Virulence factors

Shiga toxin (Stx) (also known as Verocytotoxin), is a critical virulence factor in EHEC¹. In addition, a number of non-toxin virulence factors have been reported (**Figure 1.2**)¹.

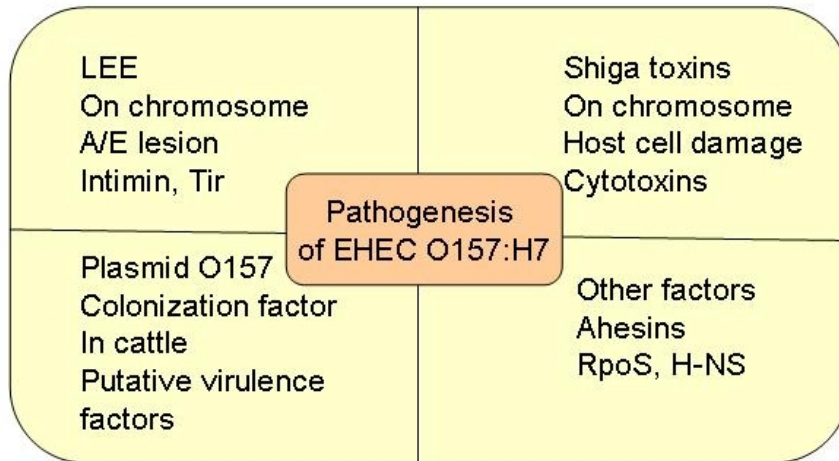


Figure 1.2 The Virulence factors in EHEC O157:H7. LEE represents the locus of enterocyte effacement; A/E indicates attaching and effacing.

1.4.1 Shiga Toxin

There are two major members in Shiga Toxin (Stx) family: Stx1 and Stx2. The homologous percentage between Stx1 and Stx2 is 56%³⁶. Three Stx2 variants (Stx2c, Stx2d and Stx2e) have been identified. Stx1 and all of these Stx2 proteins except Stx2e bind to glycolipid globotriaosylceramide-3 receptor (Gb3), while Stx2e binds to glycolipid globotriaosylceramide-4 receptor (Gb4)³⁷. Stx2 is more highly associated with HUS and more toxic than Stx1³⁸.

Each Stx consists of one A subunit and five identical B subunits, which belongs to the AB4 toxin family. The five B subunits (7.7 KDa) bind to the Gb3 on the host cell surface, resulting in the translocation of Stx complex into the host cells by endocytosis. After being translocated into the host cells, the A subunit is excised to generate the catalytically active A1 (27kDa) and A2 (4KDa) units (**Figure 1.3**). The A1 subunit inhibits protein synthesis in host cell by removing an adenine residue from

the 60S rRNA, leading to death of the host cell³⁶. The host cell death subsequently causes the breakdown of the epithelial cell barrier which results in the bloody diarrhea in EHEC-mediated gastroenteritis³⁹. Stx is also toxic to human renal endothelial cells. The decreased glomerular filtration rate leads to the acute renal failure, which is also known as haemolytic uremic syndrome (HUS). In this disease process, Stx can not only directly damage the glomerular endothelial cells but can also influence the production of pro-inflammatory cytokines by macrophages, such as tumor necrosis factor (TNF)- α and interleukin (IL)-6⁴⁰.

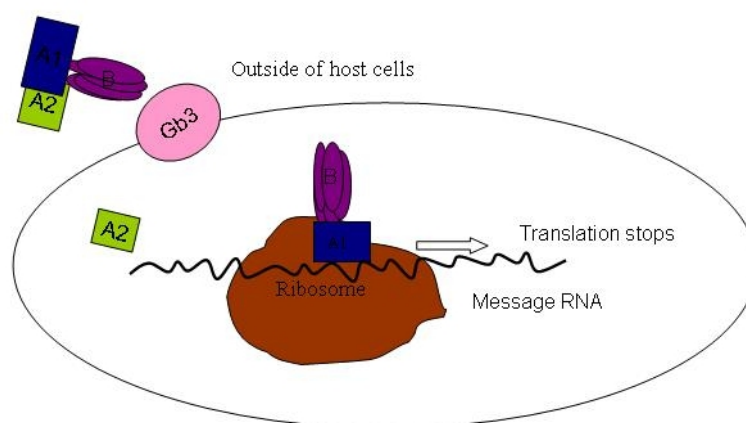


Figure 1.3 The proposed working model for Shiga-toxin³⁶. The **B** subunit interacts with cellular receptor Gb3 or Gb4, A subunit is cleaved in cytoplasm, resulting in a 27kDa N-terminal fragment (**A1**) and a 4kDa C-terminal peptide (**A2**). **A1** binds to ribosome and stop translation, leading to host cell death.

1.4.2 The locus of enterocyte effacement (LEE)

The attaching and effacing (A/E) lesion is one of the characteristic features that distinguish EHEC from many other pathogenic *E. coli* strains. Typically, the A/E lesion is characterized by host cytoskeletal changes, including high concentrations of polymerized filamentous actin and other cytoskeletal components (such as α -actinin,

talins and ezrins) in the infection sites⁴¹. Most A/E phenotype genes are encoded by the locus of enterocyte effacement (LEE)⁴²⁻⁴⁴.

The 43kb-length of the LEE pathogenicity island is composed of five operons (LEE1-5), including 41 different open reading frames. The genes encoding the translocated proteins of the type III secretion system (TTSS), such as EspA, EspB and EspD, are located in LEE1, LEE2 and LEE3⁴³. Translocated intimin receptor (Tir), which facilitates intimate binding to host epithelium in concert with other LEE-encoded proteins⁴³, is encoded in LEE5.

1.4.3 Virulence plasmid

In addition to virulence factors encoded in bacterial chromosomes, all of *E. coli* O157:H7 strains contain a plasmid called pO157, with a size ranging from 92kb to 104kb¹. Only 19 of 100 open reading frames (ORF) in this plasmid have been characterized in *E. coli* O157:H7¹. The 19 gene products include a serine protease called EspP, found to cleave human coagulation factor V and cause mucosal hemorrhage characteristic of hemorrhagic colitis⁴⁵, and a putative adhesin ToxB (*toxB*) shown to contribute to the adherence of *E. coli* O157:H7 to epithelial cells⁴⁶.

1.5 Bacterial adhesins

Adhesins are the bacterial surface components that are responsible for the adhesion of bacteria to host cells. EHEC O157:H7 adhesins can be divided into fimbrial adhesins

and non-fimbrial adhesins (including one intimin gene)⁴⁷.

1.5.1 Fimbriae family members

Many bacterial species possess long filamentous structures known as pili or fimbriae extending from their surfaces. Fimbriae have been implicated in various events, such as host–pathogen interactions, colonization and invasion⁴⁸. Non-flagellar organelles of Gram-negative bacteria include the well characterized chaperone/usher-assembled fimbriae, type IV fimbriae and curli⁸. In each of these systems, bacteria have evolved mechanisms to efficiently assemble the highly stable fimbrial structures on their surfaces⁴⁹.

Fimbriae are wiry or rod-shaped, fiber-like structures located on the surface of bacteria. Fimbriae can recognize particular receptors on the surface of different host cells (e.g. epithelial cells)⁸. The subunits encoded by fimbrial operons usually have similar genetic organization. Briefly, each operon has one or two genes that encode regulatory factors, and a major subunit, several minor subunits, a chaperone and an outer membrane usher. The fimbrial chaperone is the periplasmic protein that can specifically bind fimbrial subunits to form chaperone-fimbrial subunit complexes, which facilitates the assembly of pilus⁵⁰. The usher is an outer membrane protein that directs the assembling order of pilus subunits into a pilus⁵⁰. The genetic organization of fimbriae operon in the pathogenic EHEC is shown in **Figure 1.4**⁵¹⁻⁵².

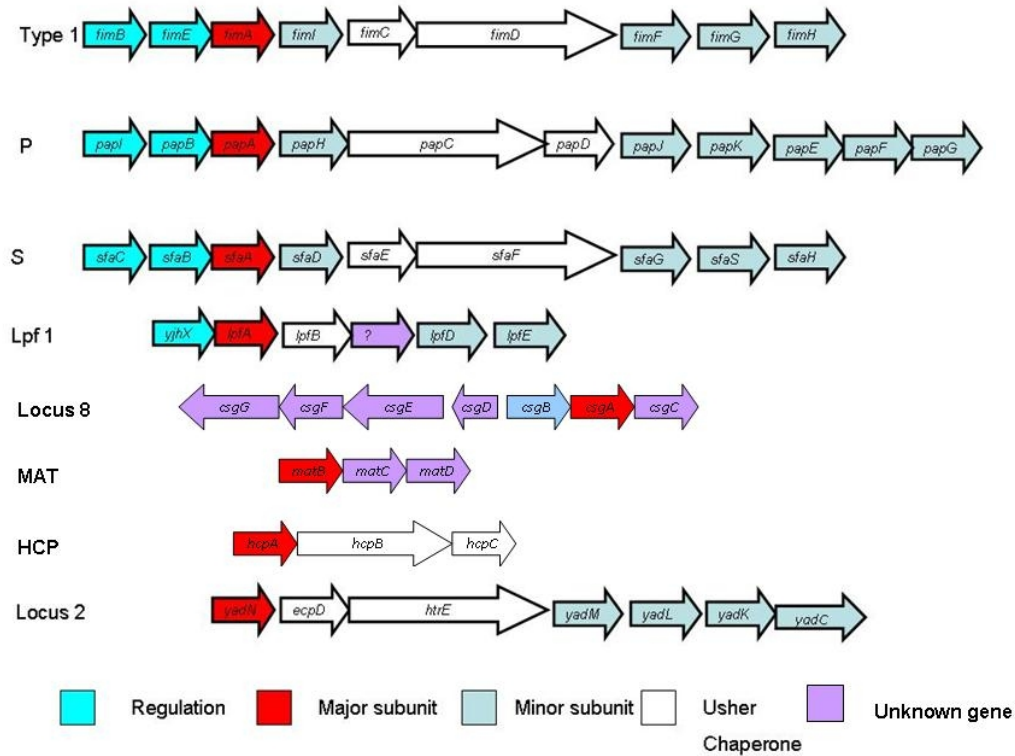


Figure 1.4 Genetic organization among fimbriae operons identified expressed in EHEC^{51,54-58}. Type I, P, S, Lpf1, locus 2 belong to chaperone and usher pathway. Red filled arrows indicate major subunit within operon; blue filled arrows refer to minor subunit within operon; white filled arrows indicate chaperone of usher within operon. This diagram is adapted from the figures in the previous publications^{51,54-58}.

According to genetic analysis, 16 potential fimbrial gene clusters have been reported in EHEC O157:H7. Thirteen of them have putative chaperone and usher genes, indicating these 13 gene clusters may be involved in the chaperone and usher pathway⁵³, while the other 3 clusters (locus 7, MAT and ppdD) may be associated to curli and type IV fimbriae. To date, 7 gene clusters have been demonstrated to be expressed in EHEC strains, including locus 13 (Lpf), locus 8 (F9), locus 7 (curli), MAT (ECP) and ppdD (HCP)⁵⁴⁻⁵⁸. However, it is still unknown whether the rest of gene clusters are functional in EHEC^{53, 56}. A well characterized type I fimbrial gene cluster (locus 14), the genetic organization of which is similar to F9 fimbrial gene

cluster (locus 8), is also located on EHEC O157:H7 chromosome⁵³. Fimbriae encoded on a plasmid in EHEC O157:H7 will also be described here.

1.5.1.1 Type I fimbriae

Type I fimbriae, one of the most studied fimbrial types, have been found in many *E. coli* strains. Typically, type I fimbriated bacteria have 200-500 copies of fimbriae on their surfaces⁵⁹. Under electron microscope, each fimbriae is a 7nm wide, 1µm long and rod-shaped fiber⁶⁰ (**Figure 1.5**). Since the *fim* genes encoding type I fimbriae, have been found in commensal and pathogenic *E. coli* strains, type I fimbriae are considered as important colonization factors and potential virulence factors⁵⁶.

The genes involved in production of type I fimbriae are located in the bacterial chromosomes, where these genes form the gene cluster⁶¹ (**Figure 1.4**). There are six genes (i.e. *fimA*, *fimC*, *fimD*, *fimF*, *fimG* and *fimH*) associated with fimbriae expression and two genes (i.e. *fimB* and *fimE*) involved in the regulation of fimbriae expression⁶¹. Due to a 16bp deletion in the invertible element, type I fimbriae may not express in EHEC O157:H7⁶².

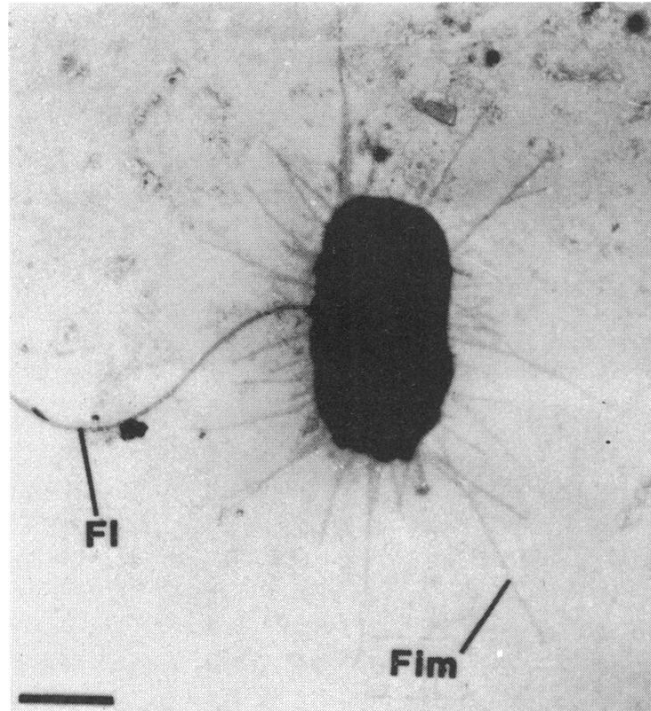


Figure 1.5 Type I fimbriae in *E.coli* under electron microscope⁶³. Fim indicates type I fimbriae; Fl indicates a long flagellum. The scale bar represents 0.5 μ m.

1.5.1.2 F9 fimbriae

F9 fimbria is one of the 16 fimbrial clusters found on EHEC O157:H7 chromosome⁵³.

Introduction of the F9 operon into the *E. coli* K12 strains increases bacterial adhesion to host cells, while a deletion of the major subunit of the F9 operon in *E. coli* O157:H7 EDL933 strain results in decreased colonization of these *E. coli* in calves⁵⁸.

1.5.1.3 Long polar fimbriae (Lpf)

Two *lpf* loci (locus 12 and locus 13) in EHEC, with high homology to the long polar fimbriae (Lpf) in *Salmonella enterica*, have been identified⁶⁴. The *lpf* form surface structures that are 7–8nm in diameter and 2–10 μ m in length extending from bacterial cell surface. The six characterized open-reading frames in the *lpf* operon of EHEC

showed considerable similarity to the *lpf* gene cluster in *S. enterica*⁵⁷. Cloning of the EHEC *lpf* operon into non-fimbriated *E. coli* K-12 results in the increased adhesion of these *E. coli* to cultured epithelial cells, indicating a role of long polar fimbriae in bacterial adhesion to host cells⁵⁷.

The protein prediction analysis reveals a high structural homology between Lpf proteins and Fim proteins of type I fimbriae⁵⁷. The major subunit encoded in the *lpf* operon, LpfA, has the similar structure as FimA, while LpfB and LpfC proteins share a high homology to FimC and FimD, the usher-chaperone subunits of type I fimbriae⁵⁷.

1.5.1.4 Other types of fimbriae

Recently, a type IV PpdD pilus has been found in *E. coli* O157:H7 and this pilus was recognized by serum from HUS patients suggesting that it was expressed on the pathogen during the infection⁵⁶. The homology between PpdD of *E. coli* K12 and *Shigella* is high (91%)⁵⁶. Under the electron microscope, PadD pili appear with a long (>20 µm), thin and rod-like shape⁵⁶. Three genes are involved in the synthesis of these pili, including *hcpA* (pilin gene), *hofB* (usher gene) and *hofC* (chaperone gene). In vitro studies of an *hcpA* mutant indicated that PpdD pili played an important role in the EHEC adhesion to epithelial cells (e.g. Caco-2, HEp-2 and Hela cells)⁵⁶.

Sfp fimbriae encoded by *sfp* cluster are located in a plasmid of sorbitol-fermenting (SF) EHEC O157. Electron microscopy reveals that Sfp fimbriae are around 0.4µm long and 3-5nm wide⁴⁵. Six genes in this cluster, *sfpA*, *sfpH*, *sfpC*, *sfpD*, *sfpJ* and *sfpG*, are highly homologous to P fimbriae. It has been demonstrated that anaerobic culture condition can induce Sfp fimbriae expression which is associated with increased adherence to host epithelial cells⁶⁵.

Curli is found to be expressed in a few EHEC O157 strains. The studies with *csgD* mutants indicate a temperature-independent phase-variation manner in the expression of EHEC O157 curli⁶⁶. It has been suggested that curli may contribute to EHEC adhesion ability, as EHEC with curli expression exhibit a more massive adhesion to HEp-2 cells, compared to EHEC with no-curli expression⁵⁴.

The MAT fimbrial gene cluster has also been found in the chromosomes of many *E. coli* strains (e.g. EHEC O157:H7), and the encoded pilus called *E. coli* Common Pilus (Ecp) is found to be expressed in several EHEC O157:H7 strains⁵³. EcpA, previously known as YadZ, is the major subunit of MAT fimbriae. The *ecpA* mutant EHEC exhibits a decreased adhesion to HEp-2 cells, indicating that Ecp may play a role in EHEC adhesion⁵⁵.

The Locus 2 operon is predicted to be a chaperone-usher fimbrial operon in EHEC O157:H7. With the use of a promoter fusion construct, It is reported that the

expression of locus 2 is not observed under standard culture conditions⁵⁹. However, a DNA microarray study revealed that the transcription level of 6 genes in the locus 2 operon increased in EHEC O157:H7 under acid-adapted acid stress, suggesting that this putative adhesion may be important for adhesion of acid-stressed EHEC³

1.5.2 Regulation of fimbriae expression

The expression of fimbriae is directed by the selection pressure under different growing conditions⁵³. In general, the fimbrial expression is regulated by local environmental conditions, global regulatory factors and genetic regulatory mechanisms^{64, 67-69}.

1.5.2.1 Local regulators (temperature and pH)

A temperature-dependent model has been reported for the expression of many fimbrial adhesins^{64, 70-71}. It has been reported that the production of SEF14 fimbriae in *S. serotype Typhimurium* are enhanced at 37 °C but not 20 °C, while SEF17 fimbriae are increased at 20 °C but not 37 °C⁷². Studies with long polar fimbriae (LPF) in *E. coli* O157:H7 have shown that the transcription level of the *lpfAlp::lacZ* is not significantly induced at 30 °C, but its expression significantly increases at stationary phase at 37 °C⁶⁴.

Studies with K99 and F41 fimbriae have shown that the pH of the culture medium greatly influences the fimbrial production⁷³. The optimal pH value for K99 and F41

fimbriae expression is 7, and thus the production of fimbriae decreases when pH is either higher or lower than 7⁷⁴. In contrast, the mRNA expression profile of acid-stressed EHEC reveals a significant increase in several known putative adhesins including *yadK*, a putative fimbrial adhesin gene that showed 5.87-fold increase, after EHEC was exposed to acid stress treatment³.

1.5.2.2 Global regulatory factors

Several global regulatory factors, such as histone-like nucleoid structuring (H-NS), Leucine-responsive regulatory protein (Lrp) and integration host factor (IHF), have been intensively studied^{71, 75-76}.

The histone-like nucleoid structuring (H-NS) protein, a 136 amino acid residues protein comprised of a C-terminal DNA binding domain and an N-terminal protein interacting domain, was found to have a negative regulatory effect on certain virulence factors encoded on the LEE pathogenicity island, subsequently affecting fimbrial expression and EHEC acid tolerance⁷⁷. Many studies have shown that H-NS is involved in regulating the *E. coli* adherence, through repressing genes encoding fimbrial adhesins. such as P fimbriae⁷¹. A microarray study revealed that *fimB* and *fimI*, encoding type I fimbrial subunits, were significantly up-regulated in *E. coli* K12 *hns* mutant⁶⁷. Other putative fimbrial adhesin genes, *yadN*, *yaiP*, *yagX* and *ycbQ* were also up-regulated in the *hns* mutant⁶⁷. This indicates H-NS may play a repressive role in fimbrial expression in *E. coli*.

Lrp is composed of two 18.8 kDa subunits⁷⁸, and it is a global regulator in *E. coli*, where Lrp controls the expression of many genes involved in amino acid biosynthesis, transport and degradation⁷⁹. Lrp also regulated expression of many fimbriae including *fim*, *sfa*, *daa*, *pap*, and *fan* operons⁸⁰. Similar to Lrp, IHF can also regulate the expression of many fimbriae⁸¹.

1.5.2.3 Genetic regulatory mechanisms

The genetic regulatory mechanisms involved in the regulation of fimbriae expression can be divided into an “ON”/“OFF” phase switch and post-transcriptional regulation.

Almost all fimbrial operons were found to encode one or two regulatory proteins and these proteins, under most circumstances, are involved in phase variation mechanism, in which the fimbriae expression state is switched between phase-on (expression) and phase-off (non-expression) states⁶⁸. The variation is controlled by two regulatory proteins, FimB and FimE. FimB has the ability to turn the switch in either direction, while FimE can only turn the switch from “on” to “off” orientation⁸². The expression of type I fimbriae was examined in 46 strains of diarrheagenic *E. coli*, and according to the mannose-sensitive hemagglutination (MSHA) test (i.e. the binding ability of *E. coli* to pig erythrocytes with or without D-mannose), only 4 strains exhibited the MSHA-positive phenotype⁶². However, none of the O157:H7 and O157: H⁻ strains express Type I fimbriae, because a 16-bp deletion was found in all these O157:H7 and O157: H⁻ strains that locked the *fim* switch in the “off” orientation⁶².

The post-transcription regulation mechanism determines the expression level of different proteins in one operon. All fimbrial operons typically contain a gene that encodes the major subunit of the fimbriae and this gene translates much larger amount of subunits compared to other subunits^{61, 83}. It has been demonstrated that the fimbriae mRNAs encoding the major subunit are relatively stable while the mRNA encoding other subunits degrades rapidly. Thus, different degradation rates of mRNAs also control the fimbriae gene expression⁶⁹.

1.5.3 Fimbrial assembly and donor strand exchange mechanisms

All structural fimbrial subunits are synthesized in the bacterial cytoplasm as proteins with an N-terminal signal sequence⁸⁴. They are then translocated into periplasm, which is dependent on a general secretory pathway. In the periplasm, almost all subunit proteins can recognize and bind to the chaperones encoded by the same gene cluster⁸⁵. After fimbrial domain proteins interacting with the chaperone, the complex can interact with the bacterial outer membrane usher encoded by the same gene cluster, and then the subunits translocate across the outer membrane and become exposed at the cell surface, contributing to the fimbrial assembly. Two components of the structural subunits contribute to this chaperone-usher pathway. The chaperone binds each fimbrial subunit, capping its interactive surfaces and maintaining them in an assembly-component conformation. Then, the chaperon-subunit complexes are transferred to the outer membrane protein, usher, where the chaperone is released. The usher then assists the subunits bind to the primer subunit and, the fimbrial

polymerization occurs. Thus, this donor strand exchange mechanism plays an essential role in the fimbriae assembly process⁸⁶ (**Figure 1.6**).

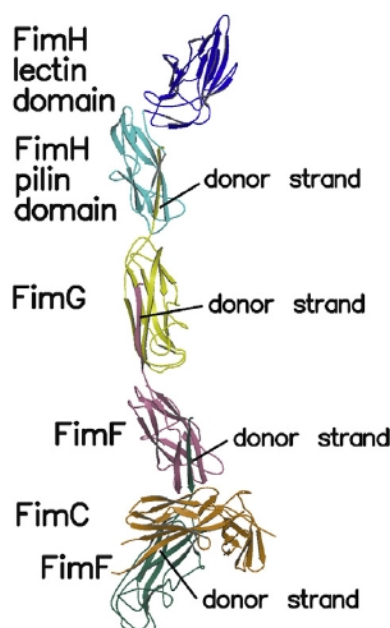


Figure 1.6 Donor strand exchange mechanism in type I fimbriae⁸⁵. The type I fimbrial domains are similar to the immunoglobulin (Ig)-like domain but lack the last β -strand. The missing β -strand of all fimbrial domains leaves a hydrophobic groove exposed to the solvent, which leads to all fimbrial subunits unstable unless they interact with the chaperone in periplasm or a complementary β -strand is donated by the N-terminal extension of the following subunit in outer membrane. After fimbrial subunits interacting with the chaperone, the chaperone-subunit complexes interact with user and then the subunits translocate across the outer membrane, contributing to the fimbrial assembly.

1.5.4 Non-fimbrial adhesins in EHEC

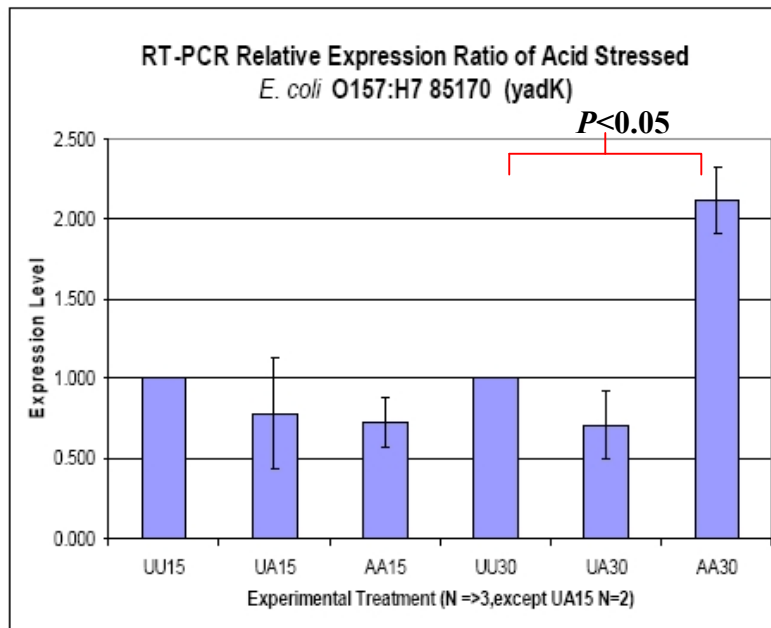
As described above, the bacterial adhesins play an essential role in the adhesion of bacteria to host cells. In addition to fimbriae adhesins, of EHEC O157:H7 also encode a number of the non-fimbrial adhesions⁴⁷, such as EHEC factor for adherence (Efa), IrgA homologous adhesin (Iha) and Intimin.

The role of *efa* was first identified in the transposon mutant of a Shiga-toxin producing EHEC clinical isolate of serotype O111:H⁻, which lost the adhesion to Chinese hamster ovary (CHO) cells⁸⁷. When a truncated *efa-1* gene was cloned in EHEC EDL933 or Sakai strains, the adhesion of these bacterial strains to human epithelial cells was impaired⁸⁸. Transformation of non-pathogenic *E. coli* with *iha* confers an increased adhesion of these *E. coli* on human epithelial cells, suggesting the role of Iha in the bacterial adhesion⁸⁹. In EHEC, intimin is responsible for the intimate attachment of bacteria to host cells and the *eae* gene which encodes intimin, is located in the LEE of bacterial chromosomes⁷.

1.6 YadK: a putative fimbrial protein

Previous microarray studies in our lab found that the expression of *yadK* gene from locus 2 fimbrial operon in EHEC, exhibited 5.87-fold increase after exposure to acid stress³. Amino acid analysis predicted YadK to be a putative fimbrial adhesin of EHEC. Increased expression of *yadK* mRNA in acid-adapted acid stress was subsequently confirmed by quantitative Real-Time PCR (RT-PCR), suggesting that this *yadK* gene is involved in the EHEC response to acid stress⁹⁰ (**Fig 1.7 A**). Studies with a $\Delta yadK$ mutant in EHEC, showed that this mutant strain lost the acid-induced adhesion phenotype observed for the parent wild-type (WT) strain⁹⁰. This adhesion phenotype was restored by complementing *yadK* expression in 85-170 $\Delta yadK$ with a *yadK*-expressing vector (**Fig 1.7 B**). This suggests that *yadK* gene plays an essential role in the adhesion of acid-stressed to host cells.

A



B

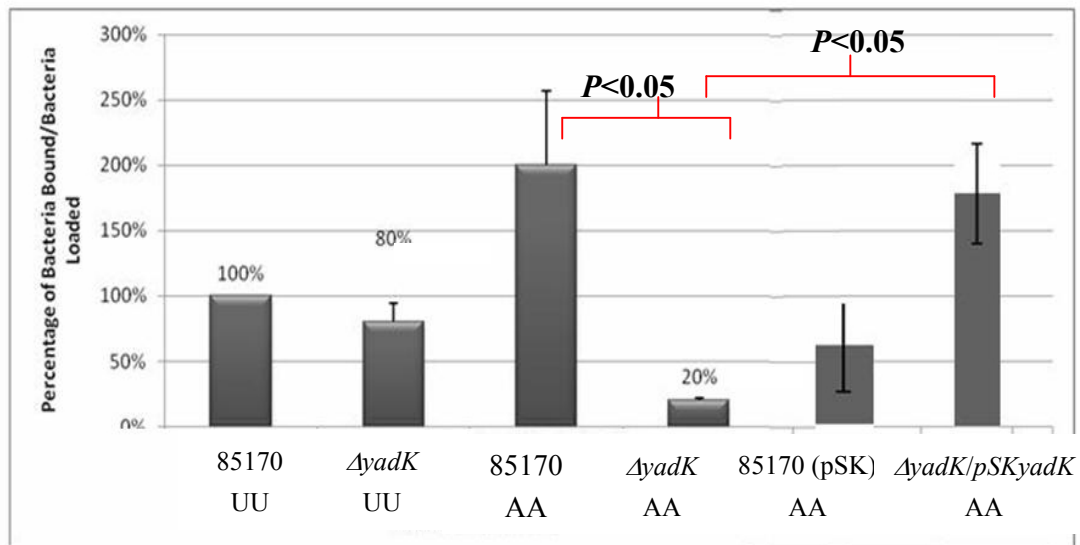


Figure 1.7 A: The *yadK* mRNA expression under no-stressed (UU) and acid-adapted acid (AA) stress⁹⁰. The mRNA expression level of *yadK* was significantly increased in AA30 compared to UU30 ($P<0.05$).

B: Adhesion of EHEC wild type and $\Delta yadK$ under stress condition⁹⁰. The adhesion of the $\Delta yadK$ mutant cells was significantly reduced compared to 85170 wild-type cells under AA; Over-expression of *yadK* in $\Delta yadK$ mutant cells ($\Delta yadK/pSKyadK$) caused the significant increase in the adhesion of these mutant cells under acid-adapted acid stress. The data represents the mean of three independent experiments \pm standard deviation bars ($n=3$ per group)⁹⁰.

The *yadK* gene is located in the locus 2 fimbrial operon of EHEC and has 591bp length (**Figure 1.8**). The *yadK* gene has been identified in EHEC O157 strains, with a low degree of homology reported to *yadK* in non-virulent *E. coli* K12 strains, suggesting that YadK is a potential virulence factor in EHEC. Protein sequence analysis reveals YadK is to be a 196 amino acid protein with 21.2kDa molecular weight.

Locus 2, in which *yadK* is located, is composed of 7 transcript genes (i.e. *yadC*, *yadK*, *yadL*, *yadM*, *htrE*, *ecpD* and *yadN*)⁹¹. Interestingly, 6 of 7 Locus 2 genes were up-regulated under acid stress³ (**Figure 1.8**). The genetic organization of Locus 2 follows the similar genetic organization as other chaperone-usher fimbrial operon. The genes in Locus 2 that are involved in regulation and biosynthesis of fimbriae are contiguous. Locus 2 has one or two genes which encode regulatory factors and the other genes encode a major subunit, several minor subunits, a chaperone and an outer membrane usher⁵¹⁻⁵². **Figure 1.9A** shows the genetic organization of Type I fimbriae and Locus 2, respectively, and the *yadK* in Locus 2 is predicted to encode a minor subunit. As the fimbrial genetic order of Locus 2 is similar to that of the chaperone-usher pathway in Type I fimbriae, the subunits encoded by Locus 2 are very likely translocated from periplasmic to outer membrane through the usher HtrE with the aid of chaperone EcpD. The major subunit YadN is close to HtrE, while the YadK minor subunit may be at the tip of these putative fimbriae (**Figure 1.9 B**).

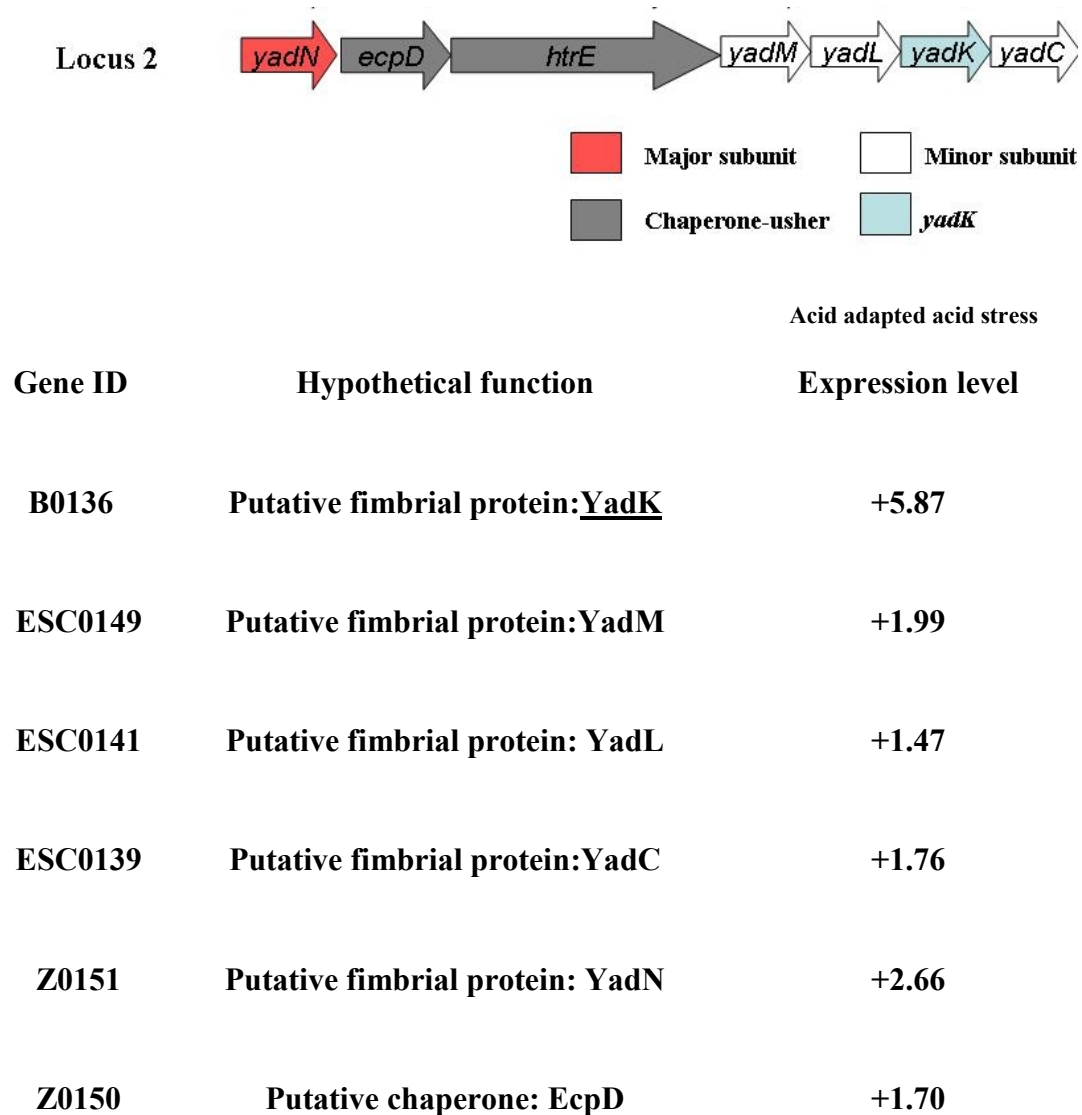
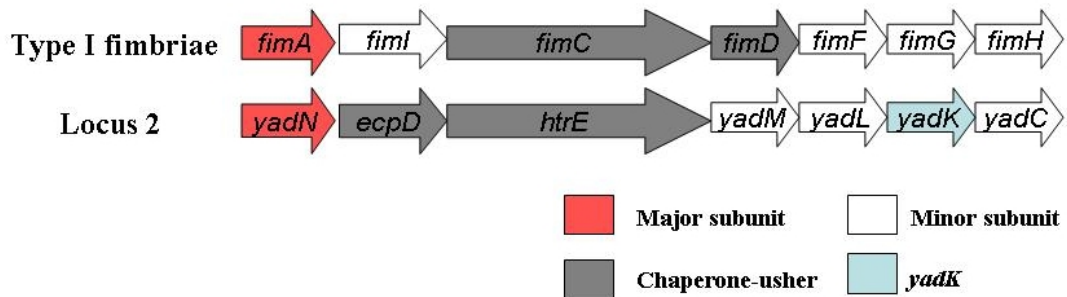


Figure 1.8 Genes in locus 2 with up-regulated transcription level on microarray chip after acid adaptation and acid stress³.

A



B

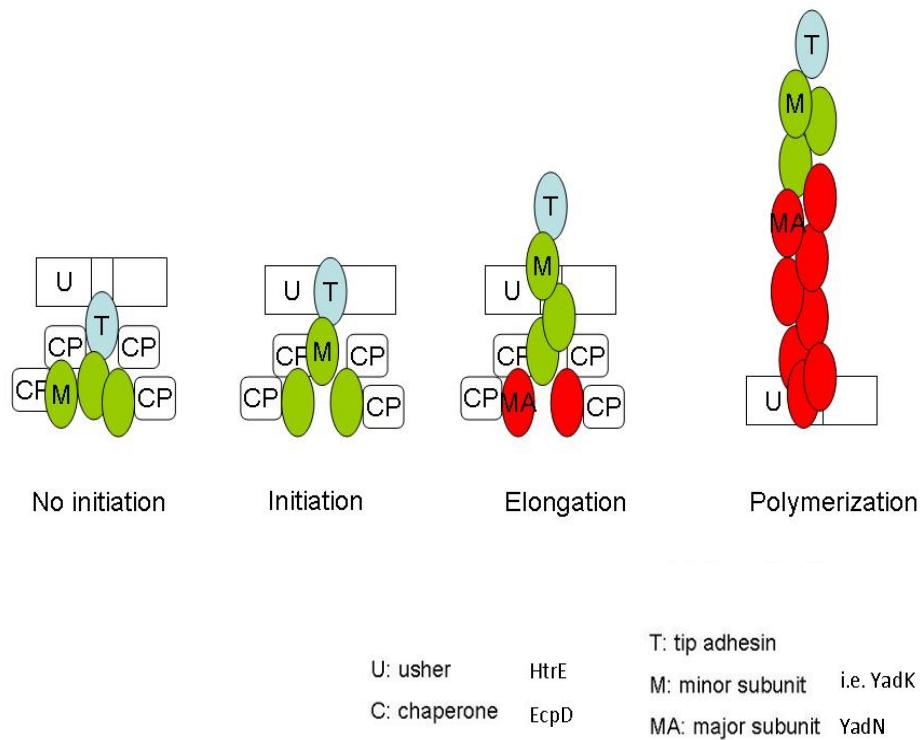


Figure 1.9 A: The genetic organization of *yadK* in Locus 2 is similar to the genetic organization of type I fimbriae⁵¹. The *yadN*, *ecpD*, and *htrE* genes encode the major structural subunit, chaperone and usher, respectively.

B: Predicted locus 2 fimbriae assembling process. The tip of adhesin is recognized by chaperone first, and forms the chaperone-subunit complex. The usher recognizes this complex and facilitate the assembly of fimbriae⁸⁶.

Several studies suggested the potential genetic regulators of *yadK* or *yad* operon, such as H-NS and AI-2^{67, 92-93}. As mentioned above, H-NS was reported to negatively regulate the fimbrial expression^{71, 94}. One microarray study revealed that gene expression of *yadN*, which encodes the major subunit in locus 2 fimbriae, was up-regulated 23-fold in *hns* mutant compared to wild type strains⁶⁷. Furthermore, the *yad* operon promoter activity in K-12 was found significantly up in *hns* mutant compared to wild type, which indicates H-NS could repress *yad* operon transcript⁹².

Autoinducer-2 (AI-2) is the only species-nonspecific autoinducer known in bacteria and is produced by both gram-positive and gram-negative organisms⁹⁵. It has been reported that AI-2 signaling is induced by acidic shock in probiotic strains of *Lactobacillus*⁹⁶. DNA microarray studies suggested that *yadK* was strongly regulated by AI-2 expression, identifying *yadK* as one of the genes that respond to AI-2 signaling activity⁹³. The expression of *yadK* and *yadN* was increased by 3.8 and 3.5-fold in the EHEC WT strain, respectively, when a higher AI-2 concentration was present in the culture media⁹³. Studies with ground beef extracts also found that the presence of AI-2 could enhance the expression of *yadK* in EHEC⁹⁷.

1.7 Rationale:

The adhesion process is an essential step for the virulence of pathogenic *E. coli*. Previous studies have demonstrated that the expression of *yadK* is significantly

up-regulated in acid stressed EHEC relative to unstressed EHEC, and that disruption of the *yadK* gene result in loss of the acid-induced adhesion phenotype observed in wild type EHEC. These data strongly suggest that the YadK protein, purported to be a fimbrial protein, functions as a subunit of an acid-induced EHEC fimbrial structure. However, there is no evidence to date that acid stress up-regulates YadK protein, and that the YadK protein participates in acid-induced adhesion of EHEC to host cells.

1.8 Hypothesis:

Acid stress up-regulates expression of the putative fimbrial protein YadK, and YadK protein plays a role in the acid-induced adhesion of EHEC to host cells.

1.9 Thesis Objectives:

I: Generation and purification of recombinant YadK protein and subsequent anti-YadK antibodies production.

In order to investigate the role of YadK protein in EHEC pathogenesis, the recombinant vectors carrying *yadK* gene were constructed and then transformed into BL21 (DE3) cells. YadK protein expression was induced and purified through the affinity chromatography technique. Then the purified YadK proteins were used to immunize a rabbit to generate anti-YadK polyclonal antibodies. The specificity of polyclonal antibodies against YadK was assayed by Western blotting.

II: Determination of the YadK protein expression under various culture conditions

EHEC and $\Delta yadK$ deletion mutants were cultured under acid-adapted acid or no-acid stress conditions, respectively. The expression level of YadK protein in EHEC under different acid stress treatment was quantified by Western blotting, using Image J program to compare band intensities relative to a standardized loading control.

III: Effects of anti-YadK antiserum on the EHEC adhesion to host cells.

Acid-adapted acid treated EHEC or unstressed EHEC were pre-incubated with anti-YadK antiserum before incubation with human epithelial cells. The adhesion of EHEC under various stresses to host cells was then examined.

2. Materials and Methods

2.1 Bacteria strains and growth conditions

All bacterial strains used in this study were listed in **Table 2.1**. Luria-Bertani (LB) agar plates (1% tryptone (EMD, Mississauga, ON, Canada); 0.5% yeast extract (VWR International, Mississauga, ON, Canada); 0.5% sodium chloride (EMD INC, Mississauga, ON, Canada); 1.5% agar (VWR International, Mississauga, ON, Canada)) with or without antibiotics (100 µg/mL of kanamycin (Sigma, Oakville, ON, Canada) or 100 µg/mL ampicillin (Sigma, Oakville, ON, Canada)) were used to subculture bacteria cells from glycerol stocks. A single isolated colony for each strain was cultured in 10 mL of LB broth (with or without antibiotics) at 37 °C for 16-18 h with agitation. All strains carrying the λ -red vector pKD46 (*Salmonella* (pKD46) and EDL933 (pKD46), Clontech, Mountain View, CA)) were grown at 30 °C, as the plasmid was sensitive to high temperature (above 35 °C).

2.2 Cell culture

The human epithelial cell line, HEp-2 (ATCC), which was used in the earlier adhesion studies, was cultured in Minimal Essential Media 1x Eagle's (MEM) (Wisent, ST-BRUNO, Quebec, Canada; with Earle's salts and L-glutamine) incubation at 37 °C and 5% CO₂, in the presence of gentamycin (Sigma, Oakville, ON, Canada) (20 µg/mL) and 10% fetal bovine serum (FBS, Wisent, ST-BRUNO, Quebec, Canada). The passage of the cultured HEp-2 cells was performed every 7 days.

Table 2.1 List of bacterial strains used in this study.

Strains	Description	Kan ^R	Amp ^R	<i>yadK</i> (EHEC)	Reference
BL21 (DE3)	<i>E. coli</i> carrying a lambda DE3 prophage	–	–	–	Ref. 98
EDL933	EHEC O157:H7	–	–	+	Ref. 99
85-170	EHEC O157:H7 derivative of 84-289 that spontaneously mutated in the laboratory	–	–	+	Ref.100
EDL933(pKD46)	EHEC transformed with λ -red plasmid pKD46	–	+	+	This Study
85-170 $\Delta yadK$	<i>yadK</i> deletion mutant of 85-170	+	–	–	Ref. 90
BL21(DE3) (pET23d-<i>yadK</i>)	BL21(DE3) transformed with pET23d- <i>yadK</i> construct	–	+	+	This Study
BL21(DE3) (pGEX-4T3-<i>yadK</i>)	BL21(DE3) transformed with pGEX-4T3- <i>yadK</i> construct	–	+	+	This study
EDL933 $\Delta yadK$	<i>yadK</i> deletion mutant in EDL933	+	+	–	This study
85-170 $\Delta yadK$/pGEX-4T3-<i>yadK</i>	85-170 $\Delta yadK$ transformed with pGEX-4T3- <i>yadK</i> construct	+	+	+	This study
85-170 $\Delta yadK$/pBlueSK-<i>yadK</i>	85-170 $\Delta yadK$ transformed with pBlueSK- <i>yadK</i> construct	+	+	+	Ref. 90
85170 (pMC1403)	85170 transformed with pMC1403	+	–	+	This study
85170 (pMC1403-PyadN)	85170 transformed with promoter <i>yadN</i> construct	+	–	+	This study

2.3 Plasmid purification

Plasmid (pET23d or pGEX-4T3; **Table 2.2**) was extracted from stock strains for colony construction, using a plasmid preparation kit and following the manufacturers' instructions (Fermentas, Burlington, ON, Canada) (**Figure 2.1**). An overnight culture of each strain was grown at 37 °C with agitation. A 2 mL overnight culture was pelleted in a 1.5 mL microcentrifuge tube by centrifugation at 12000 g for 1 min. The supernatant was discarded and 250 µL of the Re-suspension Solution (Fermentas, Burlington, ON, Canada) was used to re-suspend the pellet. 250 µL of Lysis Solution (Fermentas, Burlington, ON, Canada) and 350 µL Neutralization Solution (Fermentas, Burlington, ON, Canada) were added to the suspension and mixed gently. The suspension was pelleted by centrifugation at 12000 g for 5 min. The supernatant was transferred to the supplied GeneJET™ spin column and discarded after centrifugation. The column was washed twice with 500 µL Wash Solution (Fermentas, Burlington, ON, Canada). Finally, 50 µL Elution Buffer (Fermentas, Burlington, ON, Canada) was used to elute plasmid DNAs that were then stored at -20 °C for future use.

Table 2.2 List of plasmids used in this study.

Vectors	Antibiotics R	Restriction Enzyme	Description
pET23d	Amp ^R	BamHI, HindIII	N-terminal T7-tag C-terminal His-tag
pGEX-4T3	Amp ^R	BamHI, XhoI	N-terminal GST-tag
pKD4	Kana ^R	-	Containing kanamycin cassette
pKD46	Amp ^R	Sall	λ Red recombinant system
pMC1403	Amp ⁺	BamHI, EcoRI	Containing a promoter-less LacZ

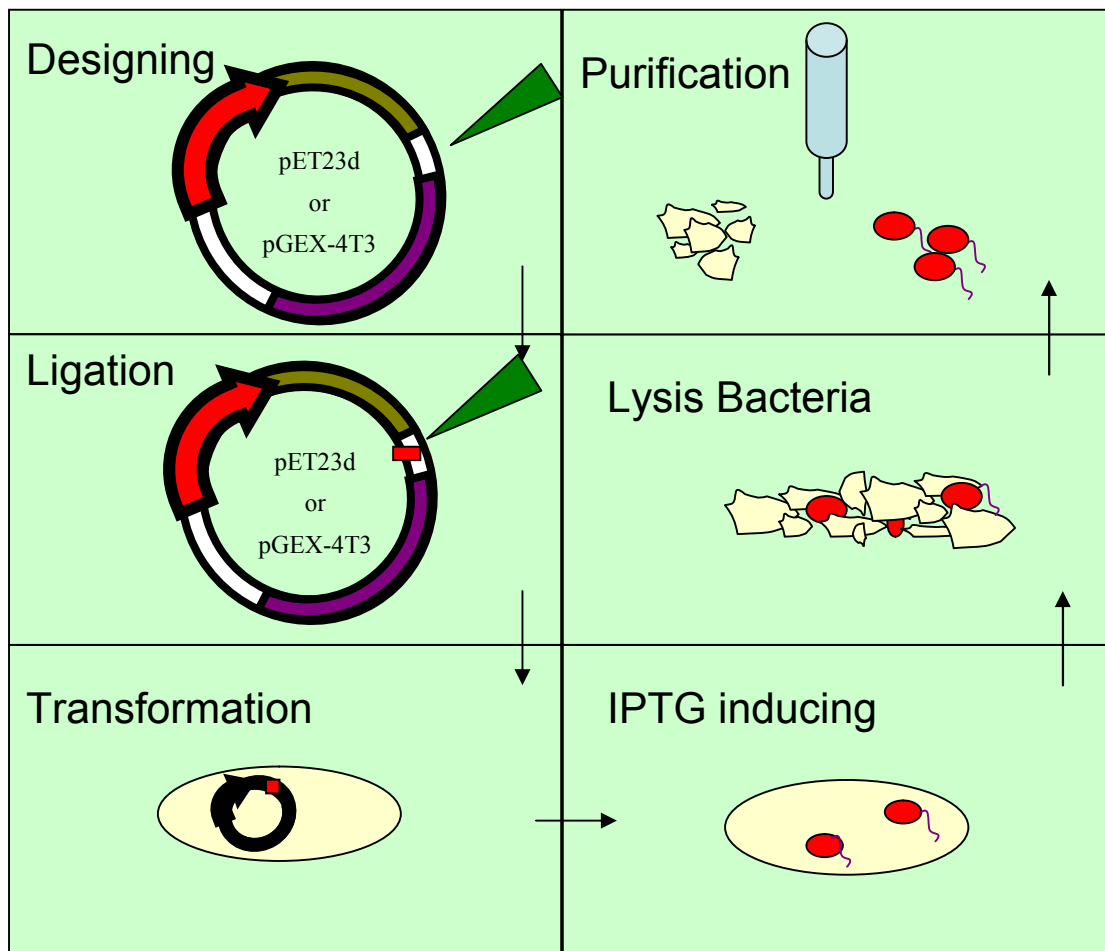


Figure 2.1 Molecular cloning constructs and protein purification procedure in this study. (Designing: Vectors and digestion sites selection).

■ indicates *yadK* gene; ▲ indicates multiple cloning site; ● indicates YadK protein; ~ indicates tag (GST or His).

2.4 PCR analysis

The primers used for cloning construction in this study are listed in **Table 2.3**. PCR reactions were performed as: 2.5 μL 10x Taq reaction buffer (Fermentas, Burlington, ON, Canada), 0.125 μL forward primer (final concentration: 10 mM), 0.125 μL

reverse primer (final concentration: 10 mM), 2 μ L of 10mM dNTP mix (Deoxynucleotide, UBI Bioinformatics, Saskatoon, SK, Canada), 0.5 μ L DNA template, 0.5 μ L of 5 U/ μ L low-fidelity Taq polymerase (Fermentas, Burlington, ON, Canada) and 18.25 μ L of sterile nuclease-free water (Gibco, Burlington, ON, Canada). All PCR reactions were performed in a 96-well Bio-Rad PCR machine. 20 μ L PCR products were resolved on 1 % agarose gels and visualized under UV light.

Table 2.3 Primers used for PCR in this study

Primer Name	Sequence (5' – 3')	Tm °C	Target Gene
T7 <i>yadK</i> full-F-BamHI	5' AAGGATCCGAATGCTATGCAGGCATCAT 3'	61.7	EDL933 <i>yadK</i>
H6 <i>yadK</i> R-HindIII	5'GCAAGCTTTTCGTAAGATACGTTAACAATAAC 3'	57.0	EDL933 <i>yadK</i>
pGEX <i>yadK</i> full_F-BamHI	5' ATGGATCCATGCTATGCAGGCATCAT 3'	61.7	EDL933 <i>yadK</i>
pGEX- <i>yadK</i> _R-XhoI	5' CGCTCGAGTTATTCGTAAGATACGTTAACAAT 3'	60.9	EDL933 <i>yadK</i>
<i>yadK</i> _F-Red recombination	5'CTGTCAGGTTGAAGTCAGTAATAATGGCGTTGTCGATCTCGTGTAGGCTGGAGCTGCTTC 3'	77.1	<i>kan^R</i> cassette pKD4/ <i>yadK</i>
<i>yadK</i> _R-Red recombination	5'GGTGCTACCGAATAAATTGCTGTTGAGGAACCATCCGTTTCATGGGAATTAGCCATGGTCC 3'	76.4	<i>kan^R</i> cassette pKD4/ <i>yadK</i>
forward EcoRI <i>pyadN</i>	5'CGCGAATTCGCATTACGATATGAAGAATCGC 3'	63.4	<i>yadK</i> promoter region
reverse BamHI <i>pyadN</i>	5'CGGGGATCCCATAACCAGAGCGGCTGC 3'	69.1	<i>yadK</i> promoter region
EcoRI <i>pyadK</i>	5'CCGAATTCAAGTCATCGCTACACTGATTGCTACT3'	61.8	<i>yadK</i> promoter region
BamHI <i>pyadK</i>	5'ACGGATCCCCACATCCTGGCCGGAATAGGCAA3'	62.8	<i>yadK</i> promoter region
EcoRI <i>pyadM</i>	5' CGGAATTCTTAATCAACGCCCTAGGT 3'	64.6	<i>yadK</i> promoter region
BamHI <i>pyadM</i>	5'TTGGATCC TAAACCCAGGCCTATTAAC3'	61.5	<i>yadK</i> promoter region

2.5 Preparation of chemically competent cells

A single isolated colony of DH5 α or BL21(DE3) (gift from Dr. Roberto Botelho's lab, Ryerson University, Toronto, ON, Canada) strain was grown in 10 mL LB overnight at 37 °C with agitation. The next day, the overnight culture was diluted at 1:100 into fresh LB and re-cultured at 37°C with agitation until the optical density (OD₆₀₀) reached 0.4. The cells were briefly chilled on ice for 10 min and harvested at 3500 rpm for 5 min at 4 °C. The cell pellets were re-suspended with 10 mL cold CaCl₂ solution (60 mM CaCl₂ (EMD, Mississauga, ON, Canada), 15% glycerol (EMD, Mississauga, ON, Canada) and 10 mM PIPES (VWR International, Mississauga, ON, Canada); filter sterilized and stored at 4 °C), and were centrifuged at 2500 rpm for 5 min at 4 °C. The supernatant was discarded and the cell pellets were re-suspended in 10 mL ice-cold CaCl₂ solution, and chilled on ice for 30 min. The cells were re-suspended in 2 mL ice-cold CaCl₂ solution and stored at -80 °C for future use.

2.6 Restriction enzyme digestion

Plasmid pET23d and PCR product (*yadK* amplified from EDL933 genomic DNA with T7*yadK*-full-F-BamHI and H6*yadK*-R-HindIII primers) were digested with BamHI and HindIII restriction enzymes (Fermentas, Burlington, ON, Canada). Briefly, 5 μ L of a DNA sample (pET23d plasmid or PCR product as above) was mixed with 2 μ L of 10X BamHI buffer (Fermentas, Burlington, ON, Canada) and 11.5 μ L of nuclease-free water. 0.5 μ L of BamHI and 1 μ L of HindIII were added the

reaction, followed by incubation in 37 °C water bath for 1 h. For pGEX construct preparation, 5 µL of DNA sample (pGEX plasmid or *yadK* amplified from EDL933 genomic DNA with pGEX-*yadK*-F-BamHI and pGEX-*yadK*-R-XhoI primers) was mixed with 2 µL of 10X BamHI buffer (Fermentas, Burlington, ON, Canada) and 11.5 µL of nuclease-free water (Gibco, Burlington, ON, Canada). Then 0.5 µL of BamHI and 1 µL of XhoI were added.

2.7 Gel extraction

After double digestion, the digested DNA sample was loaded on the 1 % agarose gel (VWR International, Mississauga, ON, Canada). The specific section of the gel containing the DNA band of interest was collected under UV light. The gel slice was weighted and transferred into a microcentrifuge tube for DNA extraction using gel extraction kit (Qiagen, Toronto, ON, Canada). The eluted pure DNA products were confirmed on 1 % agarose gel and then stored at -20 °C.

2.8 Ligation

The purified vector DNA (clean double-digested plasmid) was mixed with DNA of interest (clean double-digested PCR product) at the 1:3 ratio, following the manufacturers' suggestions. The 4 µL 5X buffer and 1 µL ligase (Fermentas, Burlington, ON, Canada) were added to the mixture (rapid DNA ligation kit; Fermentas, Burlington, ON, Canada), followed by the incubation at room temperature for less than 1 h. The ligation products could be stored at 4 °C overnight before transformation of the competent cells.

2.9 Transformation of chemically competent cells

The 5 μ L ligation product was added to 50 μ L of chemically competent (DH5 α) cells, and mixed gently on ice. The cells were chilled on ice for 30 min and then heat shocked at 42 °C for 30 s, followed by the room temperature recovery for 2 min. Then the competent cells were cultured in 1 mL SOC medium (0.5% yeast extract, 2 % tryptone, 10 mM NaCl, 2.5 mM KCl (VWR International, Mississauga, ON, Canada), 10 mM MgCl₂ (VWR International, Mississauga, ON, Canada), 10 mM MgSO₄ (VWR International, Mississauga, ON, Canada) and 20mM glucose (VWR International, Mississauga, ON, Canada)) at 37 °C with 220 rpm agitation. After 1 h incubation, 200 μ L mixtures were plated on LB agar supplemented with antibiotics for overnight growth at 37 °C. Successful transformants were re-plated on fresh LB plates with antibiotics on the next day. The presence of plasmid construct from colonies that grew in the presence of antibiotics plates was confirmed through DNA sequencing (ACGT Company, Toronto, ON), and then transformed into BL21(DE3) cells (gift from Dr. Roberto Botelho's lab at Ryerson University, Toronto, ON, Canada) for protein expression⁹⁸.

2.10 YadK protein over-expression

A single isolated colony of BL21 (DE3)/pET23d-*yadK*, 85170 Δ *yadK*/pGEX-4T3-*yadK* or 85170 Δ *yadK*/pBlueScriptSK-*yadK* strains was incubated in fresh LB broth (with selective antibiotics) and cultured overnight at 37°C with agitation (225 rpm). The next day, the cultured bacteria were diluted 1:100 into fresh LB (with selective antibiotics) and re-cultured at 37 °C with agitation until OD₆₀₀

approximated 0.6. IPTG (VWR International, Mississauga, ON, Canada) (final concentration: 1 mM) was then added to induce YadK protein expression. Then 1 mL culture cells were collected every hour to assay the time-dependent protein expression level. The 5 mL culture without adding IPTG was used as negative control.

2.11 SDS-PAGE, Coomassie blue staining and Western blotting

1x SDS-PAGE Running Buffer (25 mM Tris-HCl, 200 mM Glycine and 0.1 % (w/v) SDS (VWR International, Mississauga, ON, Canada)) and 1x transfer buffer (200 mL methanol (VWR International, Mississauga, ON, Canada), 100 mL of 10 x running buffer and 700mL H₂O) were prepared, respectively. The protein concentrations of samples were measured by Bio-Rad protein assay (Bio-Rad, Mississauga, ON, Canada). All samples were boiled with 5x sample loading buffer (10 % w/v SDS, 10 mM beta-mercapto-ethanol, 20 % v/v Glycerol, 0.2 M Tris-HCl of pH 6.8 and 0.05 % w/v Bromophenolblue (Bioshop, Burlington, ON, Canada)) and separated by 12% SDS-PAGE gel (0.02 mL TEMED, 7.5 mL of 1.5 M Tris-HCl at pH 8.8, 0.15 mL of 20% (w/v) SDS, 12.0 mL Acrylamide/Bis-acrylamide (30%/0.8% w/v) (Bioshop, Burlington, ON, Canada), 0.15 mL 10% (w/v) ammonium persulfate (APS) (Bioshop, Burlington, ON, Canada) and 10.2 mL H₂O). For coomassie blue staining, SDS-PAGE gel was stained in Coomassie blue staining solution (0.1 % coomassie brilliant blue R-250 (Bioshop, Burlington, ON, Canada), 50 % methanol and 10 % acetic acid) for 20 min at room temperature. Destaining solution (40 % methanol, 10 % acetic acid and 50 % H₂O) was used to wash the gel 1 h until background of the gel

is fully destained; For Western blotting, protein bands without Coomassie blue staining were transferred from the gel to polyvinylidene fluoride membranes (Millipore, Mississauga, ON, Canada). The membrane was blocked with 5 % milk in 1xTBST (50 mM Tris Base, 0.9% NaCl, pH7.4, 1% Tween-20) for 1 h at room temperature. The membranes were incubated with primary antibodies overnight at 4 °C, followed by incubation with secondary antibodies for 1h at room temperature. The primary antibodies are diluted in 1xTBST as follows: 1:1000 with anti-His antibodies (GE healthcare, Toronto, ON, Canada), 1:1000 with anti-GST70K antibodies¹⁰¹ (gift from Dr. Clifford Lingwood's lab at Hospital for Sick Children, Toronto) and 1:400 with anti-YadK antibodies, respectively; the secondary antibodies are diluted in 1xTBST as follows: 1:10000 with horseradish peroxidase (HRP)-conjugated goat anti-mouse antibodies (Bio-Rad, Mississauga, ON, Canada), 1:30000 with alkaline phosphatase-conjugated goat anti-rabbit antibodies (Sigma, Oakville, ON, Canada) and 1:10000 with HRP-conjugated goat anti-rabbit antibodies (Bio-Rad, Mississauga, ON, Canada), respectively. The ECL kit (GE healthcare, Toronto, ON, Canada) and X-ray film (GE healthcare, Toronto, ON, Canada) were used to detect the fluorescent signaling.

2.12 Protein extraction from BL21 (DE3)

The 50 mL of IPTG-induced BL21(DE3)/pET23-*yadK* culture were centrifuged and the pellet was re-suspended in lysis buffer (50 mg/mL lysozym (VWR International, Mississauga, ON, Canada), 1 mg/mL DNase (VWR International, Mississauga, ON,

Canada), 75 mM NaCl, 0.5 M MgCl₂ and 25 mM Tris at PH 8.0) for 30min on ice, followed by sonication at 50 % cycle for 15 min. Soluble and insoluble fractions of BL21 lysates were separated by centrifuging at 4000 rpm for 10min at 4 °C, and boiled with the sample loading buffer, respectively. Then the samples could be stored at -20 °C for future study.

2.13 Isolation of proteins from inclusion bodies

As described above, the insoluble protein fraction could be acquired from the IPTG-induced BL21(DE3)/pET23-*yadK* lysates. The insoluble protein fraction was then re-suspended in 1x phosphate buffer (GE healthcare, Toronto, ON, Canada) containing detergents (1 % Triton X-100 (VWR International, Mississauga, ON, Canada), 1 % Tween-20 (VWR International, Mississauga, ON, Canada) or 1 % SDS, respectively) for 30 min on ice. Soluble and insoluble proteins were separated by centrifugation at 4000 rpm for 10 min (4 °C). Soluble protein in 1 % SDS of 1x phosphate buffer was diluted with 1x phosphate buffer to decrease detergents concentration (till 0.02 % SDS of final concentration). 20 µL soluble samples were boiled with the sample loading buffer and stored at -20 °C for future study.

2.14 Affinity column purification

Since the recombinant YadK proteins carries a C-terminal polyhistidine tail that efficiently binds to nickel ions, affinity chromatography on nickel-nitrilotriacetic acid resin (GE healthcare, Toronto, ON, Canada) was used to purify the recombinant

YadK protein from inclusion bodies after SDS-treatment. Before purification, 10 mL of 1x binding buffer (20 mM Imidazole (VWR International, Mississauga, ON, Canada)) was used to wash the resin column (GE healthcare, Toronto, ON, Canada). The diluted soluble sample was loaded to the column and 10 mL 1x binding buffer was used to wash off the non-specifically bound samples. Finally, 3mL elution buffer (500 mM Imidazole) was used to elute T7-YadK-His proteins from the column.

Figure 2.1 represents the YadK protein purification procedure.

2.15 Anti-YadK polyclonal antibodies generation

The rabbit (purchased from Charles River Laboratories, Wilmington, MA; housed at animal vivarium of Hospital for Sick Children, Toronto, ON, Canada) was immunized with purified YadK (0.04 mg) three times at one month intervals. Blood was collected at 1 week before immunization and at 4 weeks after the 3rd immunization. Serum was isolated from clotted blood by centrifugation at 3000 rpm for 10min at 4 °C. The binding specificity of the anti-YadK in the serum was tested by Western blotting against YadK over-expressed in all of the indicated backgrounds (i.e. BL21 (DE3)/pET23d-*yadK*, 85170Δ*yadK*/pGEX-*yadK* or 85170Δ*yadK*/pSK-*yadK*). To eliminate non-specific binding of anti-YadK, three rounds of overnight incubation of anti-YadK antiserum with EDL933 Δ*yadK* bacterial lysates on the blotting membrane, followed by one round of overnight incubation of BL21(DE3)/pET23d bacterial lysates on the blotting membrane, were performed, and we named these pre-absorbed anti-YadK antiserum as anti-YadK1.

2.16 Fimbrial sample preparation

Bacteria cells were harvested by centrifuging at 3500 rpm for 5 min at 4 °C. The pellet was re-suspended in 180 µL acidic H₂O (pH 1.5) and boiled for 5 min to disassemble the pilus structures⁵⁵. Then the bacteria were boiled again for 5 min with 48 µL of 5x Sample Buffer (10 % w/v SDS, 10 mM beta-mercapto-ethanol, 20 % v/v Glycerol, 0.2 M Tris-HCl of pH 6.8 and 0.05 % w/v Bromophenolblue (Bioshop, Burlington, ON, Canada)) and 1 M NaOH.

2.17 Acid stress treatment

The acid treatment used for this study was adapted from the previously described methods⁹⁰. A single isolated colony of EHEC or EHECΔ*yadK* was grown in 10 mL LB broth (with or without 100 µg/mL kanamycin) overnight at 37 °C with agitation. The culture was diluted in 1:10 DMEM (pH 7.4) and grown at 37 °C with 5% CO₂ until OD₆₀₀ reached about 0.4-0.6. Two mL of the culture was spun down by centrifugation, and the pellet was re-suspended and re-cultured in 10 mL DMEM (pH 5) with 25 mM MES (2-(N-morpholino)ethanesulfonic acid) (Bioshop, Burlington, ON, Canada) statically at 37 °C with 5% CO₂ for 1h. After acid adaptation, the culture medium was changed to 10 mL DMEM (pH 3) for acid shocking at 37 °C with 5% CO₂ for 30 min. The cell pellets were collected by centrifugation and prepared for Western blotting. The unstressed control was prepared using 10 mL of DMEM (pH 7) with 25 mM MOPS (3-(N-morpholino) propanesulfonic acid) (VWR International, Mississauga, ON, Canada).

2.18 Preparation of electrocompetent cells

Electrocompetent EHEC and EHEC EDL933/pDK46 were used for YadK over-expression and $\Delta yadK$ mutant construct, respectively. A single isolated colony of the bacteria was cultured in to fresh 10mL LB broth (with or without antibiotics) and grown overnight at 37 °C with agitation. EDL933/pDK46 was always cultured at 30°C. The overnight culture was then diluted by 100 fold and re-cultured into fresh LB media with agitation. The bacteria were collected when an OD₆₀₀ of 0.40 was reached. The cells were briefly chilled on ice for 15 min and harvested at 4000g for 15 min at 4 °C. The cell pellet was gently re-suspended in 10 mL iced-cold sterile water and once again harvested by centrifugation. The pellet was washed with 10mL of ice-cold sterile water once and 10 mL ice-cold 10% glycerol once, respectively. The cells were harvested as above, re-suspended in 10 mL ice-cold 10% glycerol and stored at -80 °C for future use.

2.19 Bacterial adhesion to host cells

EHEC cells were initially pretreated with acid or neutral buffer as described above. Under either acid stress or unstressed treatment, EHEC cells were harvested by centrifugation at 3500 rpm for 10 min at 4°C. The pellet was re-suspended in 1mL PBS, and 300 µL of this cell solution was transferred to 1.5 mL eppendorf tubes and harvested by centrifugation. The pellet was re-suspended with either 1 mL DMEM (Wisent, ST-BRUNO, Quebec, Canada), pre-immune serum (1:50 dilution) or anti-YadK antiserum (1:50), respectively, followed by the incubation at 37°C with

agitation for 1h. The volume of bacteria to be loaded to HEp-2 cells was determined by OD₆₀₀ of bacteria.

One day before the adhesion assay experiment, HEp-2 cells were grown to 80% confluency in 25 cm² flask and diluted into MEM (Wisent, ST-BRUNO, Quebec, Canada) (with no additives) to reach a cell count of 1x10⁶ cells/mL. 500 µL of these cells were aliquoted into each well of 24-well flat bottom plates (BD Falcon, Mississauga, ON, Canada). On the day of the adhesion assay, HEp-2 cells were counted again to determine the total volume of loading bacteria. A multiplicity of infection (MOI) of ~100:1 (ratio of bacteria versus HEp-2 cells) was used for the experiments. HEp-2 cells were gently washed 3 times with 1x PBS. The appropriate volume of bacteria suspension in DMEM was added to HEp-2 cells, followed by the incubation at 37 °C with 5% CO₂ for 3-6 h. The culture media was gently removed from each well and HEp-2 cells were washed with 1x PBS after a 3 h infection period. DMEM was added to each well after washing. After a 6h infection period, HEp-2 cells and adherent EHEC cells were detached from the wells using 250µL of trypsin-EDTA (Wisent, ST-BRUNO, Quebec, Canada) for 2-3 minutes at 37°C. Serial dilutions were prepared from each sample with PBS and 15 µL of appropriate dilutions were plated on LB agar, followed by overnight culture at 37°C. The plates were quantified and the plates with 30~300 colonies were used to determine the amount of adherent bacteria.

2.20 Construction of the $\Delta yadK$ deletion mutant in EDL933

A kanamycin resistance cassette was amplified from pKD4 vector by PCR, and the PCR products were confirmed on agarose gel and subsequently purified by gel extraction. Electrocompetent EHEC EDL933/pKD46 was made fresh according to above protocol. L-arabinose (final concentration: 0.2 %) was added into the subculture to induce recombinant enzyme expression. Then 50 μ L of electrocompetent EHEC EDL933/pKD46 were transformed with 1 μ L of purified PCR product of kanamycin resistance cassette. The cells were recovered with agitation of 220rpm for 1.5 h at 30 °C. 200 μ L of the culture was plated on LB agar plates (100 μ g/mL kanamycin) and grown overnight at 37°C. Successful mutants were confirmed by PCR.

2.21 Promoter activity assay

Three predicted promoter regions (**Figure 2.2**) were selected for promoter activity assay using regulon database and compared with previous findings^{51, 92}. The promoter activity assay was modified from the protocol as previously described¹⁰².

Overnight cultures of EHEC 85170/pMC1403 or 85170/pMC1403-PyadN, 85170/pMC1403-PyadM and 85170/pMC1403-PyadK, were stressed according to the stress protocols. In brief, a single colony of an EHEC strain was inoculated in 3 mL of LB and grown overnight with shaking at 37 °C. Overnight culture media was sub-cultured into 10 mL of pre-warmed DMEM (pH 7.4) in a flask, followed by 2 h

culture. The 10 mL bacteria were transferred into 15 mL tubes, harvested at 3500 rpm for 7 min at 4 °C and re-suspended in 10 mL of pre-warmed DMEM (pH 5) and incubated statically at 37 °C with 5% CO₂ for 1 h. Then these bacteria were harvested again and the pellets were re-suspended in 10 mL pre-warmed DMEM (pH 3) and incubated statically at 37 °C with 5% CO₂ for 30 min. Then 1 mL culture was taken and spun down for pellets that were kept at -20 degree. Later, the pellets were added with 40 µL of chloroform, 20 µL 1% SDS and 1 mL Z-buffer (0.06 M Na₂HPO₄, 0.04 M NaH₂PO₄, 0.01 M KCl, 0.001 M MgSO₄ and 0.05 M beta-mercaptoethanol; stored at 4 °C). The mixture was vortexed and allowed to settle for 10 min at 30 °C. 10 µL of the bacterial supernatant and 70 µL Z-buffer were transferred to 96 well-plates. 20 µL of o-nitrophenyl-β-D-galactopyraniside (4 mg/mL suspended in Z-buffer; stored at 4°C (VWR International, Mississauga, ON, Canada)) was added to the well. The OD₄₁₄ was recorded with a plate reader and at the same time, protein concentration of bacteria extract was measured, in which 160 µL bacterial samples or bovine serum albumin standard were mixed with 40 µL Bio-Rad concentrate reagents, respectively, and kept for 5min at room temperature followed by AT OD₅₉₅ detection. The β-galactosidase activity was determined by the equation as below:

Miller Units = (1500x OD₄₂₀) / (T x ((Protein concentration x V)/1000)) where,

OD₄₁₄ is read from the reaction mixture.

T = time of the reaction in minutes.

V = volume of culture used in the assay in mLs.

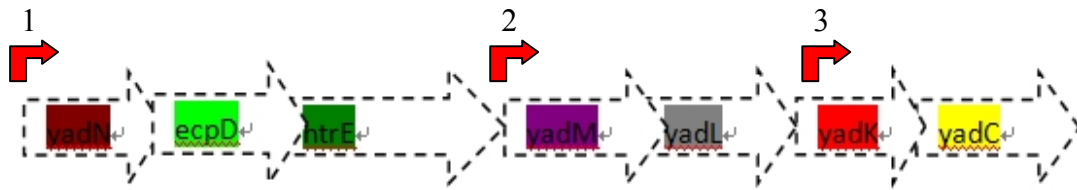


Figure 2.2. Predicted promoter regions in the locus 2.

- 1). PyadN: promoter region in front of *yadN*;
- 2). PyadM: promoter region in front of *yadM*;
- 3). PyadK: promoter region in front of *yadK*

2.22 Statistical analysis

Data in all the figures with error bars were presented as mean \pm SD. Data were analyzed using Student's t test as indicated. $P < 0.05$ was considered significant.

2.23 Image J analysis

The exposed X-ray films during Western blotting were scanned and the density of Western blotting bands was analyzed by Image J program. The ratio of density between band of interest and loading control were compared as follows:

Fold change of band intensity = (Intensity of sample band - intensity of adjacent background) / (Intensity of control band - intensity of adjacent background).

3. Results

3.1.1 Successful construction of pGEX-4T3-*yadK* vector

To establish the *yadK*-expressing vectors, the pGEX-4T3 plasmid was selected, since this plasmid contains an N-terminal GST-tag, which can be used for subsequent *YadK* protein purification. First, the *yadK* segment amplified from EDL933 was inserted into pGEX-4T3 multiple cloning sites, and then the pGEX-4T3-*yadK* vector was transformed into DH5 α competent cells, which were subsequently cultured on the Ampicillin (Amp)-positive LB plates. The plasmid DNAs were first isolated from 15 individual transformed colonies that grew on Amp⁺ plates, respectively, and then assayed by Polymerase Chain Reaction (PCR) for the presence of the *yadK* gene (**Figure 3.1.1**). One of the 15 PCR products amplified from plasmid extraction of DH5 α /pGEX-4T3-*yadK* displaying approximately 590bp band size was sequenced (**Figure 3.1.2**).

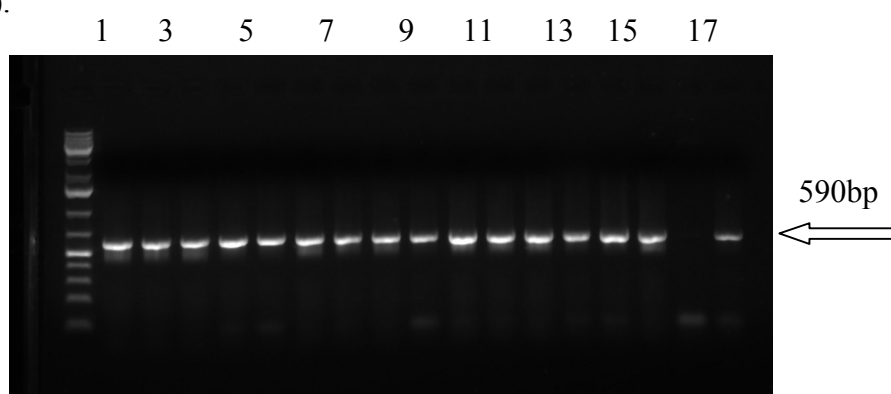


Figure 3.1.1 PCR product of full length *yadK* from DH5 α /pGEX-4T3-*yadK*. The PCR products were obtained with the use of *yadK*/BamHIF and *yadK*/XhoIR specific primers and then subjected to agarose gel electrophoresis.

1: 1 kb Ladder (Band size from top to bottom: 10kb, 8kb, 6kb, 5kb, 4kb, 3kb, 2kb, 1kb, 0.5kb)

2-16: PCR product amplified from plasmid extraction of single colonies of DH5 α /pGEX-4T3-*yadK*.

17: PCR product amplified from Negative control (pGEX-4T3).

18: PCR product amplified from Positive Control (EDL933 genomic DNA).

```

pgex-yadK      TATATAGCATGGCCITTGCAGGGCTGGCAAGCCACGTTTGGTGGTGGCGACCATCCTCCA 60
sample      -----AAGCCACGTTTGGTGGTGGCGACCATCCTCCA 32
                *****

pgex-yadK      AAATCGGATCTGGTTCGCGTGGATCCATGCTATGCAGGCATCATAAAATCGTACACTTT 120
sample      AAATCGGATCTGGTTCGCGTGGATCCATGCTATGCAGGCATCATAAAATCGTACACTTT 92
                *****

pgex-yadK      TTAGGGCTGGCAACAGCCCTTATCAGCCCTTTTGCCTATTCCGGCCAGGATGTGGATCTC 180
sample      TTAGGGCTGGCAACAGCCCTTATCAGCCCTTTTGCCTATTCCGGCCAGGATGTGGATCTC 152
                *****

pgex-yadK      ACCGCAAAGATCGTGCCAGCACCTGTGAGGTTGAAGTCAGTAATAATGGCGTTGTCGAT 240
sample      ACCGCAAAGATCGTGCCAGCACCTGTGAGGTTGAAGTCAGTAATAATGGCGTTGTCGAT 212
                *****

pgex-yadK      CTCGGCACAGTGACGCTGGACTATTTTGCAGCAATGTAACCCGACAACGGATTATGCG 300
sample      CTCGGCACAGTGACGCTGGACTATTTTGCAGCAATGTAACCCGACAACGGATTATGCG 272
                *****

pgex-yadK      GGTTGGCAAACGTTTAAATGTGAATGTGGTCTCTTGCAGTAACATTCAAACGACACAGTCG 360
sample      GGTTGGCAAACGTTTAAATGTGAATGTGGTCTCTTGCAGTAACATTCAAACGACACAGTCG 332
                *****

pgex-yadK      CAAATGAAATTAGATTTTCAGCCGAGGCGGGATCGCTTGACAGGCGAATAATCAAATT 420
sample      CAAATGAAATTAGATTTTCAGCCGAGGCGGGATCGCTTGACAGGCGAATAATCAAATT 392
                *****

pgex-yadK      TTTAGTAATGAATATGAACAGCAGGCTACCGGGGCGAAAAACGTCGGCATTGTGATTTTT 480
sample      TTTAGTAATGAATATGAACAGCAGGCTACCGGGGCGAAAAACGTCGGCATTGTGATTTTT 452
                *****

pgex-yadK      TCGGCCCAACCGAATCAGCAGACATTTAACGTGCGAGGAACGGATGGTTCTCAACAGCA 540
sample      TCGGCCCAACCGAATCAGCAGACATTTAACGTGCGAGGAACGGATGGTTCTCAACAGCA 512
                *****

pgex-yadK      ATTTATTCGGTAGCACCTGGCAATGCTGTTCCCTCAACCTGGACCTTTTATCCCGTATG 600
sample      ATTTATTCGGTAGCACCTGGCAATGCTGTTCCCTCAACCTGGACCTTTTATCCCGTATG 572
                *****

pgex-yadK      CAGCGGGTGAATAATGCCCTTCTCCTGAATCGGGAATGGTGAGAAGCCAGGTTATTGTT 660
sample      CAGCGGGTGAATAATGCCCTTCTCCTGAATCGGGAATGGTGAGAAGCCAGGTTATTGTT 632
                *****

pgex-yadK      AACGTATCTTACGAATAACTCGAGCGGCCGCATCGTGACTGACTGACGATCGCTCGCG 720
sample      AACGTATCTTACGAATAACTCGAGCGGCCGCATCGTGACTGACTGACG----- 680
                *****

pgex-yadK      CGTTTCGGTGATGACGGTGAAAACCTCTGACACATGCAGCTCCCGGAGACGGTCA 775
sample      -----

```

Figure 3.1.2 Representative gene sequencing result of *yadK* amplified from DH5 α /pGEX4T3-*yadK*. Sequence alignment was performed through ClustalW2 blast program, and the alignment result demonstrated that *yadK* with correct sequence was amplified from DH5 α /pGEX4T3-*yadK*. **pGEX-*yadK*** indicates pGEX sequence and *yadK* gene from EDL933; **sample** indicates sequence from plasmid in DH5 α /pGEX-4T3-*yadK*.

3.1.2 GST-YadK was expressed in inclusion bodies in BL21 (DE3)

To express the YadK protein in vitro, the purified pGEX-4T3 vector carrying the correct *yadK* gene sequence was transformed into BL21 (DE3) competent cells. The plasmid DNA was isolated from individual clones that grew on Amp⁺ plates and tested for the presence of *yadK* gene. Then, the BL21 (DE3) cells containing the pGEX-4T3-*yadK* vector were cultured, and IPTG was used to induce the expression of GST-YadK fusion protein.

The GST-YadK (48KDa) protein expression was first assayed by Coomassie blue staining of SDS-PAGE gel, which revealed that the GST-YadK protein expression reached the peak level around 4h after IPTG induction (**Figure 3.1.3**). Then the specificity of the GST-YadK protein was assayed by anti-GST-70K by Western blotting (**Figure 3.1.4**).

After the lysis of BL21 bacteria, Western blotting further revealed that most of GST-YadK protein was found in the insoluble fraction (**Figure 3.1.5**), and almost no GST-YadK was detectable in the soluble fraction (**Figure 3.1.6**).

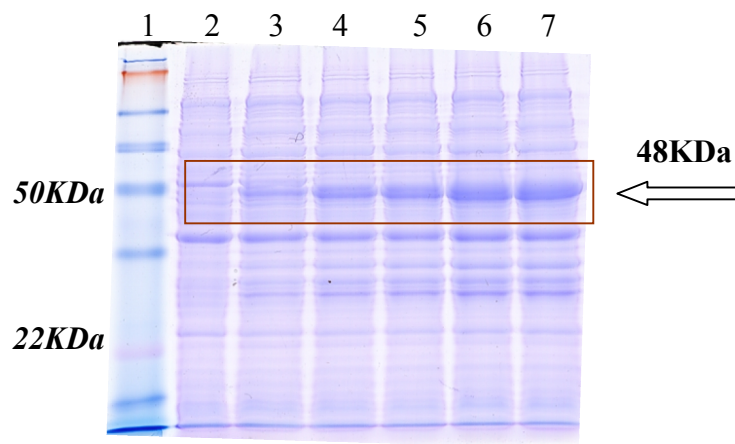


Figure 3.1.3 Coomassie blue staining of BL21(DE3) and BL21(DE3)/pGEX4T3-*yadK* lysate on SDS-PAGE gel. Approximately 20 μ g of BL21(DE3)/pGEX4T3-*yadK* lysate before or after IPTG induction were subjected to SDS-PAGE, followed by Coomassie blue staining. The protein staining result suggested that GST-YadK (48KDa) expression in BL21(DE3)/pGEX4T3-*yadK* was induced by IPTG (final concentration: 1mM).

1: Ladder (Band size from top to bottom: 250KDa, 148KDa, 98KDa, 64KDa, 50KDa, 36KDa, 22KDa, 16KDa and 6KDa). **2:** BL21(DE3) lysate;

3: BL21(DE3)/pGEX-4T3-*yadK* lysate before IPTG induction.

4-7: BL21(DE3)/pGEX-4T3-*yadK* lysate at 1h, 2h, 3h, 4h after IPTG induction.

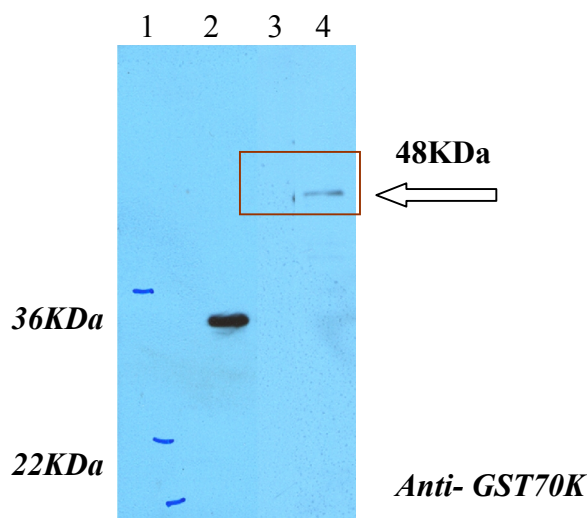


Figure 3.1.4 Western blotting of GST and BL21(DE3)/pGEX4T3-*yadK* with anti-GST70K antibodies. Approximately 20 μ g of BL21(DE3)/pGEX4T3-*yadK* lysate before or after IPTG induction were subjected to SDS-PAGE, followed by Western blotting with 1:1000 diluted anti-GST70K (1st antibody) and 1:10000 diluted HRP-conjugated goat anti-rabbit (2nd antibody) antibodies. The blotting result demonstrated that GST-YadK (48KDa) expression in BL21(DE3)/pGEX4T3-*yadK* was successfully induced by IPTG induction (final concentration: 1mM). **1:** Ladder (Band size from top to bottom: 36KDa, 22KDa and 16KDa). **2:** GST protein (28KDa; positive control).

3: BL21 (DE3)/pGEX-4T3-*yadK* lysate before IPTG induction.

4: BL21 (DE3)/pGEX-4T3-*yadK* lysate at 4h after IPTG induction.

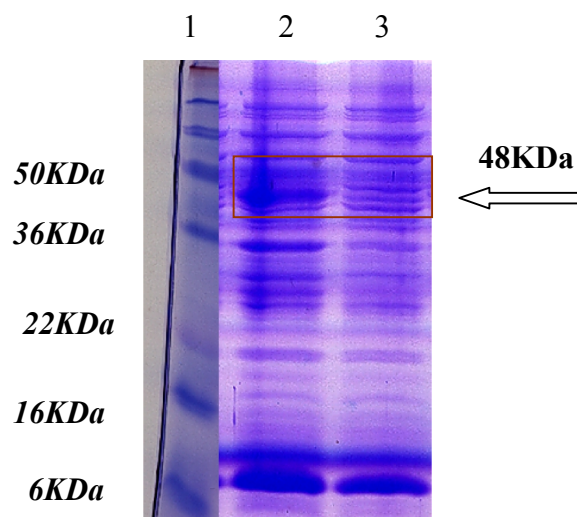


Figure 3.1.5 Coomassie blue staining of soluble and insoluble fraction of BL21(DE3)/pGEX4T3-*yadK* lysate. Approximately 20 µg of the insoluble and soluble protein fractions of BL21(DE3)/pGEX4T3-*yadK* (after IPTG induction (final concentration: 1mM)) lysate were subjected to SDS-PAGE, followed by Coomassie blue staining. The protein staining result suggested that GST-YadK fusion protein (48KDa) was mainly expressed in insoluble fraction.

1: Ladder (Band size from top to bottom: 250KDa, 148KDa, 98KDa, 64KDa, 50KDa, 36KDa, 22KDa, 16KDa and 6KDa).
2: Insoluble fraction of BL21 (DE3)/pGEX-4T3-*yadK* IPTG at 4h after IPTG induction; **3:** Soluble fraction of BL21 (DE3)/pGEX-4T3-*yadK* IPTG at 4h after IPTG induction.

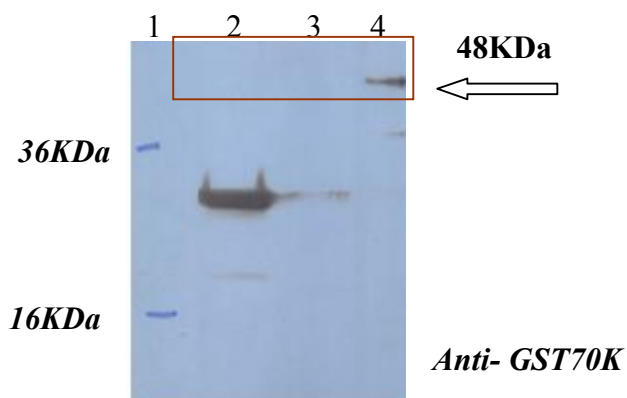


Figure 3.1.6 Western blotting of soluble and insoluble fraction of BL21(DE3)/pGEX4T3-*yadK* lysate. Approximately 20 µg of the insoluble and soluble protein fractions of BL21(DE3)/pGEX4T3-*yadK* (after IPTG induction (final concentration: 1mM)) lysate were subjected to SDS-PAGE, followed by Western blotting with 1:1000 diluted anti-GST70K (1st antibody) and 1:10000 diluted HRP-conjugated goat anti-rabbit (2nd antibody) antibodies. The blotting result further confirmed that GST-YadK fusion protein (48KDa) was mainly expressed in the insoluble fraction.

1: Ladder (Band size from top to bottom: 36KDa, 16KDa).
2: GST protein (28KDa; positive control).
3: Soluble fraction of BL21(DE3)/pGEX-4T3-*yadK* at 4h after IPTG induction.
4: Insoluble fraction of BL21(DE3)/pGEX-4T3-*yadK* at 4h after IPTG induction.

3.2.1 Successful construction of pET23d-*yadK*

As the *YadK* protein was expressed as inclusion bodies in the BL21(DE3)/pGEX-4T3-*yadK*, it is difficult to purify the *YadK* protein from inclusion bodies. Thus, another *yadK*-expressing vector was constructed. Here, the pET23d plasmid that contains an N-terminal T7-tag and a C-terminal His-tag was selected. To construct the pET23d-*yadK* vector, PCR product of the full-length *yadK* fragment was inserted into the pET23d plasmid and then transformed into DH5 α cells. Plasmid DNAs were isolated from 17 individual clones that grew from Amp⁺ plates, and tested for the presence of the *yadK* gene, respectively (**Figure 3.2.1**). The PCR products displaying approximately 590bp band size were purified and subjected to gene sequencing (**Figure 3.2.2**).

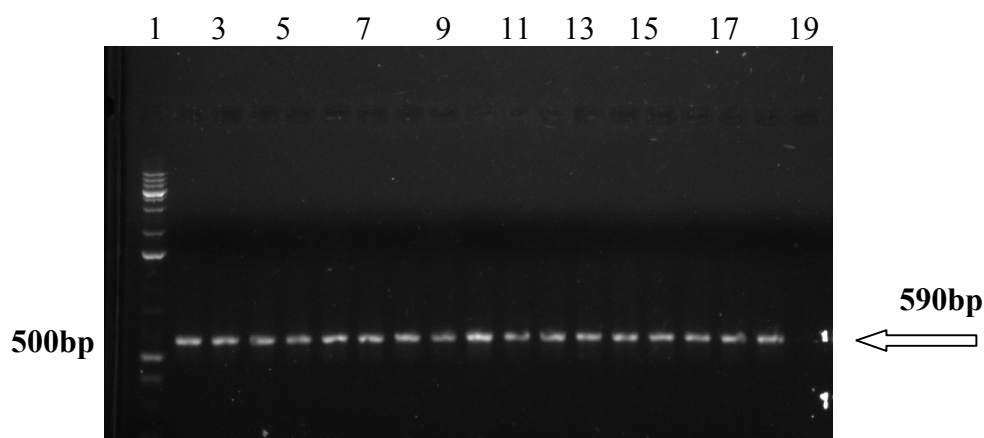


Figure 3.2.1 PCR products of *yadK* from DH5 α /pET23d-*yadK* on agarose gel. The PCR products were amplified from DH5 α /pET23d-*yadK* using the *yadK*/BamHIF and *yadK*/HindIIIIR specific primers, and subsequently subjected to agarose gel electrophoresis.

1: 1 kb Ladder (Band size from top to bottom: 10kb, 8kb, 6kb, 5kb, 4kb, 3kb, 2kb, 1kb, 0.5kb).

2-18: PCR product amplified from plasmid extraction of each DH5 α /pET23d-*yadK* colony.

19: PCR product amplified from negative control (pET23d).

```

T7-yadK-H6      -----ATGGCTAGCATGACTGGTGGACAGCAAA 28
SW8422          AATTTTGTTTAACTTTAAGAAGGAGATATACCATGGCTAGCATGACTGGTGGACAGCAAA 60
                  *****

T7-yadK-H6      TGGGTCGGATCCGAATGCTATGCAGGCATCATAAAATCGTACACTTTTTAGGGCTGGCAA 88
SW8422          TGGGTCGGATCCGAATGCTATGCAGGCATCATAAAATCGTACACTTTTTAGGGCTGGCAA 120
                  *****

T7-yadK-H6      CAGCCCTTATCAGCCTTTTGCCTATTCCGGCCAGGATGTGGATCTCACCAGCAAGATCG 148
SW8422          CAGCCCTTATCAGCCTTTTGCCTATTCCGGCCAGGATGTGGATCTCACCAGCAAGATCG 180
                  *****

T7-yadK-H6      TGCCCAGCACCTGT CAGGTTGAAGTCAGTAATAATGGCGTTGTGATCTCGGCACAGTGA 208
SW8422          TGCCCAGCACCTGT CAGGTTGAAGTCAGTAATAATGGCGTTGTGATCTCGGCACAGTGA 240
                  *****

T7-yadK-H6      CGCTGGACTATTTTCCCGACAATGTAAACCCGACAAACGGATTATGCGGGTGGCAAAACGT 268
SW8422          CGCTGGACTATTTTCCCGACAATGTAAACCCGACAAACGGATTATGCGGGTGGCAAAACGT 300
                  *****

T7-yadK-H6      TTAATGTGAATGTGGTCTCTTGCAGATAACATTCAAACGACACAGTCGCAATGAAATTAG 328
SW8422          TTAATGTGAATGTGGTCTCTTGCAGATAACATTCAAACGACACAGTCGCAATGAAATTAG 360
                  *****

T7-yadK-H6      ATTTTCAGCCGCGAGGCGGGATCGCTTGCACAGGCGAATAATCAAATTTTGTAGTAATGAAT 388
SW8422          ATTTTCAGCCGCGAGGCGGGATCGCTTGCACAGGCGAATAATCAAATTTTGTAGTAATGAAT 420
                  *****

T7-yadK-H6      ATGAACAGCAGGCTACCGGGGCGAAAAACGTCGGCATTGTGATTTTTTCGGCCCAACCGA 448
SW8422          ATGAACAGCAGGCTACCGGGGCGAAAAACGTCGGCATTGTGATTTTTTCGGCCCAACCGA 480
                  *****

T7-yadK-H6      ATCAGCAGACATTTAACGTGCGAGGAACGGATGGTTCCTCAACAGCAATTTATTCGGTAG 508
SW8422          ATCAGCAGACATTTAACGTGCGAGGAACGGATGGTTCCTCAACAGCAATTTATTCGGTAG 540
                  *****

T7-yadK-H6      CACCTGGCAATGCTGTTCCCTCAACCTGGACCTTTTATTCCCCTATGCAGCGGGTGAATA 568
SW8422          CACCTGGCAATGCTGTTCCCTCAACCTGGACCTTTTATTCCCCTATGCAGCGGGTGAATA 600
                  *****

T7-yadK-H6      ATGCCCTTCCTCCTGAATCGGGAATGGTGAGAAGCCAGGTTATTGTTAACGTATCTTACG 628
SW8422          ATGCCCTTCCTCCTGAATCGGGAATGGTGAGAAGCCAGGTTATTGTTAACGTATCTTACG 660
                  *****

T7-yadK-H6      AAAAGCTTGCGGCGCACTCGAGCACCAACCACCACCACCTGAGATCCGGCTGCTAACA 688
SW8422          AAAAGCTTGCGGCGCACTCGAGCACCAACCACCACCACCTGAGATCCGGCTGCTAACA 720
                  *****

T7-yadK-H6      AAGCCCGAAAAGGAAGCTGAGTTGGCTGCTGCCACCGCTGAGCAATAACTAGCATAAACCC 748
SW8422          AAGCCCGAAAAGGAAGCTGAGTTGGCTGCTGCCACCGCTGAGCAATAACTAGCATAAACCC 780
                  *****

T7-yadK-H6      TTGGGGCCTCTAAACGGGTCTTGAGGGGTTTTTTGCTGAAAGGAGGAAGTATATCCGGAT 808
SW8422          TTGGGGCCTCTAAACGGGTCTTGAGGGGTTTTTTGCTGAAAGGAGGAAGTATATCCGGAT 814
                  *****

```

Figure 3.2.2 Gene sequencing result of *yadK* amplified from DH5 α /pET23d-*yadK*. Sequence alignment was performed through ClustalW2 blast program, and the alignment result demonstrated that *yadK* with correct sequence was amplified from DH5 α /pET23d-*yadK*. T7-yadk-H6 indicates sequences of pET23d and full-length *yadK* from EDL933; sw8422 indicates sequence from plasmid in DH5 α /pET23d-*yadK*.

3.2.2 T7-YadK-His was also expressed as inclusion bodies in BL21 (DE3)

To express the T7-YadK-His protein, the pET23d-*yadK* vector carrying the *yadK* gene with the correct sequence was transformed into BL21(DE3) cells. The presence of pET23d-*yadK* vectors in the transformed BL21(DE3) colonies was confirmed by PCR assay. Then IPTG was used to induce the YadK protein expression of these BL21(DE3)/pET23d-*yadK* bacteria. The His-YadK-T7 protein expression was assayed by SDS-PAGE (Figure 3.2.3) and Western blotting with the use of anti-His antibody, respectively (Figure 3.2.4). However, we found that after bacterial cell lysis, most of T7-YadK-His was still found in insoluble fraction of IPTG-induced BL21(DE3)/pET23d-*yadK* (Figure 3.2.5).

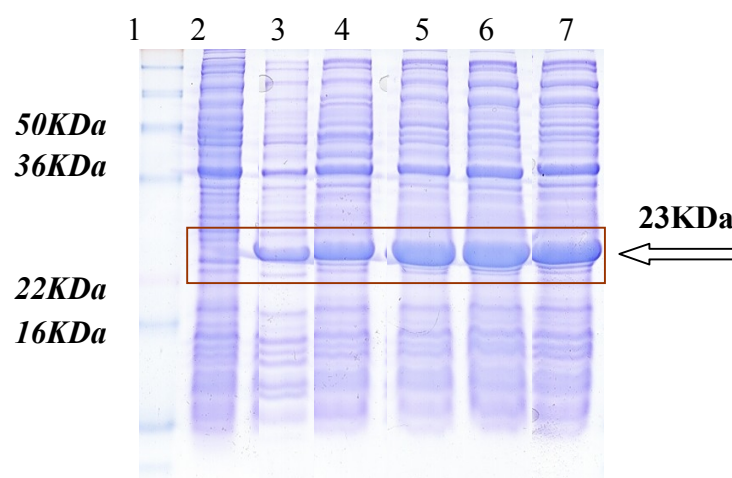


Figure 3.2.3 Coomassie blue staining of BL21 (DE3)/pET23d-*yadK* lysate. Approximately 20 μ g of BL21(DE3)/pET23d-*yadK* lysates before or after IPTG induction (at different time points) were subjected to SDS-PAGE, followed by Coomassie blue staining. The protein staining result suggested that T7-YadK-His (23KDa) expression in BL21(DE3)/pET23d-*yadK* was induced by IPTG (final concentration: 0.4 mM).

1: Ladder (Band size from top to bottom: 250KDa, 148KDa, 98KDa, 64KDa, 50KDa, 36KDa, 22KDa, 16KDa and 6KDa).

2: BL21(DE3)/pET23d lysate.

3-7: BL21(DE3)/pET23d-*yadK* lysate at 1h, 2h, 3h, 4h and 5h after IPTG induction, respectively.

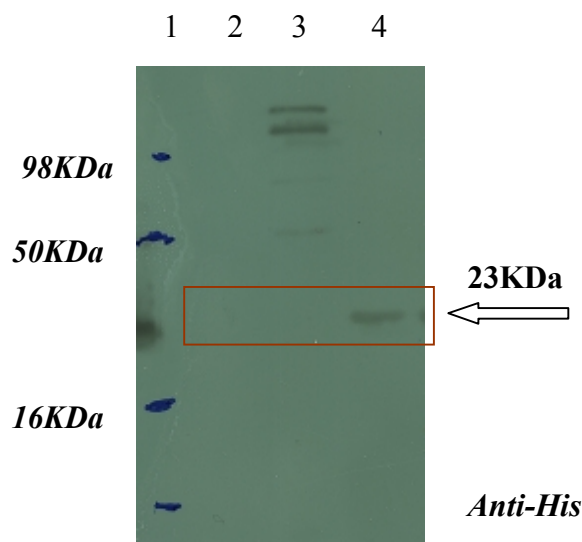


Figure 3.2.4 Western blotting of BL21(DE3)/pET23d-*yadK* lysate. Approximately 20 μ g of BL21(DE3)/pET23d-*yadK* lysates after IPTG induction (final concentration: 0.4 mM) were subjected to SDS-PAGE, followed by Western blotting with 1:1000 diluted anti-His (1st antibody) and 1:10000 diluted HRP-conjugated goat anti-mouse (2nd antibody) antibodies. The blotting result demonstrated that T7-YadK-His (23KDa) expression in BL21(DE3)/pET23d-*yadK* was induced by IPTG (final concentration: 0.4 mM).

1: Ladder (Band size from top to bottom: 98KDa, 50KDa, 16KDa).
2: BL21(DE3)/pET23d lysate; **3:** BL21(DE3)/Vac14-His lysate (T7-Vac14-His; 100KDa; positive control); **4:** BL21(DE3)/pET23d-*yadK* lysate at 5h after IPTG induction.

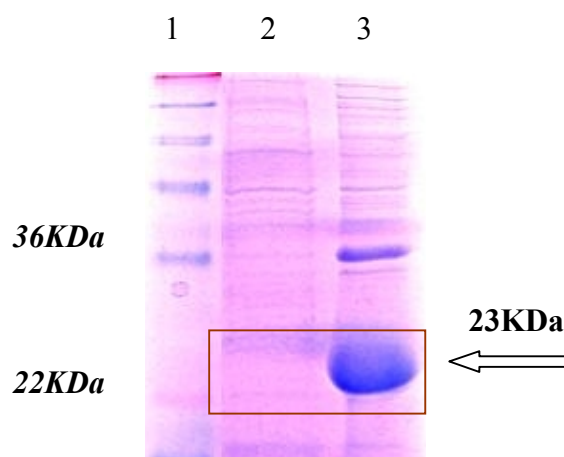


Figure 3.2.5 Coomassie blue staining of soluble and insoluble fraction of BL21(DE3)/pET23d-*yadK* lysate. Approximately 20 μ g of the soluble and insoluble protein fractions of BL21(DE3)/pET23d-*yadK* (after IPTG induction (final concentration: 0.4 mM)) lysate were subjected to SDS-PAGE, followed by Coomassie blue staining. The protein staining result suggested that T7-YadK-His (23KDa) was mainly expressed in insoluble fraction.

1: Ladder (Band size from top to bottom: 250KDa, 148KDa, 98KDa, 64KDa, 50KDa, 36KDa, 22KDa, 16KDa).
2: Soluble fraction of BL21(DE3)/pET23d-*yadK* at 5h after IPTG induction.
3: Insoluble fraction of BL21(DE3)/pET23d-*yadK* at 5h after IPTG induction.

3.2.3 T7-YadK-His purification from inclusion bodies

As described above, the T7-YadK-His expression in the BL (DE3)/pET23d-*yadK* was present as the inclusion bodies. In order to make T7-YadK-His soluble, different kinds of detergents were employed. In brief, the insoluble sample from BL(DE3)/pET23d-*yadK* was re-suspended with various detergents (i.e. Tween-20, Triton X-100 or SDS), respectively. We found that the recombinant T7-YadK-His was best solubilised in 1% SDS, compared to Tween-20 or Triton X-100 (**Figure 3.2.6**). Then the solubilized YadK protein samples were diluted with binding buffer until 0.02% SDS was present, and then loaded to the Ni-NTA agarose beads, which can specifically bind to YadK-His fusion protein. Then the samples eluted by 500mM imidazole in 1X phosphate buffer from the Ni-NTA beads were collected. To test the purity of YadK-His protein, the eluted protein was assayed by SDS-PAGE (**Figure 3.2.7**) and Western blotting with the use of anti-His (**Figure 3.2.8**). These data suggested that the purified YadK-His protein was of high purity.

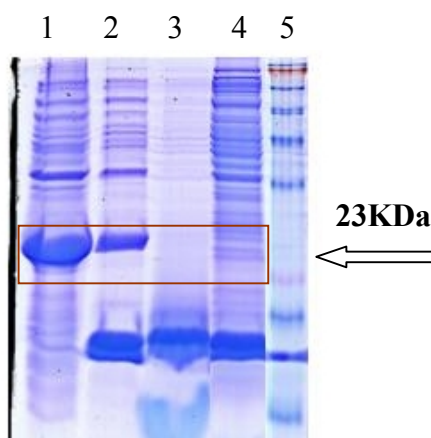


Figure 3.2.6 Coomassie blue staining of soluble fraction of detergent-treated BL21(DE3)/pET23d-*yadK* lysate. Approximately 20 μ g of BL21(DE3)/pET23d-*yadK* (after IPTG induction (final concentration: 0.4 mM)) lysate was treated by 1% SDS, Tween-20 or Triton X-100, respectively. The soluble fractions of lysate were then prepared and subjected to SDS-PAGE, followed by Coomassie blue staining. The protein staining result suggested that T7-YadK-His (23KDa) became soluble after 1% SDS treatment.

1: BL21 (DE3)/pET23d-*yadK* lysate at 5h after IPTG induction.

2: Soluble fraction treated with 1% SDS. **3:** Soluble fraction treated with 1% Tween-20. **4:** Soluble fraction treated with 1%Triton X-100.

5: Ladder (Band size from top to bottom: 250KDa, 148KDa, 98KDa, 64KDa, 50KDa, 36KDa, 22KDa, 16KDa and 6KDa).

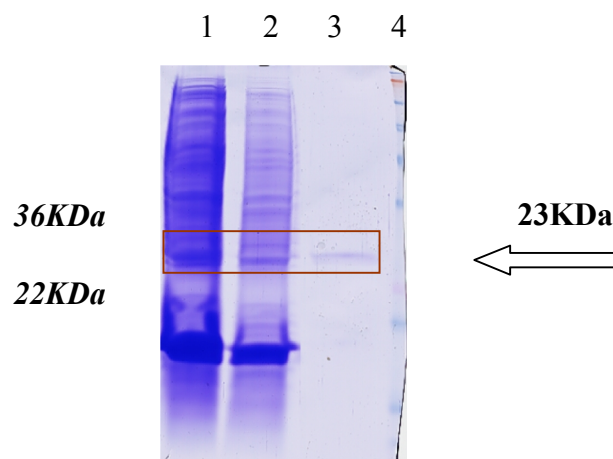


Figure 3.2.7 Coomassie blue staining of purified T7-YadK-His protein from BL21(DE3)/pET23d-*yadK* lysate. Approximately 20 μ g of BL21(DE3)/pET23d-*yadK* (after IPTG induction (final concentration: 0.4 mM)) lysate was treated by 1% SDS. The soluble fractions of lysate were prepared and loaded to the Ni-NTA agarose beads. The eluted samples were then subjected to SDS-PAGE, followed by Coomassie blue staining. The protein staining result suggested that purified YadK-His protein was of high purity.

1: BL21(DE3)/pET23d-*yadK* lysate at 5h after IPTG induction.
2: Soluble fraction in 1% SDS. **3:** Eluted sample (purified T7-YadK-His).
4: Ladder (Band size from top to bottom: 250KDa, 148KDa, 98KDa, 64KDa, 50KDa, 36KDa, 22KDa, 16KDa and 6KDa).

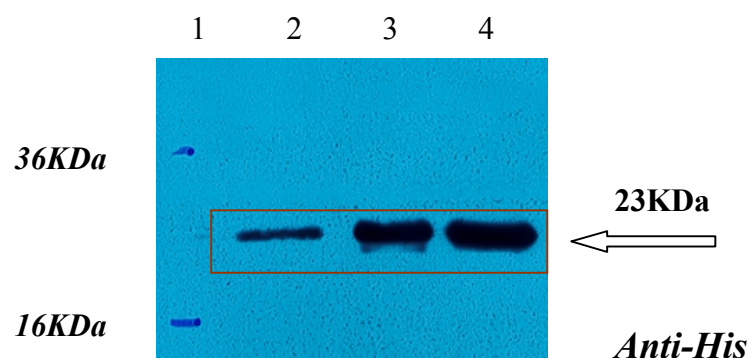


Figure 3.2.8 Western blotting of purified T7-YadK-His protein from BL21 (DE3)/pET23d-*yadK* lysate. Approximately 20 μ g of the soluble protein fraction were prepared from BL21(DE3)/pET23d-*yadK* (after IPTG induction (final concentration: 0.4 mM)) lysate treated by 1% SDS, and then loaded to the Ni-NTA agarose beads. The eluted samples were subjected to SDS-PAGE, followed by Western blotting with with 1:1000 diluted anti-His (1st antibody) and 1:10000 diluted HRP-conjugated goat anti-mouse (2nd antibody) antibodies. The blotting result further demonstrated that purified YadK-His protein was of high purity.

1: Ladder (Band size from top to bottom: 36KDa and 16KDa).
2: Eluted sample (purified T7-YadK-His).
3: Soluble fraction treated with 1% SDS.
4: BL21 (DE3)/pET23d-*yadK* at 5h after IPTG induction.

3.2.4 Generation of specific anti-YadK polyclonal antibodies

In order to generate the anti-YadK antibodies, the purified YadK protein was used to immunize the rabbits. After 3 immunizations, the sera were then collected from these YadK protein immunized rabbits.

The specificity of anti-YadK polyclonal antibodies was tested by Western blotting. The anti-YadK polyclonal sera specifically recognized the over-expressed YadK protein in 85170 Δ yadK/pGEX-4T3-yadK (GST-YadK; 48KDa), BL21 (DE3)/pET23d-yadK (T7-YadK-His; 23KDa) and EHEC85170 Δ yadK/pBluesk-yadK (21.2KDa) (Figure 3.2.9-11).

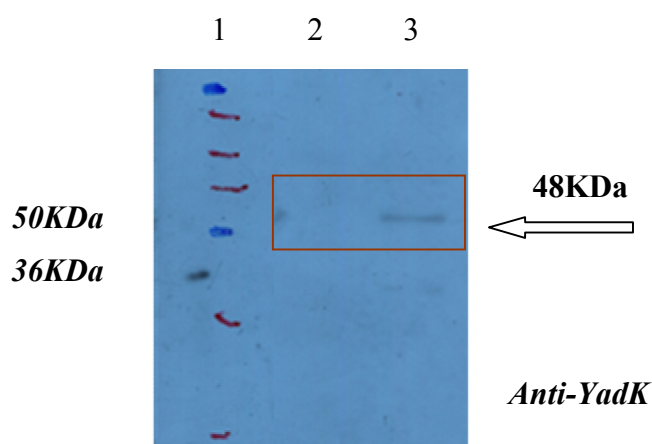


Figure 3.2.9 Western blotting of 85170 Δ yadK and 85170 Δ yadK/pGEX-4T3-yadK with anti-YadK antibodies. Approximately 20 μ g of 85170 Δ yadK/pGEX-4T3-yadK (after IPTG induction (final concentration: 1 mM)) or 85170 Δ yadK lysates were subjected to SDS-PAGE, followed by Western blotting with 1:400 diluted pre-adsorbed anti-YadK (1st antibody) and 1:10000 diluted HRP-conjugated goat anti-rabbit (2nd antibody) antibodies. The blotting result demonstrated that these polyclonal anti-YadK1 antibodies specifically recognized the over-expressed GST-YadK (48KDa) protein in 85170 Δ yadK/pGEX-4T3-yadK.

1: Ladder (Band size from top to bottom: 95KDa, 70KDa, 62KDa, 51KDa, 42KDa, 29KDa and 22KDa). **2:** 85170 Δ yadK lysate.

3: 85170 Δ yadK/ pGEX-4T3-yadK lysate after IPTG induction.

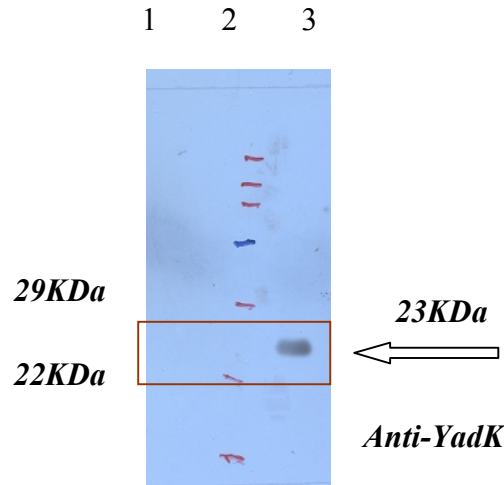


Figure 3.2.10 Western blotting of BL21(DE3) and BL21(DE3)/pET23d-yadK with anti-YadK antibodies. Approximately 20 μ g of BL21(DE3)/pET23d-yadK (after IPTG induction (final concentration: 0.4 mM)) or BL21(DE3) lysates were subjected to SDS-PAGE, followed by Western blotting with 1:400 diluted pre-adsorbed anti-YadK (1st antibody) and 1:10000 diluted HRP-conjugated goat anti-rabbit (2nd antibody) antibodies. The blotting result with ECL development kit demonstrated that these anti-YadK1 antibodies also specifically recognized the over-expressed T7-YadK-His (23KDa) protein.

1: BL21 (DE3)/pET23d lysate. **2:** Ladder (Band size from top to bottom: 95KDa, 70KDa, 62KDa, 51KDa, 42KDa, 29KDa and 22KDa). **3:** BL21(DE3)/pET23d-yadK lysate at 5h after IPTG induction.

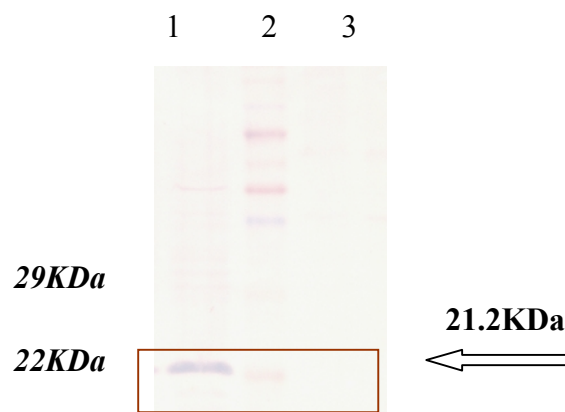


Figure 3.2.11 Western blotting of 85170 Δ yadK and 85170 Δ yadK/pBlueSK-yadK with anti-YadK antibodies. Approximately 20 μ g of 85170 Δ yadK/pBlueSK-yadK (after IPTG induction (final concentration: 1 mM)) or 85170 Δ yadK lysates were subjected to SDS-PAGE, followed by Western blotting with 1:400 diluted pre-adsorbed anti-YadK (1st antibody) and 1:10000 diluted AP-conjugated goat anti-rabbit (2nd antibody) antibodies. The blotting result demonstrated that these anti-YadK1 antibodies also specifically recognized the over-expressed YadK (21.2KDa) protein in 85170 Δ yadK/pBlueSK-yadK.

1: 85170 Δ yadK/pBlueSK-yadK lysate. **2:** Ladder (Band size from top to bottom: 95KDa, 70KDa, 62KDa, 51KDa, 42KDa, 29KDa, 22KDa and 14KDa).

3: 85170 Δ yadK lysate.

3.3 Successful construction of EDL933 $\Delta yadK$ in EDL933

Recent reports suggest that EDL933 strain exhibit significantly more biofilm formation than other EHEC 0157:H7 strains, and better adhesion ability than other strains¹⁰³⁻¹⁰⁴. Consequently, a $\Delta yadK$ mutant *was* constructed in EDL933 strain, using λ -Red recombinant system.

To disrupt *YadK* protein expression in EDL933 bacteria, EDL933 $\Delta yadK$ was constructed by inserting a Kanamycin resistance cassette into *yadK* gene. PCR was performed to screen the EDL933 $\Delta yadK$ clones grown on Kan⁺ plate (**Figure 3.3.1**). PCR products displaying approximately 1.8Kb band size were purified and sequenced (**Figure 3.3.2**). The sequencing alignment results demonstrated that EDL933 $\Delta yadK$ mutant was successfully constructed. EDL933 $\Delta yadK$ had been used in **Figure 3.4.1** as a negative control for *YadK* expression in unstressed and acid-adapted acid stressed EDL933.

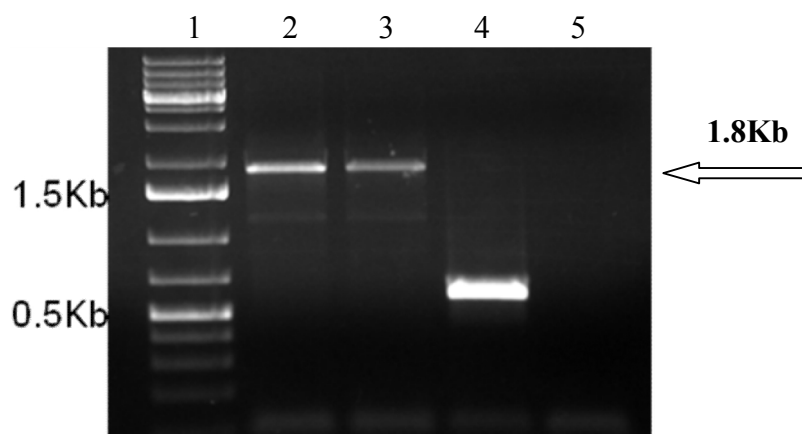


Figure 3.3.1 PCR product of *yadK*-Kan-*yadK* amplified from EDL933 $\Delta yadK$. The *yadK*-Kan-*yadK* fragment was amplified by PCR with T7*yadK*full-F-BamHI and H6*yadK*R-HindIII primers, and subsequently subjected to agarose gel electrophoresis. The successfully inserted mutant PCR product is present as ~1.8kb in size (EDL933 wild-type control: ~600bp).

- 1: Ladder
- 2: PCR product amplified from genomic DNA from EDL933 $\Delta yadK$ clone 1
- 3: PCR product amplified from genomic DNA from EDL933 $\Delta yadK$ clone 2
- 4: PCR product amplified from genomic DNA from EDL933
- 5: PCR product amplified from sterile H₂O

```

yadk      ATGCTATGCAGGCATCATAAAATCGTACACTTTTTAGGGCTGGCAACAGCCCTTATCACG 60
sample1  -----CCCTTATCACG 11
          *****

yadk      CCTTTTGCCTATTCCGGCCAGGATGTGGATCTCACCGCAAAGATCGTGCCAGCACCTGT 120
sample1  CCTTTTGCCTATTCCGGCCAGGATGTGGATCTCACCGCAAAGATCGTGCCAGCACCTGT 71
          *****

yadk      CAGGTTGAAGTCAGTAATAATGGCGTTGTCGATCTCGTGTAAGGCTGGAGCTGCTTCGAAG 180
sample1  CAGGTTGAAGTCAGTAATAATGGCGTTGTCGATCTCGTGTAAGGCTGGAGCTGCTTCGAAG 131
          *****

kana      TTCTTACTTTCTAGAGAATAGGAAC TTCGGAATAGGAAC TTCAGATCCCTCACGCT 240
sample1  TTCTTACTTTCTAGAGAATAGGAAC TTCGGAATAGGAAC TTCAGATCCCC -CACGCT 190
          *****

Kana      GCCGCAAGCACTCAGGGCGCAAGGGCTGCTAAAGGAAGCGGAACACGTAGAAAGCCAGTC 300
sample1  GCCGCAAGCACTCAGGGCGCAAGGGCTGCTAAAGGAAGCGGAACACGTAAAAAGCCAGTC 250
          *****

Kana      CTGGATGATCCTCCAGCGCGGGGATCTCATGCTGGAGTTCTTCGCCCACCCAGCTTCAA 1560
sample1  CTGGATGATCCTCCAGCGCGGGGATCTCATGCTGGAGTTCTTCGCCCACCCAGCTTCAA 86
          *****

kana      AAGCGCTCTGAAGTTCTTATAC TTTCTAGAGAATAGGAAC TTCGGAATAGGAACTAAGGA 1620
sample1  AAGCGCTCTGAAGTTCTTATAC TTTCTAGAGAATAGGAAC TTCGGAATAGGAACTAAGGA 146
          *****

kana      GGATATTCATATGGACCATGGCTAATTCCCATGAACGGATGGTTCTCAACAGCAATTTA 1680
sample1  GGATATTCATATGGACCATGGCTAATTCCCATGAACGGATGGTTCTCAACAGCAATTTA 206
          *****

yadk      TTCGGTAGCACCTGGCAATGCTGTTCCCTCAACCTGGACCTTTTATTCCTCGTATGCAGCG 1740
sample1  TTCGGTAGCACC----- 218
          *****

```

Figure 3.3.2 Sequencing result of PCR product amplified from EDL933Δ*yadK* using internal *yadK* primers. Sequence has been modified to only include the disrupted *yadK* gene, the upstream FRT site and the inserted kana resistance cassette. Sequence alignment was performed using the ClustalW2 blast program. The alignment result demonstrated that a Kanamycin resistance cassette was successfully inserted into *yadK* gene. **yadK**: *yadK* gene; **kana**: kana⁺ resistance cassette; **sample1**: sequence from successful mutant.

3.4 Increased YadK expression was observed under acid-adapted acid stress

Previous microarray studies in our lab found that the expression of *yadK* gene in EHEC, exhibited 5.87-fold increase after exposure to acid stress³. Increased expression of *yadK* mRNA in acid adapted acid stress was subsequently confirmed by quantitative Real-Time PCR (RT-PCR), suggesting that this *yadK* gene is involved in the EHEC response to acid stress⁹⁰. But it is unknown whether the expression of YadK protein in EHEC is up-regulated under acid stress.

To investigate the effects of acid stress on YadK protein expression in EHEC, Western blotting with anti-YadK polyclonal sera was employed to evaluate the YadK protein levels in EHEC under acid stress. In brief, bacterial lysates from EHEC acid-adapted acid (AA) stress group and unstressed (UU) group was pre-treated with acid H₂O to disassemble pilus structure⁵⁵. BL21(DE3)/T7-YadK-His was used as positive control. Results from three independent experiments revealed a more intense YadK band of 21.2KD size in the AA EHEC than in the UU EHEC. As loading control, chaperone protein DnaK (HSP70), was comparable between all AA and UU samples (**Figure 3.4.1**). With the use of Image J program to analyze the band density of YadK versus DnaK in Western blotting, we found that the YadK protein expression in EHEC acid-adapted acid stress group was significantly higher than that in EHEC un-stressed group (**Figure 3.4.2**).

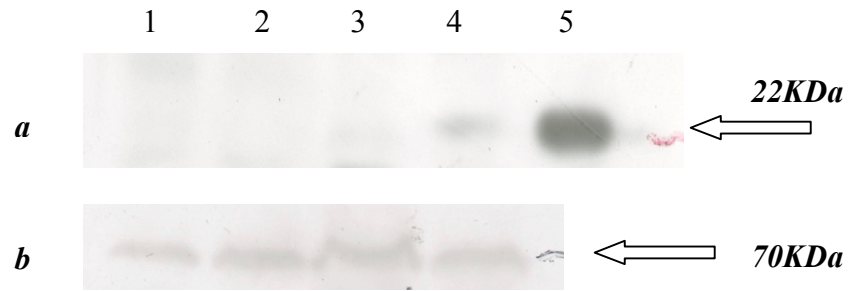


Figure 3.4.1 Western blotting of EDL933 and EDL933 Δ yadK lysates with anti-YadK antibodies. Approximately 50 μ g of EDL933 Δ yadK or EDL933 lysates under un-stressed (UU) or acid-adapted acid (AA) treatment were subjected to SDS-PAGE, respectively, followed by Western blotting with 1:400 diluted anti-YadK1 (a) or 1:1000 diluted anti-GST70K antibodies (b) (1st antibody), and 1:10000 diluted HRP-conjugated goat anti-rabbit (2nd antibody) antibodies. This result is representative of three independent experiments.

- 1: EDL933 Δ yadK (UU).
- 2: EDL933 Δ yadK (AA).
- 3: EDL933 UU.
- 4: EDL933 AA.
- 5: Δ yadK/pBlueSK-yadK after 0.4 mM IPTG induction (positive control).

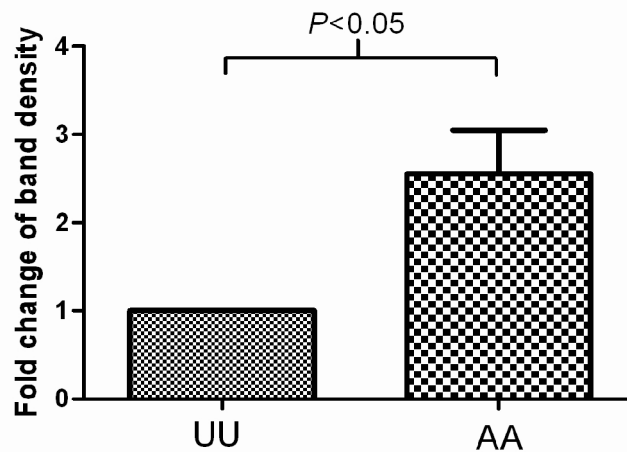


Figure 3.4.2 Quantitative analysis revealed that the YadK protein level in EHEC AA group was significantly higher than that in EHEC UU group (P<0.05; n=3 per group). The band intensity in Figure 3.4.1 was quantitated by Image J program. The intensity of adjacent background was subtracted from the intensity of sample or control band, respectively. In each independent experiment, the ratio of blotting band intensity between YadK and DnaK in unstressed (UU) group was regarded as 1, when the ratio of YadK/DnaK was compared between UU and AA group.

3.5 Anti-YadK inhibits host adhesion of acid-stressed EHEC

In the absence of anti-YadK, acid stressed EHEC showed enhanced adhesion to HEp-2 cells, relative to unstressed EHEC. When acid stressed EHEC were pre-treated with anti-YadK, the adhesion to HEp-2 cells was reduced to the level of adhesion observed for unstressed EHEC (**Figure 3.5**). On the other hand, anti-YadK had no significant effect on the adhesion of unstressed EHEC. These results indicate that anti-YadK inhibits adhesion of acid stressed EHEC to human epithelial cells, suggesting a role for YadK in the adhesion enhancement of EHEC after acid stress.

Figure 3.5 shows EHEC EDL933 strain adhesion to HEp-2 cells. This figure is representative of three independent experiments.

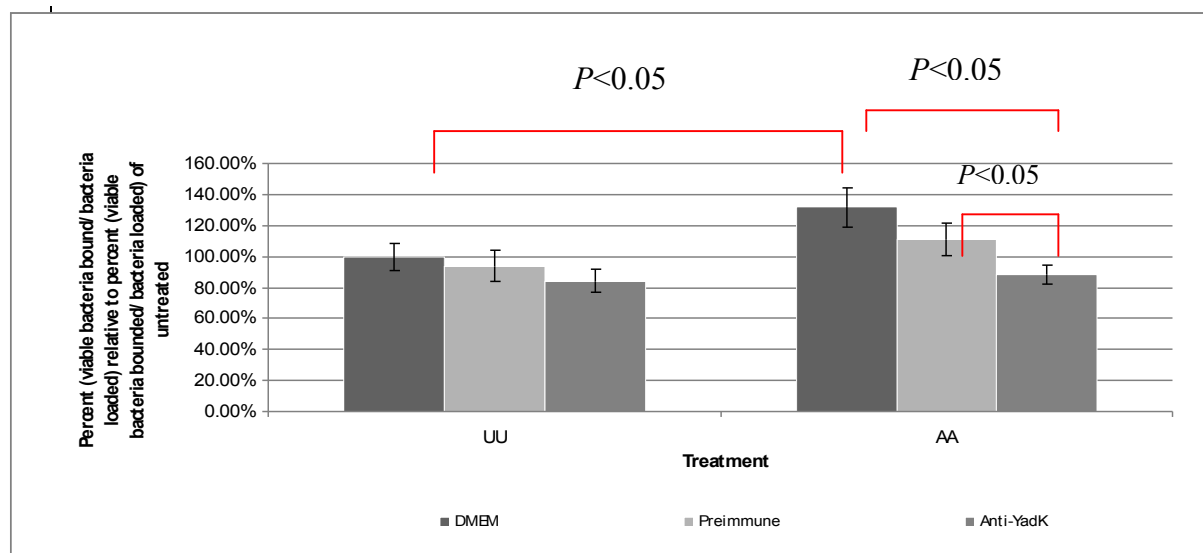


Fig 3.5 Adhesion was assessed and compared among three different incubation groups. The data represents the mean of three independent trials \pm standard deviation ($n=3$) with MOI ~ 100 . The adhesion to human epithelial cells has been normalized to UU and AA treatments, separately. DMEM indicates EDL933 incubated with DMEM for 1h; Pre-immune indicates EDL933 incubated with pre-immune serum for 1h; Anti-YadK indicates EDL933 incubated with anti-YadK for 1h; UU: unstressed; AA: acid adapted-acid stressed. 100% represents an average of 9.357×10^5 cells that bound to HEp-2 cells.

3.6.1 Successful construction of predicted promoter constructs for *yadK*

The pMC1403 plasmid, which contains a promoter-less LacZ gene, was used to make the promoter constructs with the predicted promoter regions that were involved in *yadK* gene expression. Three predicted promoter regions: PyadN, PyadM and PyadK (as indicated in **Figure 2.2**) were amplified by PCR and these PCR products were subsequently inserted into pMC1403 plasmid, respectively. The pMC1403 plasmids containing the potential promoter regions of *yadK* gene were then transformed into DH5 α cells, followed by overnight culture on Amp⁺ plates. Plasmid DNAs were isolated from different clones that grew from Amp⁺ plates and subjected to PCR assay, respectively (**Figure 3.6.1**). The PCR products displaying approximately 500~600bp band size were purified and subjected to gene sequencing (**Figure 3.6.2 A-C**). Then the promoter constructs were purified from DH5 α cells and transformed into EHEC 85170, which were subsequently used for β -galactosidase assay. These data suggest that three putative promoter regions of *yadK* gene were successfully inserted into pMC1403 plasmids, respectively.

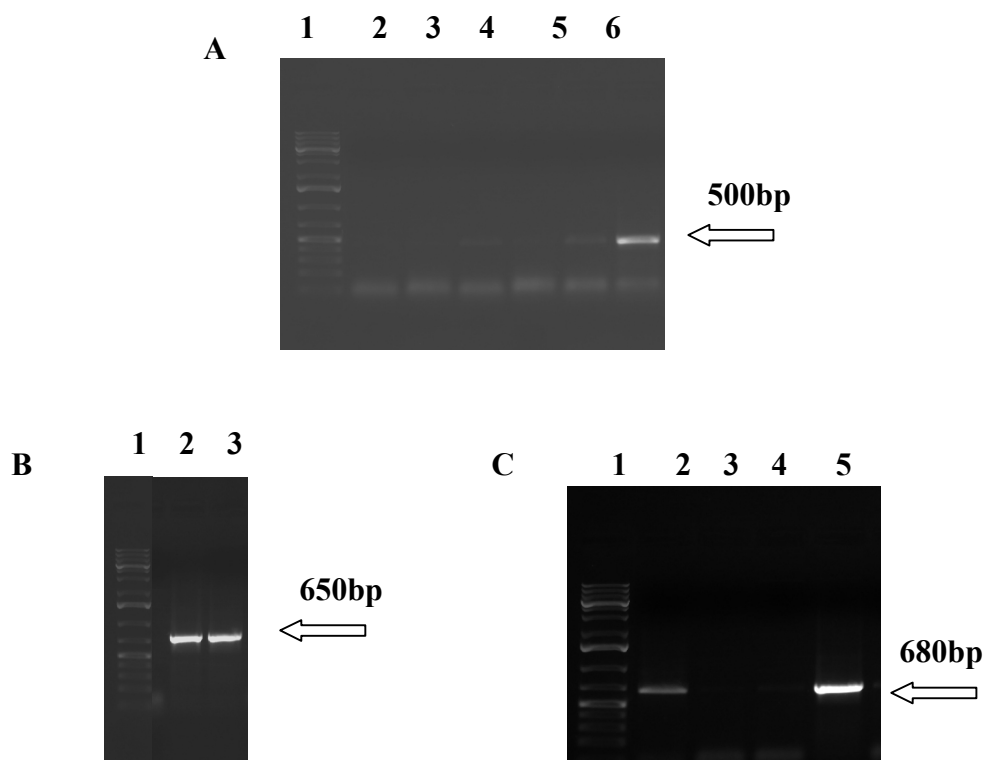


Figure 3.6.1 PCR products of putative *yadK* promoter regions from DH5 α /pMC-PyadN, DH5 α /pMC-PyadM and DH5 α /pMC-PyadK colonies, respectively. As indicated in Table 2.3, forward EcoRIPyadN and reverse BamHIIIPyadN primers were used to amplify PyadN sequence, EcoRIPyadK and BamHIIIPyadK primers for PyadK sequence, while EcoRIPyadM and BamHIIIPyadM primers were used to amplify PyadM sequence. Then these PCR products were subjected to agarose gel electrophoresis, respectively.

A): 1: Ladder (Band size from top to bottom: 10kb, 8kb, 6kb, 5kb, 4kb, 3kb, 2kb, 1kb, 0.5kb).

2-7: PCR products amplified from plasmid DNA extractions from DH5 α /pMC-PyadN independent colonies.

B): 1: Ladder (Band size from top to bottom: 10kb, 8kb, 6kb, 5kb, 4kb, 3kb, 2kb, 1kb, 0.5kb).

2-3: PCR products amplified from plasmid DNA extractions from DH5 α /pMC-PyadK independent colonies.

C): 1: Ladder (Band size from top to bottom: 10kb, 8kb, 6kb, 5kb, 4kb, 3kb, 2kb, 1kb, 0.5kb).

2-5: PCR products amplified from plasmid DNA extractions from DH5 α /pMC-PyadM independent colonies.

A

```

pyadNedl      AATTCGCATTACGATATGAAGAATCGCGGCTTTATGCTGTGGCCGCTGTTTGAGATTGCC 60
sample        -----CGCTGTTTGAGATTGCC 17
                *****

pyadNedl      CCGGAACCTCGTGTTCCTGATGGGGAGACATTACGTGAAATACTCACTTCGCTAGCAGTA 120
sample        CCGGAACCTCGTGTTCCTGATGGGGAGACATTACGTGAAATACTCACTTCGCTAGCAGTA 77
                *****

pyadNedl      CTACAACCTGCCATCTGGTATTAGCTGTATTATTTTATTTTCTTATCTTACTCCTCACTT 180
sample        CTACAACCTGCCATCTGGTATTAGCTGTATTATTTTATTTTCTTATCTTACTCCTCACTT 137
                *****

pyadNedl      CCCCTCTTACAGATTAAATATACTTAATTTACATTTTAGTTTTTTTTTAATTAATTCATGA 240
sample        CCCCTCTTACAGATTAAATATACTTAATTTACATTTTAGTTTTTTTTTAATTAATTCATGA 197
                *****

pyadNedl      AATAGCACTTCATGCAAAATAGATTAGGCATTTTTTGTGTTAAAAAACCTAGAATAGCAACA 300
sample        AATAGCACTTCATGCAAAATAGATTAGGCATTTTTTGTGTTAAAAAACCTAGAATAGCAACA 257
                *****

pyadNedl      ATTCATACACCACGTAAATATATTACACCCGTGATAATTCACCCCTATTACATCCTCC 360
sample        ATTCATACACCACGTAAATATATTACACCCGTGATAATTCACCCCTATTACATCCTCC 317
                *****

pyadNedl      AAAAAGCTTTGAGTAATATCCGCTCGCAATATTAATTTTATATAATTTTTGTAAGGATGCA 420
sample        AAAAAGCTTTGAGTAATATCCGCTCGCAATATTAATTTTATATAATTTTTGTAAGGATGCA 377
                *****

pyadNedl      TGTAATGAAAAAGCACTTCTCGCAGCCGCTCTGGTTATGCGCGGATCCCCG 472
sample        TGTAATGAAAAAGCACTTCTCGCAGCCGCTCTGGTT----- 414
                *****

```

B

```

.m7
pyadme dl      ACCTATAAAATAGGCGTATCAAGAGGCCCTTTCGTCTTCAAGAATTCTCAACCGATGGCG 60.
                -----GCGTATCAAGAGGCCCTTTCGTCTTCAAGAATTCTCAACCGATGGCG 47.
                *****

.m7
pyadme dl      GCTTTGTATTACACAGTGGTGGTTTAAAGCTTCACTAACAACAGTTTCAGCAGTAACGACA 120.
                GCTTTGTATTACACAGTGGTGGTTTAAAGCTTCACTAACAACAGTTTCAGCAGTAACGACA 107.
                *****

.m7
pyadme dl      CGCTGGTGTAAATCAACGCCCTAGGTGCTAAAGGCGCACGAATCAATAACAGTAATAACG 180.
                CGCTGGTGTAAATCAACGCCCTAGGTGCTAAAGGCGCACGAATCAATAACAGTAATAACG 167.
                *****

.m7
pyadme dl      AAATCGATCGCTGGGGATATGCCGTGACGTCTCTGTCAGCCCATATCGTGAAAACCGGG 240.
                AAATCGATCGCTGGGGATATGCCGTGACGTCTCTGTCAGCCCATATCGTGAAAACCGGG 227.
                *****

.m7
pyadme dl      TAGGTCTGAACATTGAAACACTGGAAAACGATGTGAACTGAAAAGTACCAGCGCCACCA 300.
                TAGGTCTGAACATTGAAACACTGGAAAACGATGTGAACTGAAAAGTACCAGCGCCACCA 287.
                *****

.m7
pyadme dl      CCGTACCACGTAGCGGCTCCGTTGTTTGACCCGTTTCGAAACTGACGAGGGGCGTCTG 360.
                CCGTACCACGTAGCGGCTCCGTTGTTTGACCCGTTTCGAAACTGACGAGGGGCGTCTG 347.
                *****

.m7
pyadme dl      CCGTGCTGAATATTACTGCGCCAATGGCAAATCCATTCCGTTTGCTGCGGAGGTTTACC 420.
                CCGTGCTGAATATTACTGCGCCAATGGCAAATCCATTCCGTTTGCTGCGGAGGTTTACC 407.
                *****

.m7
pyadme dl      AGGGTGAGGTGATGATCGGCAGCATGGGCAGGGTGATCAGGCATTGTACGCGGTATTA 480.
                AGGGTGAGGTGATGATCGGCAGCATGGGCAGGGTGATCAGGCATTGTACGCGGTATTA 467.
                *****

.m7
pyadme dl      ACGACAGCGGGGAATTAAATCGTGCCTGGTATGAAAACAACCAAACCATTGACTGTAAGT 540.
                ACGACAGCGGGGAATTAAATCGTGCCTGGTATGAAAACAACCAAACCATTGACTGTAAGT 527.
                *****

.m7
pyadme dl      TGCACTACCAAGTTCCTGGCGCAGCCACAAACGCAAGGGAAGCACCAACACCTTATTACTTA 600.
                TGCACTACCAAGTTCCTGGCGCAGCCACAAACGCAAGGGAAGCACCAACACCTTATTACTTA 587.
                *****

.m7
pyadme dl      ACAATCTTACCTGTCAAGTAGCAAATCACTAATATGAAAAATCTATGAAAAGGATACTA 660.
                ACAATCTTACCTGTCAAGTAGCAAATCACTAATATGAAAAATCTATGAAAAGGATACTA 647.
                *****

.m7
pyadme dl      CTAACATCCGCGTTAATAGGCCTGGGTTTAGGATCCCGTCGTTTACAACTCGTGACTG 720.
                CTAACATCCGCGTTAATAGGCCTGGGTTTAGGATCCCGTCGTTTACAACTCGTGACTG 707.
                *****

.m7
pyadme dl      GGAAAA 726.
                GGAAAA 713.
                *****

```

C

```

k1          TAGGCGTATCACGAGGCCCTTTGCTCTTCAAGAATTCAAGTCATCGCTACACTGATTGCT 60.
pyadkedi   ---GCGTATCACGAGGCCCTTTGCTCTTCAAGAATTCAAGTCATCGCTACACTGATTGCT 57.
          *****

k1          ACTGTTGCCGTGGGTGTAAAGCTTTAACAGCAATTTCCTCTGCGAGTACAACGTCGCT 120.
pyadkedi   ACTGTTGCCGTGGGTGTAAAGCTTTAACAGCAATTTCCTCTGCGAGTACAACGTCGCT 117.
          *****

k1          TCTTTAACCCTAAAAGTAACCTGACTATGGGTACCTGCGAGTGCAGATAATGGATAAT 180.
pyadkedi   TCTTTAACCCTAAAAGTAACCTGACTATGGGTACCTGCGAGTGCAGATAATGGATAAT 177.
          *****

k1          AGTAATAAAGTGATCAATGAAGTGGTCTTTGGCAATGTTTATATTTCTGAACTCGGTGCA 240.
pyadkedi   AGTAATAAAGTGATCAATGAAGTGGTCTTTGGCAATGTTTATATTTCTGAACTCGGTGCA 237.
          *****

k1          AAAAGCAAAAGTGCAACAGTTTAAAAATGCGCTTTAGCAATTGCTCTGGCCTTCCCCAAAAC 300.
pyadkedi   AAAAGCAAAAGTGCAACAGTTTAAAAATGCGCTTTAGCAATTGCTCTGGCCTTCCCCAAAAC 297.
          *****

k1          AGCGCCCAAATAGTGCTGGCACCTAATGGTATATCCTGTGCTGGTTCTCAATCGTCATCG 360.
pyadkedi   AGCGCCCAAATAGTGCTGGCACCTAATGGTATATCCTGTGCTGGTTCTCAATCGTCATCG 357.
          *****

k1          GCGGGTTTCTTAAAGTCTTACTGACGCTAGCGCAGCAACGAAACGGCTGTGGAAGTA 420.
pyadkedi   GCGGGTTTCTTAAAGTCTTACTGACGCTAGCGCAGCAACGAAACGGCTGTGGAAGTA 417.
          *****

k1          TGGACTACAGATACACCGGAAAGCAATGGCAGTACGCAATTCATTGTGCTCAAAAGATA 480.
pyadkedi   TGGACTACAGATACACCGGAAAGCAATGGCAGTACGCAATTCATTGTGCTCAAAAGATA 477.
          *****

k1          CCAGTGCTGTGACGCTTCCGCGGACACCACTCAGCCTTACGATTACCGTTAAGT 540.
pyadkedi   CCAGTGCTGTGACGCTTCCGCGGACACCACTCAGCCTTACGATTACCGTTAAGT 537.
          *****

k1          GCACGGATGACCGTTGCGGAAGGTAGATTGGTAAACGATGTAAAGACCGGGTAATTTCCGC 600.
pyadkedi   GCACGGATGACCGTTGCGGAAGGTAGATTGGTAAACGATGTAAAGACCGGGTAATTTCCGC 597.
          *****

k1          TCTCCACGACTTTACGATCACTTATCAGTAATAGCGGATAGGATATTAGAATGCTAT 660.
pyadkedi   TCTCCACGACTTTACGATCACTTATCAGTAATAGCGGATAGGATATTAGAATGCTAT 657.
          *****

k1          GCAGGCATCATAAAATCGTACACTTTTGGGCTGGCAACAGCCCTTATCAGGATCCCG 720.
pyadkedi   GCAGGCATCATAAAATCGTACACTTTTGGGCTGGCAACAGCCCTTATCAGGATCCCG 717.
          *****

k1          TCGTTTACAAAGTCGTGACTGGGAAAAACCTGGCGTTACCCAACTTAATCGCCTTGCA 780.
pyadkedi   TCGTTTACAAAGTCGTGACTGGGAAAA----- 745.
          *****

```

Figure 3.6.2 Sequencing result of potential *yadK* promoter regions amplified from pMC1403-PyadN, pMC1403-PyadK and pMC1403-PyadM in DH5 α , respectively. A): sample indicates sequence from plasmid extraction of DH5 α /pMC1403pyadN; pyadNed1: template sequence. **B):** m7: sequence from plasmid extraction of DH5 α /pMC1403pyadM; pyadmed1: template sequence. **C):** k7: sequence from plasmid extraction of DH5 α /pMC1403pyadK; pyadkedi: template sequence. Sequence alignment was performed by ClustalW2 blast program. These results suggested that three putative *yadK* promoter regions with correct sequence were inserted into pMC1403 plasmids, respectively.

3.6.2 Up-regulation of promoter activity of PyadN was observed under acid-adapted acid stress

To determine the activity of *yadK* promoter under various stress conditions, EHEC 85170/pMC1403-PyadN, 85170/pMC1403-PyadM and 85170/pMC1403-PyadK were grown overnight and exposed to acid adapted acid stress (AA) and un-stressed (UU) treatments, respectively. We found that only PyadN activity (but not PyadM and PyadK) was significantly increased under acid adapted acid stress, compared to UA or UU treatments (**Figure 3.6.3-5**), suggesting that PyadN (the predicted promoter for whole operon) may be the potential promoter region for *yadK* gene.

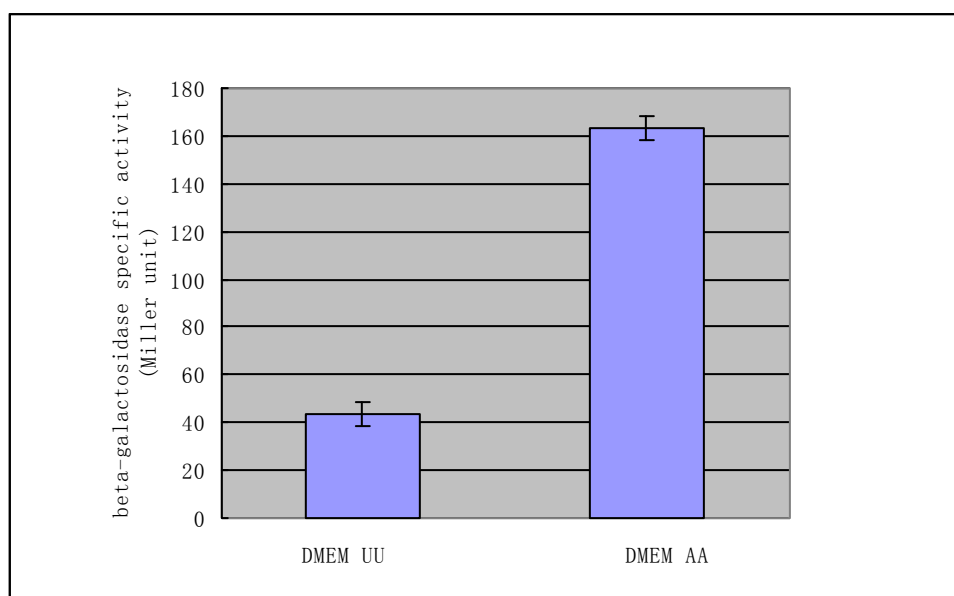


Figure 3.6.3: Promoter activity of EHEC 85170/pMC1403-PyadN under un-stressed or acid-adapted acid stress. The EHEC/PyadN bacteria lysate were resuspended in PBS and assessed for promoter activity of *yad* whole operon by β -galactosidase assay (n=3). The PyadN activity was significantly increased under acid adapted acid stress, compared to UU treatments. UU: Unstressed; AA: acid-adapted acid stress. This figure is representative of two independent experiments.

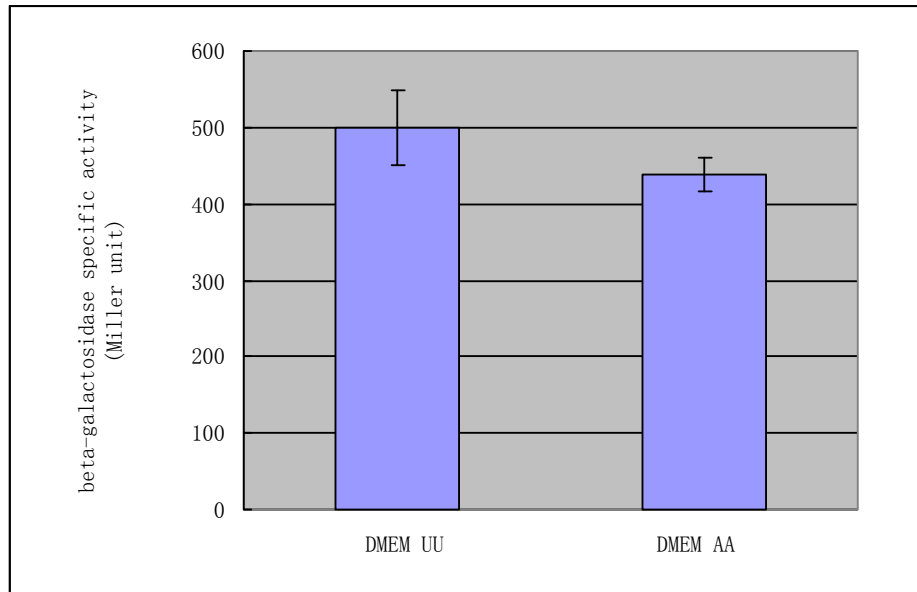


Figure 3.6.4: Promoter activity of EHEC 85170/pMC1403-PyadM under unstressed or acid-adapted acid stress. The EHEC/PyadM bacteria lysate were resuspended in PBS and assessed for promoter activity of PyadM by β -galactosidase assay (n=3). There was no significant difference in the PyadM activity between AA and UU treatments ($P > 0.05$). UU: Unstressed; AA: acid-adapted acid stress. This figure represents one experiment.

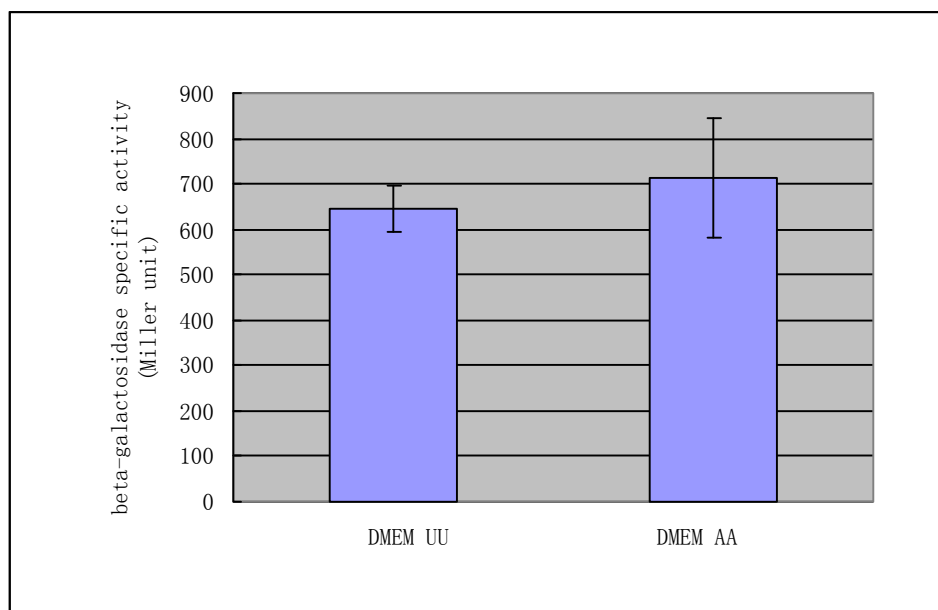


Figure 3.6.5: Promoter activity of EHEC 85170/pMC1403-PyadK under unstressed or acid-adapted acid stress. The EHEC/PyadK bacteria lysate were resuspended in PBS and assessed for promoter activity of PyadK by β -galactosidase assay (n=3). There was no significant difference in the PyadK activity between AA and UU treatments. UU: Unstressed; AA: acid-adapted acid stress. This figure is representative of one experiment.

4. Discussion

Acid stress is one of host defenses against foodborne pathogens. However, EHEC O157:H7 can survive passage through the acidic environment of GI tract due to their acid resistance system. An earlier mRNA microarray study has revealed that a variety of genes (including *yadK*) encoding virulent factors in EHEC were increased in response to the acid stress³. The increased gene expression under acid stress was also confirmed by Real-Time PCR. Disruption of *yadK* gene in EHEC resulted in the loss of acid-induced adhesion phenotype that was observed for wild-type EHEC O157⁹⁰, suggesting that *yadK* gene played an important role in mediating acid-induced EHEC adhesion to host cells. However, to date there is still little knowledge regarding the potential role of YadK protein in the pathogenesis of EHEC. It is unknown whether YadK protein is directly involved in EHEC adhesion to host cells, or whether YadK functions as a regulator on the expression or/and assembly of certain adhesins (e.g. fimbriae). The hypothesis of this thesis is that acid stress up-regulates expression of the putative fimbrial protein YadK and that the YadK protein plays an essential role in the acid-induced adhesion of EHEC to host cells.

To address this hypothesis, three research objectives were established and subsequently pursued in order to evaluate the potential role of anti-YadK specific antiserum in EHEC adhesion to host cells. To prepare a YadK-specific antiserum, it was necessary to generate recombinant tagged YadK protein in the first place. Two plasmids, pET23d-*yadK* and pGEX-4T3-*yadK* were constructed. After transformation

into BL21 (DE3), recombinant T7-YadK-His and GST-YadK were abundantly expressed as inclusion bodies. Solubilization of the recombinant proteins required denaturation. Since the binding of GST-tag (but not His-tag) to Glutathione Sepharose 4B beads is significantly decreased under denaturing conditions, the His-tag expression system (pET23d plasmid) was used in the subsequent experiments, to purify YadK protein. Soluble T7-YadK-His was obtained from inclusion bodies by SDS detergent treatment, and the T7-YadK-His protein was purified by affinity chromatography. A polyclonal anti-YadK antiserum was generated by rabbit immunization with purified T7-YadK-His protein. The anti-YadK specifically recognized over-expressed YadK (21.2KD) in EHEC, GST-YadK (48KD) in EHEC, and T7-YadK-His (23KD) in BL21 (DE3) as determined by Western blotting (**Figure 3.2.9-11**), indicating the specific recognition of YadK by this anti-YadK antiserum.

To achieve objective II, EHEC wild-type and $\Delta yadK$ mutant bacteria were treated under acid-adapted acid stress or unstressed conditions. The bacterial lysates were then prepared and subjected to Western blotting with anti-YadK polyclonal antibodies, to compare YadK expression level between UU and AA groups. In order to make an appropriate YadK negative control for EDL933 strain in Western blotting experiments, a $\Delta yadK$ mutant was constructed in EDL933 strain, using λ -Red recombinant system. EDL933 $\Delta yadK$ mutant was successfully constructed and subsequently used in Western blotting of **Figure 3.4.1**, as a YadK expression-negative control. Western blotting with anti-YadK revealed that the endogenous YadK

expression in unstressed EHEC was minimal and that expression was increased at least 2-fold by acid-adapted acid stress. This result suggested that YadK protein expression and possibly YadK fimbriae in EHEC may be up-regulated in response to acid stress.

We found that anti-YadK antibodies were able to significantly inhibit adhesion of acid-stressed EHEC to human epithelial cells, completely eliminating the acid-induced adhesion phenotype observed for wild type EHEC O157 (**Figure 3.5**). This provides convincing evidence that the YadK protein participates in the adhesion enhancement after acid stress and provides confirmation of the expression of YadK under acid stress.

To substantiate the finding of acid-induced up-regulation of *yadK*, different regions of the predicted *yadK* promoter region were cloned into the vector that contains a promoter-less *lacZ* gene. Promoter activities under various conditions (e.g. acid-adapted acid stress, unadapted acid stress and unstressed treatments) were measured. The results indicated the promoter activity for the whole operon PyadN, but not for PyadM or PyadK, was enhanced under the acid-adapted acid treatment (**Figure 3.6.2**).

Recent reports have identified two regulators involved in regulation of *yad* operon expression, H-NS and AI-2⁹²⁻⁹³. With the studies of the fimbrial operon in K12, the

yad operon promoter activity was found significantly increased in *hns* mutant compared to wild type, which indicated H-NS could repress *yad* operon transcript⁹². According to DNA microarray analysis, *yadN*, the major subunit gene in locus 2 was increased more than 23-fold in the *hns* mutant compared to wild type⁶⁷. Many studies have suggested H-NS may play a repressive function in fimbrial expression in *E. coli*, which suggests H-NS may negatively regulate *yadK* expression in EHEC⁶⁷. The *in vitro* studies demonstrate that *yadK* was induced by AI-2 signaling⁹³. The *yadK* gene was identified as one of the genes that responded to differential AI-2 concentration in culture media. Both *yadK* and locus 2 major subunit *yadN* showed a significant increase under the high AI-2 concentrations conditions⁹³. It has been reported that the presence of AI-2 in culture media influenced the expression of *yadK* in EHEC O157:H7 strains⁹⁷. Several genes involved in AI-2 signaling had been reported to be up-regulated under acid stress, indicating the regulation of *yadK* by AI-2 may be related to acid stress.

In summary, we found that YadK protein expression is up-regulated by acid stress and that YadK plays a role in acid-induced adhesion of EHEC to human epithelial cells. These results suggest that anti-YadK antibodies may be a potential therapeutic target against EHEC infection, and YadK protein could be the target for a potential vaccine in humans. Anti-YadK antibodies may also be used in the food industry to diminish the potential EHEC infection. This study provides the first evidence of an EHEC adhesin specifically expressed after acid stress and may provide a new insight into the

pathogenic mechanism of EHEC, particularly after gastric passage. A model for this mechanism is proposed in **Figure 4.1**.

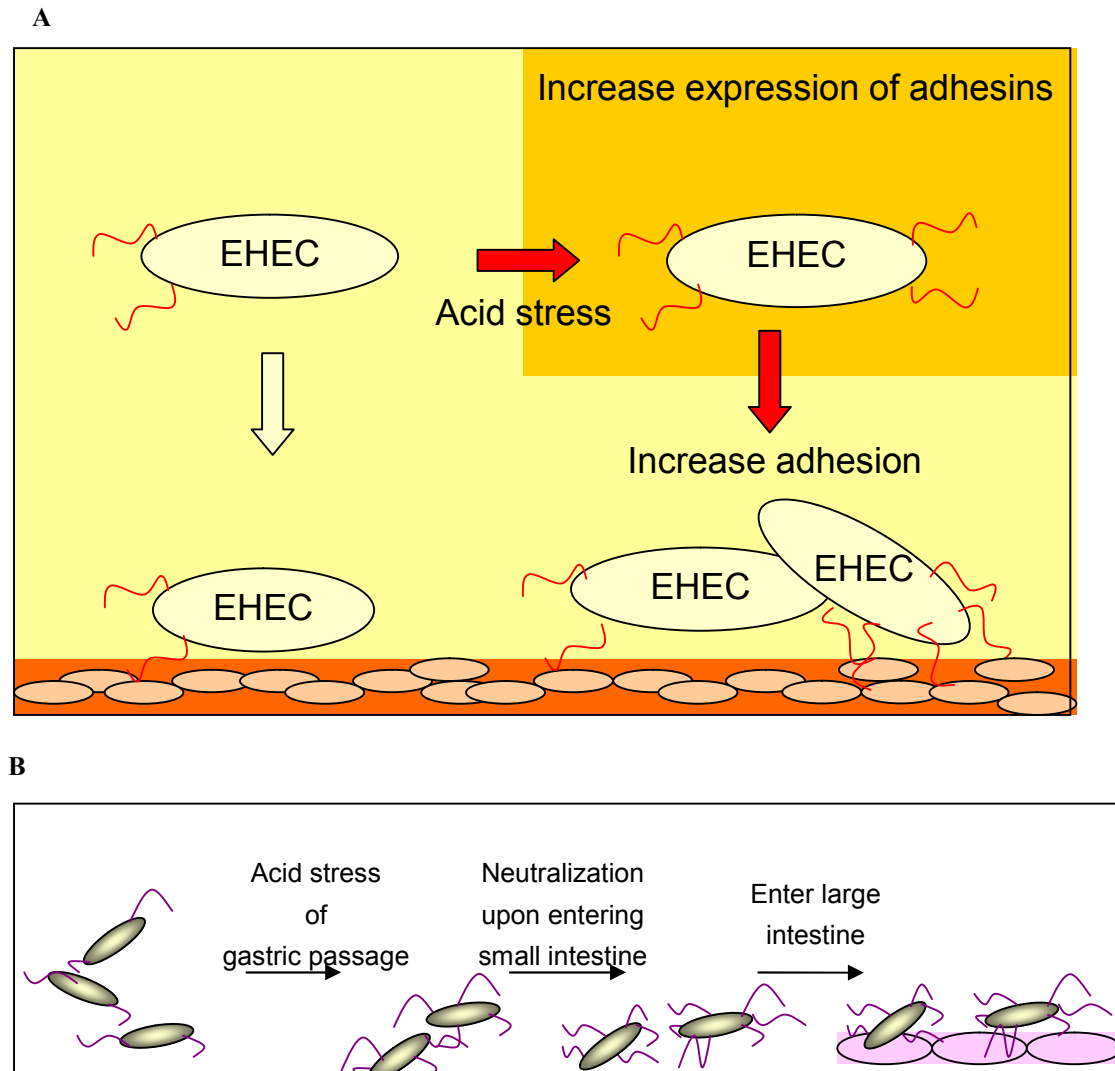





Figure 4.1 A: The effect of acid stress on EHEC adhesion to human epithelial cells. Exposure to acid appears enhanced expression of EHEC adhesins, including a putative fimbrial adhesin, YadK. As a result, acid stressed EHEC adheres to human epithelial cells much better than unstressed counterparts.

B: Enhanced EHEC adhesion to large intestine after EHEC encounter acid stress in the stomach. The exposure of EHEC to acid stress in the stomach enhanced expression of EHEC adhesions, leading to increased EHEC adhesion in large intestine.

 indicates locus 2 fimbriae adhesin,
  indicates EHEC,
  indicates human epithelial cells in large intestine.

5. Future Directions

Future work on this project should include the characterization of the structure and expression regulators of Locus 2 fimbriae in EHEC. This study provides two different YadK-tagged expression vectors, the specific anti-YadK antibodies and EDL933 Δ *yadK* strain. Biofilm formation using EDL933, EDL933 Δ *yadK* and possible complementary strains could be assessed to determine the role of YadK in microcolony formation.

YadK is predicted to be the minor subunit of Locus 2 fimbrial operon, and the transcription level of minor subunit (i.e.YadK) is usually much less than that of major subunit (i.e.YadN of Locus 2 fimbriae). Therefore, the generation of an anti-YadN antiserum may be more effective for characterization of possible fimbrial structures in EHEC through electro microscopy.

Studies have suggested that H-NS plays a repressive function in the expression of fimbrial structure in *E. coli*, which suggests H-NS may also negatively regulate *yadK* expression in EHEC. Three promoter constructs (pMC1403-PyadN, pMC1403-PyadM and pMC1403-PyadK) made in this study could be used to transform the EDL933 Δ *hns* mutant and assess the role of H-NS in YadK expression.

AI-2 in culture media has been reported to influence *yadK* expression in EHEC O157:H7 strains⁹⁷. Several genes involved in AI-2 signaling had been reported to be up-regulated in acid stress, which indicates the regulation of *yadK* by AI-2 may be related to acid stress. AI-2 experiment could be performed to determine the AI-2 activity under various stresses (e.g. acid-adapted acid stress, un-adapted acid stress and no-acid stress). Future studies could be performed to investigate the regulation of AI-2 on other fimbrial gene expression (i.e. *yagZ* and *lpfA*).

6. References

1. Lim JY, Hong JB, Sheng H, et al. Phenotypic diversity of *Escherichia coli* O157:H7 strains associated with the plasmid O157. *J Microbiol.* Jun 2010;48(3):347-357.
2. Turner M. Microbe outbreak panics Europe. *Nature.* Jun 9 2011;474(7350):137.
3. House B, Kus JV, Prayitno N, et al. Acid-stress-induced changes in enterohaemorrhagic *Escherichia coli* O157 : H7 virulence. *Microbiology.* Sep 2009;155(Pt 9):2907-2918.
4. Frankel G, Candy DC, Everest P, et al. Characterization of the C-terminal domains of intimin-like proteins of enteropathogenic and enterohemorrhagic *Escherichia coli*, *Citrobacter freundii*, and *Hafnia alvei*. *Infect Immun.* May 1994;62(5):1835-1842.
5. Karaolis DK, McDaniel TK, Kaper JB, et al. Cloning of the RDEC-1 locus of enterocyte effacement (LEE) and functional analysis of the phenotype on HEp-2 cells. *Adv Exp Med Biol.* 1997;412:241-245.
6. Schmidt H, Beutin L, Karch H. Molecular analysis of the plasmid-encoded hemolysin of *Escherichia coli* O157:H7 strain EDL 933. *Infect Immun.* Mar 1995;63(3):1055-1061.
7. Batchelor M, Prasannan S, Daniell S, et al. Structural basis for recognition of the translocated intimin receptor (Tir) by intimin from enteropathogenic *Escherichia coli*. *EMBO J.* Jun 1 2000;19(11):2452-2464.
8. Proft T, Baker EN. Pili in Gram-negative and Gram-positive bacteria - structure, assembly and their role in disease. *Cell Mol Life Sci.* Feb 2009;66(4):613-635.
9. LeBlanc JJ. Implication of virulence factors in *Escherichia coli* O157:H7 pathogenesis. *Crit Rev Microbiol.* 2003;29(4):277-296.
10. Jacobsen L, Durso L, Conway T, et al. *Escherichia coli* O157:H7 and other *E. coli* strains share physiological properties associated with intestinal colonization. *Appl Environ Microbiol.* Jul 2009;75(13):4633-4635.
11. Lim JY, Yoon J, Hovde CJ. A brief overview of *Escherichia coli* O157:H7 and its plasmid O157. *J Microbiol Biotechnol.* Jan 2010;20(1):5-14.
12. Pomajzl RJ, Varman M, Holst A, et al. Hemolytic uremic syndrome (HUS)--incidence and etiologies at a regional Children's Hospital in 2001-2006. *Eur J Clin Microbiol Infect Dis.* Dec 2009;28(12):1431-1435.
13. Rangel JM, Sparling PH, Crowe C, Griffin PM, Swerdlow DL. Epidemiology of *Escherichia coli* O157:H7 outbreaks, United States, 1982-2002. *Emerg Infect Dis.* Apr 2005;11(4):603-609.
14. Michino H, Araki K, Minami S, et al. Massive outbreak of *Escherichia coli* O157:H7 infection in schoolchildren in Sakai City, Japan, associated with

- consumption of white radish sprouts. *Am J Epidemiol.* Oct 15 1999;150(8):787-796.
15. Torres AG, Jeter C, Langley W, et al. Differential binding of *Escherichia coli* O157:H7 to alfalfa, human epithelial cells, and plastic is mediated by a variety of surface structures. *Appl Environ Microbiol.* Dec 2005;71(12):8008-8015.
 16. McGannon CM, Fuller CA, Weiss AA. Different classes of antibiotics differentially influence shiga toxin production. *Antimicrob Agents Chemother.* Sep 2010;54(9):3790-3798.
 17. Lapeyraque AL, Fremeaux-Bacchi V, Robitaille P. Efficacy of eculizumab in a patient with factor-H-associated atypical hemolytic uremic syndrome. *Pediatr Nephrol.* Apr 2011;26(4):621-624.
 18. Bearson S, Bearson B, Foster JW. Acid stress responses in enterobacteria. *FEMS Microbiol Lett.* Feb 15 1997;147(2):173-180.
 19. Olesen I, Jespersen L. Relative gene transcription and pathogenicity of enterohemorrhagic *Escherichia coli* after long-term adaptation to acid and salt stress. *Int J Food Microbiol.* Jul 15 2010;141(3):248-253.
 20. Yin X, Zhu J, Feng Y, et al. Differential gene expression and adherence of *Escherichia coli* O157:H7 in vitro and in ligated pig intestines. *PLoS One.* 2011;6(2):e17424.
 21. Jeong KC, Hung KF, Baumler DJ, et al. Acid stress damage of DNA is prevented by Dps binding in *Escherichia coli* O157:H7. *BMC Microbiol.* 2008;8:181.
 22. Foster JW. *Escherichia coli* acid resistance: tales of an amateur acidophile. *Nat Rev Microbiol.* Nov 2004;2(11):898-907.
 23. Richard HT, Foster JW. Acid resistance in *Escherichia coli*. *Adv Appl Microbiol.* 2003;52:167-186.
 24. Castanie-Cornet MP, Penfound TA, Smith D, et al. Control of acid resistance in *Escherichia coli*. *J Bacteriol.* Jun 1999;181(11):3525-3535.
 25. Castanie-Cornet MP, Foster JW. *Escherichia coli* acid resistance: cAMP receptor protein and a 20 bp cis-acting sequence control pH and stationary phase expression of the gadA and gadBC glutamate decarboxylase genes. *Microbiology.* Mar 2001;147(Pt 3):709-715.
 26. Bhagwat AA, Chan L, Han R, et al. Characterization of enterohemorrhagic *Escherichia coli* strains based on acid resistance phenotypes. *Infect Immun.* Aug 2005;73(8):4993-5003.
 27. Hsin-Yi C, Chou CC. Acid adaptation and temperature effect on the survival of *E. coli* O157:H7 in acidic fruit juice and lactic fermented milk product. *Int J Food Microbiol.* Oct 22 2001;70(1-2):189-195.
 28. Leyer GJ, Wang LL, Johnson EA. Acid adaptation of *Escherichia coli* O157:H7 increases survival in acidic foods. *Appl Environ Microbiol.* Oct 1995;61(10):3752-3755.
 29. Tosun H, Gonul SA. The effect of acid adaptation conditions on heat resistance of *Escherichia coli* O157: H7. *Pol J Microbiol.* 2005;54(4):295-299.

30. Cheng HY, Yang HY, Chou CC. Influence of acid adaptation on the tolerance of *Escherichia coli* O157:H7 to some subsequent stresses. *J Food Prot.* Feb 2002;65(2):260-265.
31. Parry-Hanson AA, Jooste PJ, Buys EM. Relative gene expression in acid-adapted *Escherichia coli* O157:H7 during lactoperoxidase and lactic acid challenge in Tryptone Soy Broth. *Microbiol Res.* Sep 20 2010;165(7):546-556.
32. de Jesus MC, Urban AA, Marasigan ME, et al. Acid and bile-salt stress of enteropathogenic *Escherichia coli* enhances adhesion to epithelial cells and alters glycolipid receptor binding specificity. *J Infect Dis.* Oct 15 2005;192(8):1430-1440.
33. Bergholz TM, Vanaja SK, Whittam TS. Gene expression induced in *Escherichia coli* O157:H7 upon exposure to model apple juice. *Appl Environ Microbiol.* Jun 2009;75(11):3542-3553.
34. King T, Lucchini S, Hinton JC, et al. Transcriptomic analysis of *Escherichia coli* O157:H7 and K-12 cultures exposed to inorganic and organic acids in stationary phase reveals acidulant- and strain-specific acid tolerance responses. *Appl Environ Microbiol.* Oct 2010;76(19):6514-6528.
35. Huang YJ, Tsai TY, Pan TM. Physiological response and protein expression under acid stress of *Escherichia coli* O157:H7 TWC01 isolated from Taiwan. *J Agric Food Chem.* Aug 22 2007;55(17):7182-7191.
36. Johannes L, Romer W. Shiga toxins--from cell biology to biomedical applications. *Nat Rev Microbiol.* Feb 2010;8(2):105-116.
37. Matise I, Cornick NA, Samuel JE, et al. Binding of shiga toxin 2e to porcine erythrocytes in vivo and in vitro. *Infect Immun.* Sep 2003;71(9):5194-5201.
38. Ostroff SM, Tarr PI, Neill MA, et al. Toxin genotypes and plasmid profiles as determinants of systemic sequelae in *Escherichia coli* O157:H7 infections. *J Infect Dis.* Dec 1989;160(6):994-998.
39. Pina DG, Johannes L. Cholera and Shiga toxin B-subunits: thermodynamic and structural considerations for function and biomedical applications. *Toxicon.* Mar 15 2005;45(4):389-393.
40. Yuhas Y, Nofech-Mozes Y, Weizman A, et al. Enhancement of pentylenetetrazole-induced seizures by *Shigella dysenteriae* in LPS-resistant C3H/HeJ mice: role of the host response. *Med Microbiol Immunol.* Mar 2002;190(4):173-178.
41. Nataro JP, Kaper JB. Diarrheagenic *Escherichia coli*. *Clin Microbiol Rev.* Jan 1998;11(1):142-201.
42. McDaniel TK, Kaper JB. A cloned pathogenicity island from enteropathogenic *Escherichia coli* confers the attaching and effacing phenotype on *E. coli* K-12. *Mol Microbiol.* Jan 1997;23(2):399-407.
43. Perna NT, Mayhew GF, Posfai G, et al. Molecular evolution of a pathogenicity island from enterohemorrhagic *Escherichia coli* O157:H7. *Infect Immun.* Aug 1998;66(8):3810-3817.

44. Zhu C, Feng S, Sperandio V, et al. The possible influence of LuxS in the in vivo virulence of rabbit enteropathogenic *Escherichia coli*. *Vet Microbiol*. Dec 15 2007;125(3-4):313-322.
45. Brunder W, Schmidt H, Karch H. EspP, a novel extracellular serine protease of enterohaemorrhagic *Escherichia coli* O157:H7 cleaves human coagulation factor V. *Mol Microbiol*. May 1997;24(4):767-778.
46. Tatsuno I, Horie M, Abe H, et al. toxB gene on pO157 of enterohemorrhagic *Escherichia coli* O157:H7 is required for full epithelial cell adherence phenotype. *Infect Immun*. Nov 2001;69(11):6660-6669.
47. Torres AG, Kanack KJ, Tutt CB, et al. Characterization of the second long polar (LP) fimbriae of *Escherichia coli* O157:H7 and distribution of LP fimbriae in other pathogenic *E. coli* strains. *FEMS Microbiol Lett*. Sep 15 2004;238(2):333-344.
48. Kline KA, Dodson KW, Caparon MG, et al. A tale of two pili: assembly and function of pili in bacteria. *Trends Microbiol*. May 2010;18(5):224-232.
49. Pizarro-Cerda J, Cossart P. Bacterial adhesion and entry into host cells. *Cell*. Feb 24 2006;124(4):715-727.
50. Jones CH, Jacob-Dubuisson F, Dodson K, et al. Adhesin presentation in bacteria requires molecular chaperones and ushers. *Infect Immun*. Nov 1992;60(11):4445-4451.
51. Low AS, Holden N, Rosser T, et al. Analysis of fimbrial gene clusters and their expression in enterohaemorrhagic *Escherichia coli* O157:H7. *Environ Microbiol*. Jun 2006;8(6):1033-1047.
52. Lindberg S, Xia Y, Sonden B, et al. Regulatory Interactions among adhesin gene systems of uropathogenic *Escherichia coli*. *Infect Immun*. Feb 2008;76(2):771-780.
53. Low AS, Dziva F, Torres AG, et al. Cloning, expression, and characterization of fimbrial operon F9 from enterohemorrhagic *Escherichia coli* O157:H7. *Infect Immun*. Apr 2006;74(4):2233-2244.
54. Kim SH, Kim YH. *Escherichia coli* O157:H7 adherence to HEp-2 cells is implicated with curli expression and outer membrane integrity. *J Vet Sci*. Jun 2004;5(2):119-124.
55. Rendon MA, Saldana Z, Erdem AL, et al. Commensal and pathogenic *Escherichia coli* use a common pilus adherence factor for epithelial cell colonization. *Proc Natl Acad Sci U S A*. Jun 19 2007;104(25):10637-10642.
56. Xicohtencatl-Cortes J, Monteiro-Neto V, Ledesma MA, et al. Intestinal adherence associated with type IV pili of enterohemorrhagic *Escherichia coli* O157:H7. *J Clin Invest*. Nov 2007;117(11):3519-3529.
57. Torres AG, Giron JA, Perna NT, et al. Identification and characterization of lpfABCC'DE, a fimbrial operon of enterohemorrhagic *Escherichia coli* O157:H7. *Infect Immun*. Oct 2002;70(10):5416-5427.
58. Naylor SW, Low JC, Besser TE, et al. Lymphoid follicle-dense mucosa at the terminal rectum is the principal site of colonization of enterohemorrhagic

- Escherichia coli* O157:H7 in the bovine host. *Infect Immun.* Mar 2003;71(3):1505-1512.
59. Schembri MA, Kjaergaard K, Sokurenko EV, et al. Molecular characterization of the *Escherichia coli* FimH adhesin. *J Infect Dis.* Mar 1 2001;183 Suppl 1:S28-31.
 60. Telford JL, Barocchi MA, Margarit I, et al. Pili in gram-positive pathogens. *Nat Rev Microbiol.* Jul 2006;4(7):509-519.
 61. Capitani G, Eidam O, Glockshuber R, et al. Structural and functional insights into the assembly of type 1 pili from *Escherichia coli*. *Microbes Infect.* Jul 2006;8(8):2284-2290.
 62. Iida K, Mizunoe Y, Wai SN, et al. Type 1 fimbriation and its phase switching in diarrheagenic *Escherichia coli* strains. *Clin Diagn Lab Immunol.* May 2001;8(3):489-495.
 63. Lowe MA, Holt SC, Eisenstein BI. Immunoelectron microscopic analysis of elongation of type 1 fimbriae in *Escherichia coli*. *J Bacteriol.* Jan 1987;169(1):157-163.
 64. Torres AG, Milflores-Flores L, Garcia-Gallegos JG, et al. Environmental regulation and colonization attributes of the long polar fimbriae (LPF) of *Escherichia coli* O157:H7. *Int J Med Microbiol.* Jun 2007;297(3):177-185.
 65. Musken A, Bielaszewska M, Greune L, et al. Anaerobic conditions promote expression of Sfp fimbriae and adherence of sorbitol-fermenting enterohemorrhagic *Escherichia coli* O157:NM to human intestinal epithelial cells. *Appl Environ Microbiol.* Feb 2008;74(4):1087-1093.
 66. Uhlich GA, Keen JE, Elder RO. Mutations in the csgD promoter associated with variations in curli expression in certain strains of *Escherichia coli* O157:H7. *Appl Environ Microbiol.* May 2001;67(5):2367-2370.
 67. Hommais F, Krin E, Laurent-Winter C, et al. Large-scale monitoring of pleiotropic regulation of gene expression by the prokaryotic nucleoid-associated protein, H-NS. *Mol Microbiol.* Apr 2001;40(1):20-36.
 68. Joyce SA, Dorman CJ. A Rho-dependent phase-variable transcription terminator controls expression of the FimE recombinase in *Escherichia coli*. *Mol Microbiol.* Aug 2002;45(4):1107-1117.
 69. Mol O, Oudega B. Molecular and structural aspects of fimbriae biosynthesis and assembly in *Escherichia coli*. *FEMS Microbiol Rev.* Oct 1996;19(1):25-52.
 70. Xie H, Cai S, Lamont RJ. Environmental regulation of fimbrial gene expression in *Porphyromonas gingivalis*. *Infect Immun.* Jun 1997;65(6):2265-2271.
 71. Goransson M, Forsman K, Uhlin BE. Regulatory genes in the thermoregulation of *Escherichia coli* pili gene transcription. *Genes Dev.* Jan 1989;3(1):123-130.
 72. Walker SL, Sojka M, Dibb-Fuller M, et al. Effect of pH, temperature and surface contact on the elaboration of fimbriae and flagella by *Salmonella* serotype Enteritidis. *J Med Microbiol.* Mar 1999;48(3):253-261.

73. van der Woude MW, Arts PA, Bakker D, et al. Growth-rate-dependent synthesis of K99 fimbrial subunits is regulated at the level of transcription. *J Gen Microbiol.* May 1990;136(5):897-903.
74. van Verseveld HW, Bakker P, van der Woude T, et al. Production of fimbrial adhesins K99 and F41 by enterotoxigenic *Escherichia coli* as a function of growth-rate domain. *Infect Immun.* Jul 1985;49(1):159-163.
75. Gally DL, Rucker TJ, Blomfield IC. The leucine-responsive regulatory protein binds to the fim switch to control phase variation of type 1 fimbrial expression in *Escherichia coli* K-12. *J Bacteriol.* Sep 1994;176(18):5665-5672.
76. Muller CM, Aberg A, Straseviciene J, et al. Type 1 fimbriae, a colonization factor of uropathogenic *Escherichia coli*, are controlled by the metabolic sensor CRP-cAMP. *PLoS Pathog.* Feb 2009;5(2):e1000303.
77. Mellies JL, Elliott SJ, Sperandio V, et al. The Per regulon of enteropathogenic *Escherichia coli* : identification of a regulatory cascade and a novel transcriptional activator, the locus of enterocyte effacement (LEE)-encoded regulator (Ler). *Mol Microbiol.* Jul 1999;33(2):296-306.
78. Willins DA, Ryan CW, Platko JV, et al. Characterization of Lrp, and *Escherichia coli* regulatory protein that mediates a global response to leucine. *J Biol Chem.* Jun 15 1991;266(17):10768-10774.
79. Hung SP, Baldi P, Hatfield GW. Global gene expression profiling in *Escherichia coli* K12. The effects of leucine-responsive regulatory protein. *J Biol Chem.* Oct 25 2002;277(43):40309-40323.
80. Tani TH, Khodursky A, Blumenthal RM, et al. Adaptation to famine: a family of stationary-phase genes revealed by microarray analysis. *Proc Natl Acad Sci U S A.* Oct 15 2002;99(21):13471-13476.
81. Corcoran CP, Dorman CJ. DNA relaxation-dependent phase biasing of the fim genetic switch in *Escherichia coli* depends on the interplay of H-NS, IHF and LRP. *Mol Microbiol.* Dec 2009;74(5):1071-1082.
82. Holden N, Blomfield IC, Uhlin BE, et al. Comparative analysis of FimB and FimE recombinase activity. *Microbiology.* Dec 2007;153(Pt 12):4138-4149.
83. Lund B, Lindberg F, Normark S. Structure and antigenic properties of the tip-located P pilus proteins of uropathogenic *Escherichia coli*. *J Bacteriol.* Apr 1988;170(4):1887-1894.
84. Nuccio SP, Baumler AJ. Evolution of the chaperone/usher assembly pathway: fimbrial classification goes Greek. *Microbiol Mol Biol Rev.* Dec 2007;71(4):551-575.
85. Le Trong I, Aprikian P, Kidd BA, et al. Donor strand exchange and conformational changes during E. coli fimbrial formation. *J Struct Biol.* Dec 2010;172(3):380-388.
86. Verger D, Rose RJ, Paci E, et al. Structural determinants of polymerization reactivity of the P pilus adaptor subunit PapF. *Structure.* Nov 12 2008;16(11):1724-1731.
87. Nicholls L, Grant TH, Robins-Browne RM. Identification of a novel genetic locus that is required for in vitro adhesion of a clinical isolate of

- enterohaemorrhagic *Escherichia coli* to epithelial cells. *Mol Microbiol.* Jan 2000;35(2):275-288.
88. Tatsuno I, Kimura H, Okutani A, et al. Isolation and characterization of mini-Tn5Km2 insertion mutants of enterohemorrhagic *Escherichia coli* O157:H7 deficient in adherence to Caco-2 cells. *Infect Immun.* Oct 2000;68(10):5943-5952.
 89. Tarr PI, Bilge SS, Vary JC, Jr., et al. Iha: a novel *Escherichia coli* O157:H7 adherence-conferring molecule encoded on a recently acquired chromosomal island of conserved structure. *Infect Immun.* Mar 2000;68(3):1400-1407.
 90. Chingcuanco F, Levesque CM, Barnett Foster DE. Role of a novel fimbrial adhesin in acid-induced host adhesion of *Escherichia coli* O157:H7. 109th Congress of American Society for Microbiology (ASM 2009), Philadelphia, USA. May, 2009.
 91. Perna NT, Plunkett G, 3rd, Burland V, et al. Genome sequence of enterohaemorrhagic *Escherichia coli* O157:H7. *Nature.* Jan 25 2001;409(6819):529-533.
 92. Korea CG, Badouraly R, Prevost MC, et al. *Escherichia coli* K-12 possesses multiple cryptic but functional chaperone-usher fimbriae with distinct surface specificities. *Environ Microbiol.* Jul 2010;12(7):1957-1977.
 93. DeLisa MP, Valdes JJ, Bentley WE. Mapping stress-induced changes in autoinducer AI-2 production in chemostat-cultivated *Escherichia coli* K-12. *J Bacteriol.* May 2001;183(9):2918-2928.
 94. Torres AG, Slater TM, Patel SD, et al. Contribution of the Ler- and H-NS-regulated long polar fimbriae of *Escherichia coli* O157:H7 during binding to tissue-cultured cells. *Infect Immun.* Nov 2008;76(11):5062-5071.
 95. Miller MB, Bassler BL. Quorum sensing in bacteria. *Annu Rev Microbiol.* 2001;55:165-199.
 96. Moslehi-Jenabian S, Gori K, Jespersen L. AI-2 signalling is induced by acidic shock in probiotic strains of *Lactobacillus* spp. *Int J Food Microbiol.* Nov 15 2009;135(3):295-302.
 97. Soni KA, Lu L, Jesudhasan PR, et al. Influence of autoinducer-2 (AI-2) and beef sample extracts on *E. coli* O157:H7 survival and gene expression of virulence genes *yadK* and *hhA*. *J Food Sci.* Apr 2008;73(3):M135-139.
 98. Giedroc DP, Khan R, Barnhart K. Overexpression, purification, and characterization of recombinant T4 gene 32 protein22-301 (g32P-B). *J Biol Chem.* Jul 15 1990;265(20):11444-11455.
 99. Li Z, Bell C, Buret A, et al. The effect of enterohemorrhagic *Escherichia coli* O157:H7 on intestinal structure and solute transport in rabbits. *Gastroenterology.* Feb 1993;104(2):467-474.
 100. Tzipori S, Karch H, Wachsmuth KI, et al. Role of a 60-megadalton plasmid and Shiga-like toxins in the pathogenesis of infection caused by enterohemorrhagic *Escherichia coli* O157:H7 in gnotobiotic piglets. *Infect Immun.* Dec 1987;55(12):3117-3125.

101. Mamelak D, Mylvaganam M, Whetstone H, et al. Hsp70s contain a specific sulfogalactolipid binding site. Differential aglycone influence on sulfogalactosyl ceramide binding by recombinant prokaryotic and eukaryotic hsp70 family members. *Biochemistry*. Mar 27 2001;40(12):3572-3582.
102. Griffith KL, Wolf RE, Jr. Measuring beta-galactosidase activity in bacteria: cell growth, permeabilization, and enzyme assays in 96-well arrays. *Biochem Biophys Res Commun*. Jan 11 2002;290(1):397-402.
103. Lee JH, Kim YG, Cho MH, et al. Transcriptomic analysis for genetic mechanisms of the factors related to biofilm formation in *Escherichia coli* O157:H7. *Curr Microbiol*. Apr 2011;62(4):1321-1330.
104. Puttamreddy S, Minion FC. Linkage between cellular adherence and biofilm formation in *Escherichia coli* O157:H7 EDL933. *FEMS Microbiol Lett*. Feb 2011;315(1):46-53.